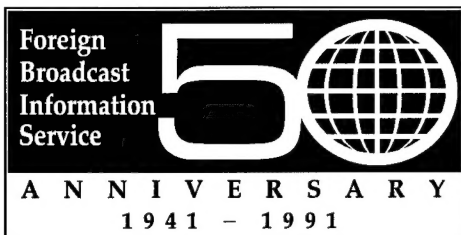


JPRS-UEQ-91-009
31 JULY 1991



JPRS Report

Science & Technology

***USSR: Engineering &
Equipment***

19980116 211

DTIC QUALITY INSPECTED 2

REPRODUCED BY
U.S. DEPARTMENT OF COMMERCE
NATIONAL TECHNICAL
INFORMATION SERVICE
SPRINGFIELD, VA 22161

DISTRIBUTION STATEMENT A

Approved for public release;
Distribution Unlimited

Science & Technology

USSR: Engineering & Equipment

JPRS-UEQ-91-009

CONTENTS

31 July 1991

Optics, High Energy Devices

- Improving the Design of Magnetic Compasses
[L.A. Kardashinskiy-Braude, V.V. Voronov; SUDOSTROYENIYE, Jan 91] 1
- Behavior of Industrial Hydrolysis Tailings During Heating to High Temperatures
[K.T. Norkulova, Yu.T. Tashpulatov, et al.; DOKLADY AKADEMII NAUK UzSSR, Nov 90] 3

Mechanics of Gases, Liquids, Solids

- Approximate Evaluation of Attenuation of Shock Waves by Permeable Barriers
[B.Ye. Gelfand, S.M. Frolov; ZHURNAL PRIKLADNOY MEKHANIKI I TEKHNICHESKOY FIZIKI, No 4, Jul-Aug 90] 4
- Acoustic Fields of Moving Sources
[A.V. Generalov; DOKLADY AKADEMII NAUK SSSR, Vol 316 No 4, Feb 91] 4
- Numerical Analysis of Oblique Penetration of Elastoplastic Body With Stellate Cross-Section into Layer of Compressible Fluid
[S.A. Afanasyeva, S.A. Chernyshev, et al.; DOKLADY AKADEMII NAUK SSSR, Vol 316 No 3, Jan 91] 4
- Vibrations of Piecewise-Homogeneous Elastic Body Immersed in Homogeneous Elastic Medium: Two-Dimensional Problem
[I.I. Safarov, A.B. Atoev, et al.; IZVESTIYA AKADEMII NAUK UZBEKSKOY SSR: SERIYA TEKHNICHESKIKH NAUK, No 6, Nov-Dec 90] 5
- Steady-State Diffraction of Longitudinal Wave by Cylindrical Shell
[M.Kh. Abdukhaparov, S.A. Abdukadyrov; IZVESTIYA AKADEMII NAUK UZBEKSKOY SSR: SERIYA TEKHNICHESKIKH NAUK, No 6, Nov-Dec 90] 5
- Physical and Chemical Action of Medium on Materials Undergoing Self-Organization During Friction
[B.I. Kostetskiy, O.V. Zazimko; FIZIKO-KHIMICHESKAYA MEKHANIKA MATERIALOV, No 6, Dec 90] 5
- Numerical and Experimental Study of Plane Ice Field and Cylindrical Pile Interaction
[V.I. Danilenko, S.I. Rogachko; IZVESTIYA AKADEMII NAUK SSSR; MEKHANIKA TVERDOGO TELA, No 6, Nov-Dec 90] 6
- Flexure of Polygonal Plate with Circular Center Hole and Two Straight Notches of Unequal Lengths
[S.A. Kuliyeu; IZVESTIYA AKADEMII NAUK SSSR: MEKHANIKA TVERDOGO TELA, No 6, Nov-Dec 90] 6
- Stability of Steady Rotations of Symmetric Gyroscope Filled With Liquid
[V.V. Rumyantsev; IZVESTIYA AKADEMII NAUK SSSR: MEKHANIKA TVERDOGO TELA, No 6, Dec 90] 7
- Refinement of Theory of Flat Shells
[V.V. Vasilyev, S.A. Lurye; IZVESTIYA AKADEMII NAUK SSSR: MEKHANIKA TVERDOGO TELA, No 6, Nov-Dec 90] 7
- Exact Solution to Problem of Flexure for Semiinfinitely Large Plate Totally Bonded to Elastic Medium Occupying Half-Space
[N.G. Moiseyev, G.Ya. Popov; IZVESTIYA AKADEMII NAUK SSSR: MEKHANIKA TVERDOGO TELA, No 6, Nov-Dec 90] 8
- Asymptotic Analysis and Refinement of Timoshenko-Reissner Theories on Plates and Shells
[A.L. Goldenveyser, Yu.D. Kaplunov, et al; IZVESTIYA AKADEMII NAUK SSSR: MEKHANIKA TVERDOGO TELA, No 6, Nov-Dec 90] 8
- Reconstructing Image of Defect From Scattered Wave Field in Acoustic Approximation
[I.I. Vorovich, M.A. Sumbatyan; IZVESTIYA AKADEMII NAUK SSSR: MEKHANIKA TVERDOGO TELA, No 6, Nov-Dec 90] 9
- Three-Dimensional Motion of Elastic Bodies
[A.F. Ulitko; IZVESTIYA AKADEMII NAUK SSSR: MEKHANIKA TVERDOGO TELA, No 6, Nov-Dec 90] 9
- Motion of Two Parallel Circular Cylinders in Viscous Fluid in Field of Acoustic Wave
[A.N. Guz, A.P. Zhuk; IZVESTIYA AKADEMII NAUK SSSR: MEKHANIKA TVERDOGO TELA, No 6, Nov-Dec 90] 9

Density Distribution in Pulsed Gas Jets Flowing Into Rarefied Medium [A.V. Yeremin, I.M. Naboko; <i>ZHURNAL PRIKLADNOY MEKHANIKI I TEKHNICHESKOY FIZIKI</i> , No 6, Nov-Dec 90]	10
Effect of Phase Transitions on Propagation of Sound Through Fog: Theory and Experiment [D.A. Gubaydullin, A.I. Ivandayev; <i>ZHURNAL PRIKLADNOY MEKHANIKI I TEKHNICHESKOY FIZIKI</i> , No 6, Nov-Dec 90]	10
Effect of Entropic Sublayer on Stability of Supersonic Shock Layer and Laminar-to-Turbulent Transition of Boundary Sublayer [V.I. Lysenko; <i>ZHURNAL PRIKLADNOY MEKHANIKI I TEKHNICHESKOY FIZIKI</i> , No 6, Nov-Dec 90]	10
Transient Processes in Free Pack Following Sudden Loss of Pressure During Gas Filtration [V.A. Antipin, A.A. Borisov, et al.; <i>ZHURNAL PRIKLADNOY MEKHANIKI I TEKHNICHESKOY FIZIKI</i> , No 6, Nov-Dec 90]	11
Relaxation Characteristics of Turbulent Shear Flow in Wake of Transversely Oriented Cylinder Near Plate [V.I. Kornilov, D.K. Mekler; <i>ZHURNAL PRIKLADNOY MEKHANIKI I TEKHNICHESKOY FIZIKI</i> , No 6, Nov-Dec 90]	11
Axial Compression of Nonhomogeneous Cone [M.A. Zadoyan, N.B. Safaryan; <i>ZHURNAL PRIKLADNOY MEKHANIKI I TEKHNICHESKOY FIZIKI</i> , No 6, Nov-Dec 90]	12
Interaction of Vibration Relaxation and Dissociation Reactions During Supersonic Flow of Viscous Gas Past Blunt Body [A.G. Tirskiy, V.G. Shcherbak; <i>ZHURNAL PRIKLADNOY MEKHANIKI I TEKHNICHESKOY FIZIKI</i> , No 6, Nov-Dec 90]	12
Effect of Reflected Particles on Flow of Gas With Suspended Particles Past Blunt Bodies [Yu.M. Davydov, I.Kh. Yenikeyev, et al.; <i>ZHURNAL PRIKLADNOY MEKHANIKI I TEKHNICHESKOY FIZIKI</i> , No 6, Nov-Dec 90]	13
Comparison Between Two Patterns Collision of Counterflowing Jets With Different Values of Bernoulli Constant [N.N. Lukerchenko; <i>ZHURNAL PRIKLADNOY MEKHANIKI I TEKHNICHESKOY FIZIKI</i> , No 6, Nov-Dec 90]	13
Effective Third-Order Moduli of Elasticity of Composite Materials [V.A. Buryachenko, A.M. Lipanov; <i>ZHURNAL PRIKLADNOY MEKHANIKI I TEKHNICHESKOY FIZIKI</i> , No 6, Nov-Dec 90]	13
Long Waves With Finite Amplitude in Polydisperse Gaseous Suspensions [N.A. Gumerov; <i>ZHURNAL PRIKLADNOY MEKHANIKI I TEKHNICHESKOY FIZIKI</i> , No 4, Jul-Aug 90]	14
Transient Vibrations of Slim Rod in Elastic Half-Space [L.N. Yungerman; <i>ZHURNAL PRIKLADNOY MEKHANIKI I TEKHNICHESKOY FIZIKI</i> , No 4, Jul-Aug 90]	14
Comparing Electric Field of Lightning With Electric Field of Glancing Spark [Ye.A. Zobov, A.N. Sidorov; <i>ZHURNAL PRIKLADNOY MEKHANIKI I TEKHNICHESKOY FIZIKI</i> , No 4, Jul-Aug 90]	15
Model of Interaction of High-Intensity Ion Beam and Metallic Absorber [V.I. Boyko, V.P. Kishkin, et al.; <i>ZHURNAL PRIKLADNOY MEKHANIKI I TEKHNICHESKOY FIZIKI</i> , No 4, Jul-Aug 90]	15
Development Models for Evaluation of Heat Transfer Under Conditions of Supersonic Turbulent Separation Flow [A.A. Zheltovodov, Ye.G. Zaulichnyy, et al.; <i>ZHURNAL PRIKLADNOY MEKHANIKI I TEKHNICHESKOY FIZIKI</i> , No 4, Jul-Aug 90]	15
Effect of Wave Processes on Viscous-Nonviscous Interaction of Subsonic or Supersonic Jet and Respectively Supersonic or Subsonic Companion Stream in Channel and in Tube [I.S. Belotserkovets, V.I. Timoshenko; <i>ZHURNAL PRIKLADNOY MEKHANIKI I TEKHNICHESKOY FIZIKI</i> , No 4, Jul-Aug 90]	16
Nonisothermal Separation Flow Past Sphere [K.B. Koshelev, M.P. Strongin; <i>ZHURNAL PRIKLADNOY MEKHANIKI I TEKHNICHESKOY FIZIKI</i> , No 4, Jul-Aug 90]	16
Modes of Free Oscillations in System of Four Quasi-Two-Dimensional Vortices [A.M. Batchayev; <i>ZHURNAL PRIKLADNOY MEKHANIKI I TEKHNICHESKOY FIZIKI</i> , No 4, Jul-Aug 90]	17

Dynamics of Condensation Front During Metal Ore Reduction by Laser Beam Under High Gas Pressure [A.G. Gnedovets, Ye.B. Kulbatskiy, et al.; ZHURNAL PRIKLADNOY MEKHANIKI I TEKHNICHESKOY FIZIKI, No 4, Jul-Aug 90]	17
Absorption of Sound Near Semiinfinite Rigid Plane [V.A. Murga; ZHURNAL PRIKLADNOY MEKHANIKI I TEKHNICHESKOY FIZIKI, No 4, Jul-Aug 90]	18
Experimental Study of Transient Radiation Emission by Jet of Impact-Heated Gas Mixture Containing CO ₂ [A.V. Yeremin, V.S. Ziborov; ZHURNAL PRIKLADNOY MEKHANIKI I TEKHNICHESKOY FIZIKI, No 4, Jul-Aug 90]	18
Aerodynamics of Apparatus With Stationary Granular Bed [Sh.A. Yershin, U.K. Zhabbasbayev, et al.; ZHURNAL PRIKLADNOY MEKHANIKI I TEKHNICHESKOY FIZIKI, No 4, Jul-Aug 90]	19
Jet Flow Pattern of Rarefied Gas Near Surface of Plane Barrier [B.F. Pavlov; VESTNIK LENINGRADSKOGO UNIVERSITETA, SERIYA 1: MATEMATIKA, MEKHANIKA, ASTRONOMIYA, No 4, Oct 90]	19
Accounting for Finiteness of Mach Numbers in Simplest Linear Model of Local Interaction Theory [O.A. Aksenova; VESTNIK LENINGRADSKOGO UNIVERSITETA, SERIYA 1: MATEMATIKA, MEKHANIKA, ASTRONOMIYA, No 4, Oct 90]	19
Optical Methods of Studying Inhomogeneities in Gaseous Media [S.A. Meladze; VESTNIK LENINGRADSKOGO UNIVERSITETA, SERIYA 1: MATEMATIKA, MEKHANIKA, ASTRONOMIYA, No 4, Oct 90]	20
Accessible Region for Single-Impulse Flight From Kepler Orbit [S.N. Kirpichnikov; VESTNIK LENINGRADSKOGO UNIVERSITETA, SERIYA 1: MATEMATIKA, MEKHANIKA, ASTRONOMIYA, No 4, Oct 90]	20
Structural Strength of Steel-Copper Pseudoalloys [V.N. Antsiferov, N.N. Maslennikov, et al.; FIZIKO-KHIMICHESKAYA MEKHANIKA MATERIALOV, Vol 26 No 6, Dec 90]	20
Mechanical Strength of VT-22 Titanium Alloy in Various Structural States [V.V. Shevelkov, L.F. Kratovich; FIZIKO-KHIMICHESKAYA MEKHANIKA MATERIALOV, Vol 26 No 6, Dec 90]	21
Classification of Hydrogen Storage Alloys [B.A. Kolachev; FIZIKO-KHIMICHESKAYA MEKHANIKA MATERIALOV, Vol 26 No 6, Dec 90]	21
Temperature Fields in Spherisymmetric Multilayer Systems [Yu.I. Dudarev, M.Z. Maksimov, et al.; INZHENERNO-FIZICHESKIY ZHURNAL, Vol 59 No 6, Dec 90]	21
Dielectric Properties of Filled Glass-Ceramic Material [V.V. Novikov, L.N. Tartakovskaya, et al.; INZHENERNO-FIZICHESKIY ZHURNAL, Vol 56 No 6, Dec 90]	22
Apparatus for Measuring Parameters of Air Streams at Ocean Surface [S.I. Gavrilovich, S.A. Levchenko, et al.; INZHENERNO-FIZICHESKIY ZHURNAL, Vol 59 No 6, Dec 90]	22
Thermal Expansion of Polycrystalline SiC and Nonreproducibility of Its Linear Dimensions [A.M. Tolkachev, V.A. Tits, et al.; INZHENERNO-FIZICHESKIY ZHURNAL, Vol 59 No 6, Dec 90]	23
Transverse Flow of Two-Phase Stream Past Cylindrical Heat Exchanger Surface [N.A. Kudryavtsev, M.V. Mironova, et al.; INZHENERNO-FIZICHESKIY ZHURNAL, Vol 59 No 6, Dec 90]	23

Industrial Technology, Planning, Productivity

Robot-Based Assembly Center [Yu.V. Kitayev; MEKHANIZATSIYA I AVTOMATIZATSIYA PROIZVODSTVA, No 2, 91]	24
The Problem of Developing Domestic Conveyor Building [V.K. Dyachkov; MEKHANIZATSIYA I AVTOMATIZATSIYA PROIZVODSTVA, No 2, 91]	25
Control System for a Multicoordinate Manipulator [V.A. Muravitskiy, A.V. Melnichuk; MEKHANIZATSIYA I AVTOMATIZATSIYA PROIZVODSTVA, No 2, 91]	31
Rotary Automated Assembly Line [L.T. Pasholok, I.V. Shchiviyev, et al.; MEKHANIZATSIYA I AVTOMATIZATSIYA PROIZVODSTVA, No 2, 91]	33

Ministry Becomes Joint-Stock Association [N. Panichev Interview; IZVESTIYA, 2 Jul 91]	36
Development of Control Programs for NC Machines in a Manufacturing Process CAD System [A.M. Gilman, Yu.B. Yegorov; STANKI I INSTRUMENT, Dec 90]	38
A System for the Computerized Exploratory Design and Manufacture of Tools for Resource-Saving Machining Processes [G.N. Kirsanov; STANKI I INSTRUMENT, Dec 90]	38
A Unified Intelligence Structure for Engineering and Biological Systems [G.N. Rapoport, A.G. Gerts; STANKI I INSTRUMENT, Dec 90]	38
The Survivability of Flexible Manufacturing Systems [V.G. Mitrofanov, A.S. Starostin; STANKI I INSTRUMENT, Dec 90]	39
Modeling Computer-Integrated Manufacturing [V.V. Pavlov; STANKI I INSTRUMENT, Dec 90]	39
Information Science Problems in Computerized Manufacturing [Yu.M. Solomentsev; STANKI I INSTRUMENT, Dec 90]	39
Prospective Automated Transport and Warehousing Systems [S.I. Bochek, A.G. Solomina; MEKHANIZATSIYA I AVTOMTIZATSIYA PROIZVODSTVA, Jan 91] ..	40
A Robot Vision System for Determining the Color, Shape, and Position of Objects in a Robot's Live Zone [V.I. Syryamkin, V.S. Titov, et al.; MEKHANIZATSIYA I AVTOMTIZATSIYA PROIZVODSTVA, Jan 91]	40
Overhead Transport Robot To Automate Loading, Unloading, Transport, and Warehousing Operations [V.I. Burenkov, V.N. Kazakov; MEKHANIZATSIYA I AVTOMTIZATSIYA PROIZVODSTVA, No 1, Jan 91]	41
Scientific-Technical Progress in Machine Building [A.A. Panov, Yu.N. Losev; MEKHANIZATSIYA I AVTOMTIZATSIYA PROIZVODSTVA, Jan 91]	41
Methods of Increasing and Stabilizing Precision When Manufacturing Products [I.M. Baranchukova; MEKHANIZATSIYA I AVTOMTIZATSIYA PROIZVODSTVA, Jan 91]	41
The Entropy Approach in Determining the Ultimate Bounds of the Development of an Automated Control System [A.A. Smekhov; MEKHANIZATSIYA I AVTOMTIZATSIYA PROIZVODSTVA, Jan 91]	42
Equipment for Remote Control of Underground Hoisting Units [N.P. Prokhorenko, N.P. Matviyenko, et al.; MEKHANIZATSIYA I AVTOMTIZATSIYA PROIZVODSTVA, Jan 91]	42
Designing Mechanisms To Move Blanks [V.A. Zaderenko; MEKHANIZATSIYA I AVTOMTIZATSIYA PROIZVODSTVA, Jan 91]	42
Determining an Industrial Robot's Work Space [V.F. Krasnikov; MEKHANIZATSIYA I AVTOMTIZATSIYA PROIZVODSTVA, Jan 91]	43
Development of a Technology for the High-Speed Milling of Cast Iron Components for the Krasnyy Proletariy Automated Plant [G.V. Borovskiy, I.G. Kondratyev, et al.; PROBLEMY MASHINOSTROYENIYA I NADEZHNOСТИ MASHIN, No 3, 91]	43
Ways of Developing Conventional Machining Methods Under the Conditions of an Automated Plant [M.A. Esterzon; PROBLEMY MASHINOSTROYENIYA I NADEZHNOСТИ MASHIN, No 3, 91]	43
Selected Features of the Technological Design of Flexible Manufacturing Systems [V.I. Buveykovskiy; PROBLEMY MASHINOSTROYENIYA I NADEZHNOСТИ MASHIN, No 3, 91]	44
Monitoring, Testing, and Diagnosis in Computerized Manufacturing [A.I. Kamyshev; PROBLEMY MASHINOSTROYENIYA I NADEZHNOСТИ MASHIN, No 3, 91]	44
NC Systems as a Part of the Hierarchical Structure for Managing an Automated Plant [V.A. Ratmirov; PROBLEMY MASHINOSTROYENIYA I NADEZHNOСТИ MASHIN, No 3, 91]	45
Principles of Creating an Automated System for the Technological Preparation of Production for an Automated Plant [A.M. Berman; PROBLEMY MASHINOSTROYENIYA I NADEZHNOСТИ MASHIN, No 3, 91]	45
The Automated Plant CAD System of the Krasnyy proletariy Machine Tool Production Association in Moscow [A.I. Levin; PROBLEMY MASHINOSTROYENIYA I NADEZHNOСТИ MASHIN, No 3, 91]	46
Simulation in Problems of the Design and Functioning of Automated Plants [V.T. Portman, Ye.I. Sklyarevskaya; PROBLEMY MASHINOSTROYENIYA I NADEZHNOСТИ MASHIN, No 3, 91]	46
Forecasting the Economic Indicators of an Automated Plant's Production Activity [L.Yu. Lishchinskiy; PROBLEMY MASHINOSTROYENIYA I NADEZHNOСТИ MASHIN, No 3, 91] ..	47
Prospects and Concepts of Creating Automated Plants [O.I. Averyanov, B.I. Cherpakov, et al.; PROBLEMY MASHINOSTROYENIYA I NADEZHNOСТИ MASHIN, No 3, 91]	47

Improving the Design of Magnetic Compasses

917F0240A Leningrad SUDOSTROYENIYE
in Russian No 1, Jan 91

[Article by L.A. Kardashinskiy-Braude and V.V. Voronov under the "Marine Instrument Making" rubric: "Improving the Design of Magnetic Compasses"]

629.12.053.11:55.380.84

[Text] The increasing interest in the shipping industry has increased requirements regarding course indicators' precision and reliability. The precision of a gyrocompass, while adequate under ordinary sailing conditions, is significantly reduced at high latitudes, and in regions near the poles a gyrocompass loses its serviceability altogether. It should be kept in mind that the magnetic pole does not coincide with the geographic pole. In principle, therefore, a magnetic compass can maintain its serviceability as a course indicator at all points of the northern sea route, including in the region of the geographic pole. Realizing this possibility, however, requires improving the design of the magnetic compass. The following may be mentioned as the key preferred directions for improving marine magnetic course indicators:

- creating a compass with an increased directional moment;
- developing a sensor with suspension and centering but without dry friction;
- introducing improved methods and means of reducing deviation so as to minimize it and provide stability during navigation at various latitudes;
- selecting the optimal location on a ship on which to install the magnetic sensor and using more precise remote transmission of its readings in analog and digital form;
- combining magnetic compasses and gyrocompasses.

This article examines the individual solutions to the aforesaid problems.

A magnetic compass with an increased directional moment. Increasing the magnetic moment M of the coil helps reduce a compass's static error and makes it possible to use the compass at high latitudes. But a high M can cause a significant reduction in the period of the coil's natural vibrations T at low latitudes where the horizontal component of the magnetic induction of the earth's field N is five- to tenfold that in the polar region. The phenomenon of resonance—i.e., the coincidence of the vibration frequency of the coil and the frequency of the disturbance (tossing, yawing)—may result, and the compass will have a high dynamic error. The main requirements for a magnetic compass with increased sensitivity may be formulated as follows:

- the magnetic moment M should be sufficient so that the compass's static error given minimal induction values N does not exceed the admissible value;
- the period T must not extend beyond the minimal bounds in which frequency resonance may appear;
- the compass must remain autonomous and independent of the power source.

One article¹ has examined the theoretical foundation of a new type of magnetic compass sensor meeting the specified requirement. It is proposed that the sensor's magnetic moment be increased by a factor of 5 to 10 while the inertial moment of the coil, on the other hand, be reduced severalfold. Such a sensor may be created on the basis of modern magnetic materials in which the magnetic moment does not depend on the shape but is instead determined solely by the volume (mass) of the substance. The coil of such a compass has a very high oscillation ability. The period of the sensor's natural vibrations ranges between 1 and 5 seconds. In other words, it is always less than the rocking period (in conventional compasses it is the other way around).

The system's high oscillation ability, which is close to a mode of continuous vibrations, makes it unsuitable for direct reading of a course. For this reason, the sensor has been furnished with a second complementary magnetic system with a working scale that has a high inertial moment and insignificant magnetic moment. Thanks to this fact, it is not sensitive to high-frequency vibrations of the main coil. This makes it possible to take averaged readings of the vibrated system.

An inventor's certificate² has been awarded for the design of a two-stage magnetic compass with a system of two coils as its sensor. Figure 1 is a schematic of the two-stage magnetic compass. The main magnetic system (8) consists of a set of several round flat magnets. The system represents a vertical cylinder that is magnetized along the diameter. The system has two jewel cones (4) and (9) resting on the tips of needles (3) and (10). The needle (3) is mounted in a frame (12), and the needle (10) is mounted in a shell (7). A float (11) compensates for the weight of the main magnetic system. A complementary magnetic system is mounted coaxially to the system. This complementary system consists of the following: a scale (5), a float (1), and two small magnets (6) and (13) located along the NS axis of the main magnetic system. The complementary system has a jewel cone (2) based on the upper tip of the needle (3).

Tests of a laboratory prototype of the two-stage magnetic compass confirmed its theoretical substantiation. The main advantages of the new sensor are the stability of the free vibration period T of the complementary magnetic system, the independence of the quantity T of the magnetic induction of the earth's field, and the compass's high sensitivity at high latitudes with minimal static and dynamic errors in all navigation regions.

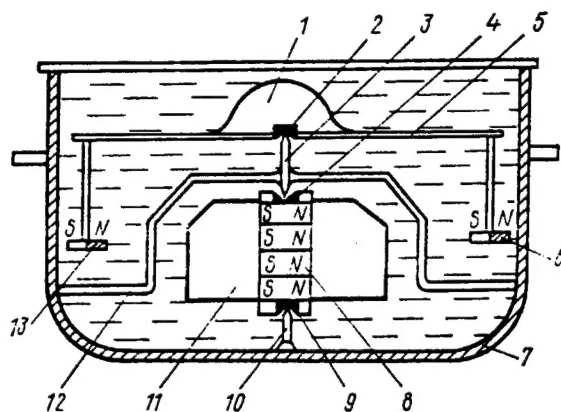


Figure 1. Diagram of a Two-Stage Magnetic Compass

A sensor with suspension and centering but without dry friction. Dry friction in the coil support is the reason for the occurrence of static error that has high values at high latitudes. In the region of the geographic pole where $N < 3 \mu T$, a magnetic compass ceases to be a reliable course indicator owing to dry friction. The weight of the coil is compensated for by placing a float at the interface of the two layers of liquid with different densities as has been described in one Japanese patent.³ The proposed new element is contactless centering of the coil. For this, the intent is to use two rings made of an electret (a dielectric that maintains its polarization for a long time). Figure 2 shows a compass design with electrostatic centering of the sensor. A float (5) with a scale (3) and magnets (7) lies at the interface of two liquids: a denser liquid (6) and a less dense liquid (4). The outer ring (2) made of an electret is mounted on the shell of the bowl (8) whereas the inner ring (1) is mounted on the float (5). The opposing surfaces of the rings should have the same charges. Modern electrets⁴ based on fluoroplastic have a charge density up to $30 \text{ N} \times \text{C}/\text{cm}^2$ that remains unchanged for 5 years. The centering radial forces given a gap of 10 mm between the rings amounts to $6 \times 10^{-2} \text{ N}$. When the gap is reduced by half, the centering force increases by about a factor of 8. This is sufficient to hold the sensor in the center of the shell under any compass operating conditions, i.e., in the presence of tossing, yawing, and vibrations.

In the proposed design, the dry friction of the support is eliminated and the compass's sensitivity increased significantly. Only wet friction remains in the instrument. It causes some error due to drag of the sensor in the case of circulation and yawing of the vessel. Using low-viscosity liquids and a circulated form of sensor helps reduce this type of deviation. The design of a compass with an electret sensor suspension is promising because it meets international requirements regarding autonomy and high sensitivity.

Compensating for higher-order deviations in compasses with an increased magnetic moment. The appearance of magnetic compasses using sensors with a high magnetic

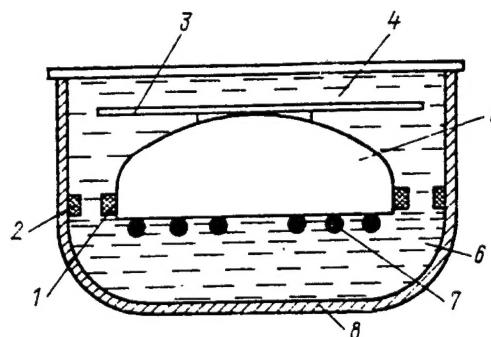


Figure 2. Diagram of a Compass With a Sensor That Is Free From Dry Friction

moment has created the problem of reducing higher-order deviations. This problem was solved in its own time for sensors using three pairs of needles with comparatively low magnetic moments. In the two-stage magnetic compass,¹ the main magnetic system has the unusual shape of a vertical cylinder magnetized along the diameter (see Figure 1). Research has shown that the most suitable material for these purposes is the alloy 23Kh15KGTM, which was created at the Physics of Metals Institute of the USSR Academy of Sciences. The alloy has the following key characteristics:

Coercive force, $\text{kA} \times \text{m}^{-1}$	50
Residual induction, T	1.4
Magnetic energy, $\text{T} \times \text{kA}/\text{m}$	40
Specific magnetization, $\text{A} \times \text{m}^2/\text{g}$	0.1

Research has shown that giving a magnet the shape of a flat ring or disk with magnetization along the diameter makes it possible to reduce higher-order deviation to a value not exceeding 0.1° provided that the sensor is in a nonuniform magnetic field created by a semicircular, quadrantal, and heeling deviation compensator and by elements of the vessel's structure. Using the alloy 23Kh15KGTM makes it possible to have a sensor with a magnetic moment of $10 \text{ A} \times \text{m}^2$ given a mass of 100 g. It has become possible to develop magnetic compasses with an increased directional moment and minimal errors and to use them on seagoing vessels.

References

1. V.V. Voronov, S.Yu. Moninets, "A Magnetic Compass With Two Coils," *Navigatsiya i upravleniye sudnom* (Ship Navigation and Control), V/O Mortekhin-formreklama, Moscow, 1989.
2. Ye.L. Smirnov, V.V. Voronov, and S.Yu. Moninets, "Magnetic Compass," *Inventor's Certificate No 1455237, OTKRYTIYA, IZOBRETENIYA, PROMY-SHLENNYYE OBRAZTSY, TOVARNYYE ZNAKI*, No 4, 1989.
3. Japanese Patent No 57-5965, 1982.

4. "Electrets," Collection of translations from English, Mir, Moscow, 1983.

Behavior of Industrial Hydrolysis Tailings During Heating to High Temperatures

917F0214A Tashkent DOKLADY AKADEMII NAUK
UzSSR in Russian No 11, Nov 90 pp 31-32

[Article by K.T. Norkulova, Yu.T. Tashpulatov, corresponding member, UzSSR Academy of Sciences, L.N. Semenova, and M.A. Sirazhdinova, Scientific Research Institute of Cotton Cellulose Chemistry and Technology]

UDC 547.455.526.154-058.666.71/72

[Abstract] An experimental study of brick manufacture from loess with a mixture of a "betonite" (concrete) and "collactivite" (byproduct of hydrolysis in industrial xylite production) added for improvement of the brick quality was made, of concern being the behavior of this additive mixture during heating up to the required 1040° brick baking temperature. Thermograms for thermogravimetric analysis of betonite, collactivite, and their 1:1 mixture were recorded on a Paulik-Erdey MOM derivatograph while specimens of these materials were being heated from 20°C to 1050°C at a rate of 10°C/min, before and after use in treatment of pentose hydrolyzates with sulfuric acid. The basic brick material, loess alone, was also thus treated and its behavior during heating analyzed. An endothermic effect within the 110-125°C

range, associated with removal of water, was detected in each material. Two other endothermic effects at 680°C and at 780° respectively, attributable to decomposition of carbonates (Na,K,Ca, Mg) reacting with sulfuric acid, were detected in betonite before but not after treatment of pentose hydrolyzates. The mass of 15x30x75 mm³ large plain loess bricks remained constant (92.4 g) during baking. The loss of mass by specimens of betonite, collactivite, and their mixture after use in treatment of pentose hydrolyzates was increasing during baking, evidently because organic compounds (formic and acetic acids, dyes, and pentose sugars) they had adsorbed were burning out. As the mixture of betonite and collactivite was added to loess bricks in amounts ranging from 5% to 50%, the mass of bricks decreased by a factor ranging from 1.025 to 1.32 correspondingly. Broken pieces of these bricks revealed pores below the surface, evidently formed by gaseous products of collactivite combustion during the baking process. Inasmuch as its combustion nears completion within the 700-800°C range, while baking continues further and ends at 1040°C, only internal pores without egress to the surface remain in such a brick. Its mechanical strength is higher than that of plain loess brick. Heat released by combustion of collactivite is, moreover, usable for baking and thus serves as an energy consumption economizer. Maximum decomposition of betonite and loess is 15% and 13% respectively, that of collactivite is 95%. Figures 2; references 1.

Approximate Evaluation of Attenuation of Shock Waves by Permeable Barriers

917F0195E Novosibirsk *ZHURNAL PRIKLADNOY MEKHANIKI I TEKHNICHESKOY FIZIKI* in Russian No 4, Jul-Aug 90 pp 42-46

[Article by B.Ye. Gelfand and S.M. Frolov, Moscow]

UDC 532.593

[Abstract] Attenuation of a plane shock wave by an permeable immovable thick barrier is evaluated on the basis of the gas flow equation $(v + a)dp/dx + ap(v + a)dv/dx = [(\gamma - 1)v - a]f(pv^2/2)$ (v - velocity of gas, a - acoustic velocity, ρ - density of gas, p - pressure, γ - c_p/c_v , x - space coordinate in direction of gas flow through barrier), where $f = C_D(1 - q)/s$ characterizes aerodynamic drag in the barrier (C_D - drag coefficient, q - permeability of barrier layer, s - structural pitch of barrier in direction of gas flow) and is constant at high values of the Reynolds number. Into this equation is inserted the relation $\phi(M, \gamma)(dM/dx) = -f/2$ characterizing the compression shock front (M -Mach number), where $M(x_1) = M_0$ at the entrance to the barrier and $M(x_2) = M_1$ at the exit from the barrier, so that the solution to this equation will be $G(M_0, \gamma) - G(M_1, \gamma) = f(x_2 - x_1)/2$. The shock wave intensity function $G(M)$ is now semiempirically approximated as $G(M) = 4(0.4M - 1)/(M^2 - 1) + 4\log(M^2 - 1) + 0.8\log(M + 1)/(M - 1)$. This approximation is validated by available experimental data on quenching of shock waves in gasdynamic laser systems by grids or screens. It is subsequently extended to attenuation of shock waves by n successive barriers: $G(M_n) = G(M_0) - \sum \eta_i$ ($i = 1, \dots, n$). Figures 4; tables 1; references 15.

Acoustic Fields of Moving Sources

917F0215A Moscow *DOKLADY AKADEMII NAUK SSSR* in Russian Vol 316 No 4, Feb 91 pp 851-855

[Article by A.V. Generalov, Scientific-Industrial Association "Trud" (Labor), Kuybyshev]

UDC 534.23

[Abstract] The problem of acoustic field of a source moving near barriers in a boundless medium is solved for general boundary conditions, this problem not having been tackled before and the solution to it being readily obtained from the known solution to the corresponding problem of a stationary source in such a medium is known. A point source of sound moving along an arbitrary trajectory near elastic barriers in a nonhomogeneous medium is considered. The barriers can be beams, plates, shells, or other structures mounted in stationary frames. The problem is solved for the velocity potential of the acoustic field and thus reduced to the corresponding nonhomogeneous wave equation the solution of which must satisfy certain boundary conditions, two conditions at the barrier surface and two conditions along the frame contour, also the condition of radiation

at infinity. Assuming steady static processes, this equation leads to one for the amplitudinal spectral density with the same but appropriately rewritten boundary conditions. Inasmuch as the Fourier transform representing this spectral density is the exact solution to the original equation, it is possible to determine the acoustic field of a moving source can when Green's function of the stationary source is known. The procedure is demonstrated on the example of homogeneous medium within absolute boundaries and is extended to larger guided sources such as multipole sources of arbitrary N -th order. Article was submitted by Academician N.D. Kuznetsov on 3 May 1990. References 7.

Numerical Analysis of Oblique Penetration of Elastoplastic Body With Stellate Cross-Section into Layer of Compressible Fluid

917F0200A Moscow *DOKLADY AKADEMII NAUK SSSR* in Russian Vol 316 No 3, Jan 91 pp 562-565

[Article by S.A. Afanasyeva, S.A. Chernyshev, and N.T. Yugov, Scientific Research Institute of Applied Mathematics and Mechanics, Tomsk]

UDC 539.4

[Abstract] Oblique penetration of an elastoplastic solid body with a stellate cross-section into a layer of compressible fluid is considered, the deformation of such a body in the process being treated as a three-dimensional problem and analyzed on the basis of a numerical solution for a specific object. The object was a 4.8 cm long steel cylinder with 1.49 cm long conical nose plunging at a supersonic speed into a 2.8 cm thick water layer at a 5° angle from the normal to its free surface, body and fluid then interacting at a speed equal to 1.333 times the speed of sound in water. The cross-section of the cylinder was a four-pointed star formed by four identical isosceles triangles, their vertices lying 90° apart on a circumscribed circle with a radius $R = 0.4$ cm and their arcuate bases spanning each a 90° arc around a circular center hub with a radius $r = 2^{1/2}R/4 \approx 0.173$ cm. The cross-section of the nose was similar but tapered to a point at the tip. Deformations of the solid body and configurations of the fluid body around the cavity were simulated both numerically and graphically covering a period of time from $0.12 \mu s$ to $24 \mu s$ after the initial impact at time $t = 0$, in addition to which were calculated the axial pressure profiles at successive instants of time. The results indicate that the deformation of such an obliquely plunging body and especially the flexure of its nose can be sufficiently large to destabilize the mode of its farther penetration into thicker layers of fluid. The deformation can, however, be minimized by optimizing the design of the star rays and the nose. Article was submitted by Academician L.I. Sedov on 3 May 1990. Figures 4; references 10.

Vibrations of Piecewise-Homogeneous Elastic Body Immersed in Homogeneous Elastic Medium: Two-Dimensional Problem

917F0199A Tashkent IZVESTIYA AKADEMII NAUK UZBEKSKOY SSR: SERIYA TEKHNICHESKIKH NAUK in Russian No 6, Nov-Dec 90 pp 24-28

[Article by I.I. Safarov, A.B. Atoev, and N.U. Kuldashiev, Institute of Mechanics and Earthquake-Resistant Equipment imeni M.T. Urazbayev, UzSSR Academy of Sciences]

UDC 539.3

[Abstract] Free and forced vibrations of a multilayer cylinder immersed in a boundless elastic medium are analyzed, the cylinder being regarded as a piecewise-homogeneous elastic body and the medium being regarded as a homogeneous elastic one. The field equation is formulated for the displacement vector $U = \text{grad}(\text{vector})\phi + \text{curl}(\text{vector})\psi$ ($\text{div}(\text{vector})\psi = 0$), functions ϕ and ψ each satisfying the wave equation. Boundary conditions of either rigid contact or sliding contact between layers are considered, Sommerfeld's conditions of radiation at infinity being stipulated for both functions. The problem is solved for the wave potential in a polar system of coordinates, by the same method the authors used for solving the problem of diffraction of seismic waves by elastic cylindrical structures. From the solution to the Helmholtz equation for each of the given boundary conditions are then determined the corresponding stress distributions in layers of the cylinder and their dependence on the dimensionless wave number. Numerical data pertaining to hollow cylinders with $n = 1, \dots, 5$ layers and the stress distribution in the innermost layer due to incidence of longitudinal and transverse waves indicate that longitudinal incident waves produce maximum stress along the radius at angle $\theta = \pi/2$ and transverse incident waves produce maximum stress at angles $\theta = \pi/4, 3\pi/4$. Figures 4; references 5.

Steady-State Diffraction of Longitudinal Wave by Cylindrical Shell

917F0199B Tashkent IZVESTIYA AKADEMII NAUK UZBEKSKOY SSR: SERIYA TEKHNICHESKIKH NAUK No 6, Nov-Dec 90 pp 28-32

[Article by M.Kh. Abdukhaparov and S.A. Abdukadyrov, Institute of Mechanics and Earthquake-Resistant Apparatus imeni M.T. Urazbayev, UzSSR Academy of Sciences]

UDC 539.3

[Abstract] Incidence of a plane harmonic tension-compression wave on a cylindrical shell is considered, analysis of resulting dynamic stresses in the shell being reduced to solution of the two-dimensional problem of steady-state diffraction by a rigid cylinder in a boundless elastic medium. This problem is formulated for the

displacement potential of such a wave in a polar system of coordinates with the origin on the axis of the cylinder, deformation of the shell being described by equations of the classical Kirchhoff-Love theory. The displacement potentials of both reflected and diffracted waves are determined from the solution to the corresponding Helmholtz equation with boundary conditions of either rigid contact or sliding contact between shell and medium, and with Sommerfeld's conditions of radiation at infinity. The solution to this problem yields the total stress distribution, of particular concern being stress concentration and dynamicity. The two principal stress components, bond stress and flexural stress, are then calculated separately for a comparative evaluation. A numerical analysis of their distributions and amplitude-frequency characteristics reveals that bond stresses dominate over flexural ones with an amplitude one order of magnitude higher over a wide frequency range and the location of their maximum depending on the mode of shell interaction with the medium: along the radius at angle $\theta = \pi$ in the case of a rigid contact, along the radii at angles $\theta = 0$ and $\theta = \pi$ in the case of a sliding contact. In the case of a sliding contact with the medium, moreover, longitudinal vibrations of the shell around its circumference are characterized by a sharp resonance, the natural frequency being a complex quantity whose real part does not significantly differ from that of a cylindrical shell in vacuum. Figures 1; references 8.

Physical and Chemical Action of Medium on Materials Undergoing Self-Organization During Friction

917F0194B Kiev FIZIKO-KHIMICHESKAYA MEKHANIKA MATERIALOV in Russian Vol 26 No 6, Dec 90 pp 47-53

[Article by B.I. Kostetskiy and O.V. Zazimko, Ukrainian Academy of Agriculture, Kiev]

UDC 621.891:620.178.162

[Abstract] Tribological systems are examined from the standpoint of latest developments in theoretical physics regarding self-organization of materials and formation of ordered dissipative structures during friction, the practical purpose being a study of ways to minimize wear. External friction is accordingly regarded as a process which converts external mechanical energy into internal energy. The effects of all inevitable influencing factors on this process depend not only on a set of energy and kinetic conditions, definable in terms of integral parameters, but on mechanical, physical-chemical, and thermal properties of the materials as well. The fundamental energy condition characterizing self-organization in a tribological system is dynamic equilibrium between activation and passivation, the two underlying mechanisms, namely expenditure of the entire small amount of not dissipated but stored energy on formation of secondary structures. There is a fundamental kinetic condition

characterizing self-organization generation and annihilation of secondary structures at the same rate, an important parameter of this mechanism being the equilibrium stabilization time. The mechanical, thermal, and physical-chemical properties which determine the self-organization of materials during friction are those which also determine the exchange interactions of these materials and the ambient medium. The physical-chemical exchange interaction processes in effect modify the composition of secondary structures and weaken the adhesion forces so that those structures become shielded. Schematic analysis and experimental study of self-organization have revealed the range and the level of friction and wear normalization in various tribological systems, both widening the range and changing the level being the obvious means of control aimed at optimization of the friction coefficient and minimization of the wear rate. This can be done by utilizing various phenomena such as chemical modification of secondary structures, inversion of the dependence of the wear rate on the concentration of additives in the lubricant, synergistic and antagonistic influences of oxidizers and surfactants on the Rebinder effect during rubbing and cutting of metals, anomalous diffusion, plasticity, and nonstoichiometry of secondary structures, ordering and dislocationless fragmentation of secondary structures, and also the laws of mechanical-chemical abrasion processes. This is demonstrated on friction pairs of Cr15 ball-bearing steel (Rockwell C hardness 60-63) with pure nonpolar vaseline as lubricant and with various additives in it. Abrasive wear evidently depends on the kind and the concentration of additives in the lubricant, there existing an intermediate optimum range between insufficient and excessive concentrations for each. Abrasive wear also depends on the surrounding gas, as clearly demonstrated by tests in air, an oxidizing atmosphere, and in inert pure argon. The dependence on these factors was also studied on friction of St-45 plain carbon steel against 40Cr alloy steel (Rockwell C hardness 50-52). Wear of these and many materials (cast irons, steels, Al, Ni, TiN) in industrial machinery and in experimental laboratory friction pairs was reliably measured by the methods of x-ray spectrum and Auger spectrum analyses. Figures 6; tables 1; references 9.

Numerical and Experimental Study of Plane Ice Field and Cylindrical Pile Interaction

917F01971 Moscow *IZVESTIYA AKADEMII NAUK SSSR: MEKHANIKA TVERDOGO TELA in Russian*
No 6, Nov-Dec 90 pp 179-183

[Article by V.I. Danilenko and S.I. Rogachko, Moscow]

UDC 539.3

[Abstract] A broad experimental study was made concerning interaction of a plane ice field and a cylindrical pile, the procedure consisting of the following successive steps: 1) cutting a rectangular block of ice (1 m thick, 8 m square base) from a natural ice field by means of a saw

tool mounted on a bulldozer, 2) pressing this block to the lower edge of the ice cap with the aid of a vertically mounted hydraulic cylinder and then rotating it through a 45° angle, 3) removing the vertical force exerted by the cylinder on the block so that the latter would remain pressed to the cap by the force of buoyancy alone, 4) extracting from the thus produced artificial basin lumps of ice and freezing them at subzero temperature so as to form a plane field. The test apparatus consisted of a truss bridge across the basin and a carriage moving across the basin along a track on the bridge with a cylindrical pile dipping vertically into the basin fastened to the floor of this carriage. Over a period of several days and depending on the weather, a plane ice field was forming naturally in the basin. Upon its buildup to the thickness required for testing, a free ridge formed ahead of the pile was cut off. The readings of load and displacement transducers were recorded on oscillograms by a light-beam oscillograph throughout the test period. Specimens of still ice were sampled from the basin after the experiment, for a determination of their physical and structural characteristics. Compressive strength was measured under an axial load acting in one test perpendicularly to the freeze-on plane and in one test parallel to it. Tests for flexural strength and the critical stress concentration factor as indicator of resistance to cracking were performed on smooth bars and on notched ones. Two successive experiments were performed in a 7x6 m² large basin at approximately the same temperature, an ice cap being cut with a cylindrical pile 416 mm in diameter at a speed of about 10 mm/s: a 110 mm thick ice cap in the first test and a 150 mm thick ice cap in the second test several days later. A theoretical study of ice cap fracture under such conditions was made on the basis of a mathematical model for numerical analysis of the process by the method of finite elements. The results indicate an appreciable change of the stressed state upon formation of a crack, stress concentration along a peripheral crack causing tension zones to form along the lateral surfaces of the ice wedge. When the tensile stresses exceed the tensile strength of ice, then these zones may become the site of lateral cracks leading to normal breakoff. The authors thank staff members from the Departmental Scientific Research Laboratory for Industrial Hydrological Off-Shore Oil and Gas Exploration Equipment at the Institute of Maritime Construction Engineering imeni V.V. Kuybyshev who participated in the experiments, also R.V. Goldshteyn and N.M. Osipenko for assistance in designing the method. Figures 3; references 5.

Flexure of Polygonal Plate with Circular Center Hole and Two Straight Notches of Unequal Lengths

917F0197H Moscow *IZVESTIYA AKADEMII NAUK SSSR: MEKHANIKA TVERDOGO TELA in Russian*
No 6, Nov-Dec 90 pp 173-179

[Article by S.A. Kuliyeu, Baku]

UDC 539.3

[Abstract] A homogeneous isotropic plate of uniform thickness h is considered which has the shape of a regular polygon, specifically a regular hexagon, and has a circular center hole with two narrow rectangular notches of unequal lengths cut diametrically toward any two opposite corners of that hexagon. The problem of its elastic equilibrium under various loads is solved not conventionally by mapping the doubly-connected region S onto a concentric annulus but by the simpler method of determining this region S section of the plate in the median plane, where two analytic functions satisfy given boundary conditions. This method is applied to a plate under a load consisting of a distributed transverse force q , moments at the edges, and bending forces $p(S)$. The particular solution w_1 to the equation $\Delta\Delta w = q/D$ ($D = Eh^3/12(1-\nu^2)$ denoting the cylindrical stiffness, ν - Poisson's ratio) has presumably been found, the stress intensity coefficient and the deflection function w are to be calculated. As the first special case is considered pure flexure of such a plate under constant bending moments at both outer and inner edges only. As the second special case is considered such a plate under a force uniformly distributed over the edges of the hole and the two notches only. The two formulas for the deflection w agree exactly with the corresponding Timoshenko formulas (S.P. Timoshenko and S. Voinovskiy-Krieger, "Plates and Shells", Izd. Nauka, 1966). For comparison is also considered an elliptical plate with a center hole and two diametral notches along its major axis under a bending moment uniformly distributed over the elliptical periphery only, the edges of its hole and two notches being free. Figures 1; references 10.

Stability of Steady Rotations of Symmetric Gyroscope Filled With Liquid

917F0197A Moscow IZVESTIYA AKADEMII NAUK
SSSR: MEKHANIKA TVERDOGO TELA in Russian
No 6, Nov-Dec 90 pp 4-9

[Article by V.V. Rumyantsev, Moscow]

UDC 531.383

[Abstract] Steady rotations of a heavy body with a fixed point in a uniform gravitational force field are analyzed, as such a body being considered a gyroscope of arbitrary shape but with the center of gravity on one of the principal axes of inertia and with a cavity completely filled with a viscous homogeneous fluid which moves together with the body as an integral part of it. The orientation of this entity in a system of coordinates $O\xi\eta\zeta$ with the origin O at the fixed point, $O\xi$ being the vertical axis, is defined in terms of three Euler angles: θ (nutation), ψ (precession), and φ (rotation proper). Inasmuch as projection k of the angular momentum onto the vertical axis $O\xi$ remains constant over the entire rotation period, because the moment of the gravitational force with respect to this axis is zero, therefore the condition for steady rotation is $[dW] = 0$ with every fixed $k = k_0$

of that constant ($W = k_0^2/2J + \Pi$, Π - potential energy, J - moment of inertia with respect to the ξ -axis independent of angle ψ). This condition yields all steady axes in a Cartesian system of coordinates $Oxyz$ and their geometrical locus. The angular velocity about any of these axes aligned with axis $O\xi$ is $\omega = k_0/J_0$ (J_0 - moment of inertia with respect to that particular axis). Moreover $\Pi = Mgay_3$ and $J = Ay_1^2 + By_2^2 + Cy_3^2$, where $[g <] \inf i$ ($i = 1, 2, 3$) denote the cosines of angle which axis $O\xi$ forms with axes Ox , Oy , Oz respectively ($\gamma_1 = \sin\theta\sin\varphi$, $\gamma_2 = \sin\theta\cos\varphi$, $\gamma_3 = \cos\theta$), Mg being the weight of the body and $a = z_0 > 0$ being the altitude of its center of gravity. The condition for stationarity of function $W(\gamma_{1,2})$ is expressed as a system of two nonlinear equations for the first-order derivatives $\delta W/\delta\gamma_1$ and $\delta W/\delta\gamma_2$ respectively. The system of three equations for the second-order derivatives $\delta^2 W/\delta\gamma_1^2$, $\delta^2 W/\delta\gamma_2^2$, $\delta^2 W/\delta\gamma_1\delta\gamma_2$ then yields the sufficient conditions for stability of rotations with respect to angle θ , generalized velocities θ^* , ψ^* , φ^* , and kinetic energy T_{rot} in accordance with Moiseyev-Rumyantsev theorems 6 and 7 (N.N. Moiseyev and V.V. Rumyantsev, "Dynamics of Body with Cavities Containing Fluid" Part 1, Izd. Nauka, 1965) stating that function W must have an isolated minimum and any perturbed motion sufficiently close to it must approach, asymptotically in time, a steady rotation of the mechanical system as a single body. Two special cases are considered, the first one being such a gyroscope with the center of gravity at the fixed point. The second case is such a gyroscope whose ellipsoid of inertia coincides with the ellipsoid of rotation about the Oz axis and whose center of gravity lies on that axis. Figures 1; references 4.

Refinement of Theory of Flat Shells

917F0197F Moscow IZVESTIYA AKADEMII NAUK
SSSR: MEKHANIKA TVERDOGO TELA in Russian
No 6, Nov-Dec 90 pp 139-146

[Article by V.V. Vasilyev and S.A. Lurye, Moscow]

UDC 539.3

[Abstract] The three-dimensional equations of the theory of elasticity for homogeneous orthotropic shells are reduced to two-dimensional equations for flat homogeneous orthotropic shells on the basis of physical hypotheses. This is done by expanding displacements $U(x_1, x_2, x_3)$, $V(x_1, x_2, x_3)$, $W(x_1, x_2, x_3)$ of any point on the normal to the median surface (Ox_1 and Ox_2 axes in the two principal directions, Ox_3 axis in the direction of the outward normal) into $u_0(x_1, x_2) + x_3 u_1(x_1, x_2) + \sum u_i(x_1, x_2) v_i(x_3)$ ($i = 2, \dots, I$), $v_0(x_1, x_2) + x_3 v_1(x_1, x_2) + \sum v_j(x_1, x_2) \theta_j(x_3)$ ($j = 2, \dots, J$), $w_1(x_1, x_2) + \sum w_k(x_1, x_2) \psi(\inf k(x_3))$ ($k = 2, \dots, K$) respectively. Functions u_0 , v_0 , w_1 correspond to translations of the normal as a solid body in x_1, x_2, x_3 directions respectively and functions u_1, v_1 correspond to its rotations about the x_2 axis and the x_1 axis respectively. The series terms, usually in Legendre polynomials, describe deformation of the normal and the resulting fundamental stressed-strained state, functions

u_i, θ_j, ψ_k being stipulated and functions u_i, v_j, w_k to be determined from that system of two-dimensional equations. According to this theory, a shell element of finite thickness (x_3 coordinate) but infinitesimally small length and width (x_1, x_2 coordinates) has $(I+1) + (J+1) + K$ degrees of freedom. The corresponding equations of balance are obtained by application of the principle of virtual displacements. Multiplication of the three-dimensional equations by the corresponding approximating functions and subsequent integration of the products over the shell thickness, taking into account the appropriate boundary conditions, yield those equations of balance for the fundamental state and also for higher-order states. Calculation of stresses and strains is then formulated as a variational problem for its solution in displacements, whereupon the stationarity condition for the Lagrange functional (minimum of functional) in variations is reduced from "triple integral - double integral = 0" to "double integral + double integral of the sum of three finite ($2, \dots, I, 2, \dots, J, 2, \dots, K$) series = 0". The new two-dimensional theory is regarded as being consistent with respect to energy, if the variational equations which that stationarity condition yields coincide with the earlier derived equations of balance and if that stationarity condition yields natural boundary conditions of zero displacements at constrained edges and zero stresses at free edges. A theory consistent in this sense is then constructed for the fundamental state and for higher-order states. As an example is considered an axisymmetric isotropic cylindrical shell freely supported at both ends and under a internal pressure sinusoidally distributed along its lateral surface. References 12.

Exact Solution to Problem of Flexure for Semiinfinitely Large Plate Totally Bonded to Elastic Medium Occupying Half-Space

917F0197D Moscow IZVESTIYA AKADEMII NAUK
SSSR: MEKHANIKA TVERDOGO TELA in Russian
No 6, Nov-Dec 90 pp 112-123

[Article by N.G. Moiseyev and G.Ya. Popov, Odessa]

UDC 539.3

[Abstract] Under consideration is a plate of finite thickness ($-h \leq z \leq h$) but semiinfinite width ($0 < x < +\infty$) and infinite length ($y < +\infty$) with one surface totally bonded to an elastic medium which occupies the upper half-space ($x > -\infty, y < +\infty, z > 0$) and its edge $x = 0$ otherwise free, this plate being loaded in flexure by longitudinal and transverse as well as normal forces distributed over its free other surface. The problem is to determine effective action on the plate and contact stresses at its boundary with the medium. The problem is formulated as a system of integrodifferential equations with a stress column-vector on the left-hand side and a displacement column-vector on the right-hand side. Following a Fourier transformation with respect to y , the problem is reduced to the Riemann problem. In order to solve the latter, it is necessary to factorize its matrix

coefficient $G(t)$. This is done, whereupon the factorizing matrix $G_0(z) = T(z)X_0(z)$ is put in the canonical form for solution of the Riemann problem. The original problem of flexure is then solved for given zero boundary conditions, which reduce it to a system of linear algebraic equations for the vector of unknown coefficients C_j on the right-hand side $\sum C_j f_j(x)$ ($j = 0, \dots, 4$). From the solution are obtained expressions for the bending moment on such a plate under a longitudinally distributed vertical load. References 16.

Asymptotic Analysis and Refinement of Timoshenko-Reissner Theories on Plates and Shells

917F0197E Moscow IZVESTIYA AKADEMII NAUK
SSSR: MEKHANIKA TVERDOGO TELA in Russian
No 6, Nov-Dec 90 pp 124-138

[Article by A.L. Goldenveyser, Yu.D. Kaplunov, and Ye.V. Nolde, Moscow]

UDC 539.3

[Abstract] Application of the asymptotic Timoshenko-Reissner to flexure of plates is considered, this being a $[O(\eta^{4-4q}) = 0]$ theory which takes into account transverse shear and rotational inertia. Its differential equations are constructed so that the stressed-strained state of elastic thin bodies such as shells and plates can be split into internal and peripheral states, which makes it possible to integrate these equations by two separate iteration processes when the integration interval is rather narrow. This asymptotic $[O(\eta^{4-4q}) = 0]$ is first compared with the asymptotic $[O(\eta^{2-2q})]$ a very slight modification of the Kirchhoff-Love theory. When applied to static flexure of isotropic plates, both theories are shown not to rigorously require introduction of two-dimensional quantities such as forces and moments as well as linear and angular displacements of the median plane for a three-dimensional stress and strain analysis, which also the Kirchhoff-Love theory does not require. They are introduced, however, for comparing the asymptotic Timoshenko-Reissner theory with Timoshenko-Reissner engineering theories based on physical hypotheses. Boundary conditions for differential equations describing the internal stressed-strained state in this, as in any other asymptotic theory, are stipulated so as to ensure exponential decay of the boundary layer. Solutions to static boundary-value problems of flexure obtained by the "Kirchhoff equation + two reduced boundary conditions" scheme and by the "equation of Timoshenko-Reissner engineering theory + three boundary conditions" scheme should be numerically very close for the region of a plate far from the edges, no higher precision evidently being attained by satisfying one more boundary condition. The advantage of Timoshenko-Reissner engineering theories over the Kirchhoff-Love theory thus lies not in higher precision but only in the variational formulation of boundary conditions. For a comparison with the asymptotic Timoshenko-Reissner

theory, one may assume that "redundant" integral in its differential equations has been eliminated and their order thus reduced to one not higher than the order of those of the Kirchhoff-Love theory. It then becomes evident that the $[O(\eta^{4-4q}) = 0]$ precision of its differential equations is higher than the $[O(\eta^{2-2q}) = 0]$ precision of reduced boundary conditions and than the $[O(\eta^{1-q}) = 0]$ precision of canonical boundary conditions. For dynamic flexure of plates is constructed a two-dimensional asymptotic $[O(\eta^{4-4q}) = 0]$ theory which includes initial conditions and in which the homogeneous resolvent equation has been refined by raising the precision of the operator of reduced normal inertia, most expediently done by Lurye's symbolic method (A.I. Lurye, PRIKLADNAYA MATEMATIKA I MEKHANIKA Vol 6 Nos 2-3, 1942). This is demonstrated on a numerical example of a plate with an index characterizing dynamicity of flexure not larger than index q characterizing variability of the stressed-strained state. Tables 1; references 29.

Reconstructing Image of Defect From Scattered Wave Field in Acoustic Approximation

917F0197C Moscow IZVESTIYA AKADEMII NAUK SSSR: MEKHANIKA TVERDOGO TELA in Russian No 6, Nov-Dec 90 pp 79-84

[Article by I.I. Vorovich and M.A. Sumbatyan, Rostov-na-Donu]

UDC 539.3

[Abstract] The problem is to reconstruct the contour L of an unknown cavity existing in an elastic medium from the wave field scattered by it, assuming that either only longitudinal or only transverse waves can propagate through the medium. In this approximation the problem reduces to the simplest inverse problem of diffraction for the scalar wave equation. It is formulated in the two-dimensional approximation for a body in an acoustic medium and a plane incident wave $p_0 = e^{ikx}$ (k - wave number), only stellar regions being considered so that the contour of the body can be described parametrically in a polar system of coordinates: $p(\varphi)$ (φ - angular coordinate). The boundary condition at the contour is $p|_{\leq} \inf L = 0$ for an acoustically soft one and $\delta p / \delta n|_{\leq} \inf L = 0$ for an acoustically stiff one, a soft contour being considered here. The integral representation of the scattered field $F(\varphi)$ contains two unknown functions $g(\theta)$ and $p(\theta)$ of the scattering angle θ , which need to be determined. The operator $D^{-1}: F(\varphi) \rightarrow p(\theta)$ of this inverse problem cannot be continuous, because the operator $D: p(\theta) \rightarrow F(\varphi)$ of the straight problem is, and therefore this inverse problem is ill-conditioned in the Tikhonov sense. It is also a nonlinear problem, but can be solved iteratively by the numerical method of steepest descent. Adaptability of the regularization algorithm to a nonlinear problem like this is ensured by smoothness of the functional and its being a quadratic one in the vicinity of its minimum. The algorithm is constructed by rewriting the expressions for $F(\varphi)$ and $g(\theta)$ in a finite-dimensional form at nodes φ_i, θ_j of the grid ($\varphi_i = \theta_j$) and using the quadrature relation for rectangles. This algorithm is then extended

to more difficult situations such as scattering (diffraction) of plane waves successively incident at different angles. Figures 3; references 17.

Three-Dimensional Motion of Elastic Bodies

917F0197B Moscow IZVESTIYA AKADEMII NAUK SSSR: MEKHANIKA TVERDOGO TELA in Russian No 6, Nov-Dec 90 pp 55-66

[A.F. Ulitko, Kiev]

UDC 539.3

[Abstract] Three-dimensional motion of elastic bodies with attendant nonuniform and time-dependent bulk deformation is analyzed, considering a strained state accurately enough described a linear Cauchy tensor and assuming absence of kinematic constraints. The nonlinear theory for this case is simplified, not being completely linearizable even for small strains which satisfy linear Cauchy relations. The simplest description of such a motion is described most simply, according to the Trefftz-Hamel-Kappus elasticity theory of finite displacements (R. Kappus, ZEITSCHRIFT DER ANGEWANDTEN MATHEMATIK UND MECHANIK Vol 12 No 5, 1939). On this basis are derived two theorems pertaining to motion of the center of mass and to change of momentum under applicable boundary conditions, each reducing a volume integral of the respective vector into a surface integral of a force vector in accordance with the Gauss-Ostrogradskiy equality. With absolute motion of an elastic body then represented as the sum of transport motion (translation plus momentary rotation) and relative motion, first the Lamé equations of elasticity and then the Euler equations of motion for this case are thus partially linearized prior to their solution by integration for appropriate initial conditions (zero initial conditions if the body was at standstill and undeformed at time $t = 0$). Figures 1; references 11.

Motion of Two Parallel Circular Cylinders in Viscous Fluid in Field of Acoustic Wave

917F0197G Moscow IZVESTIYA AKADEMII NAUK SSSR: MEKHANIKA TVERDOGO TELA in Russian No 6, Nov-Dec 90 pp 158-164

[Article by A.N. Guz and A.P. Zhuk, Kiev]

UDC 533.6.013.42

[Abstract] Motion of two parallel circular cylinders one behind the other in a boundless viscous fluid in the direction of an acoustic wave propagating through this fluid is analyzed, the cylinders having generally unequal radii. The acoustic wave is described in a rectangular global system of coordinates $Oxyz$ with the origin at a point half-way between the parallel axes of the two cylinders, the Ox axis in the direction of wave propagation crossing those two axes at right angles, and the Oz axis half-way between those two axes running parallel to them. The average force of the wave field acting on the surface of each cylinder is calculated by time-averaging the hydrodynamic force $F_{1,2}$, this force being expressed

as a surface integral of the stress tensor $\sigma = (-p + \lambda' \operatorname{div} v)E + 2\mu'e$ (p - acoustic pressure, v - velocity vector, e - strain rate tensor, E - unit tensor, μ' - dynamic viscosity, $\lambda' = -2\mu'/3$). The velocity field is $v = \operatorname{grad} \Phi + \operatorname{grad} \Psi_1$, the potentials Φ and Ψ_1 of the resultant velocity field being calculated by solving the diffraction problem for a plane wave and two free cylinders. Solution of this problem involves integration of two equations, one for each potential in a triply-connected region, for the boundary condition $v = U_{1,2}$ ($U_{1,2}$ - linear velocity of respective cylinder due to action of that hydrodynamic force) at the surface of each cylinder and for conditions of radiation at infinity. This problem is formulated in two cylindrical local systems of coordinates, one for each cylinder with the origin on its axis. The problem was solved numerically for two circular cylinders in propanol (density 0.7854 g/cm³ at 20°C) and an acoustic wave propagating with a velocity amplitude of 1247 m/s. Figures 4; references 5.

Density Distribution in Pulsed Gas Jets Flowing Into Rarefied Medium

917F0201J Novosibirsk ZHURNAL PRIKLADNOY MEKHANIKI I TEKHNIЧЕСКОY FIZIKI
in Russian No 6, Nov-Dec 90 pp 123-127

[Article by A.V. Yeremin and I.M. Naboko, Moscow]

UDC 534.202.2

[Abstract] The density distribution in pulsed gas jets discharging into a rarefied medium is described by analytically fitting experimental data. Experiments were performed with axisymmetric jets in media under a high vacuum of the order of 10^{-5} mm Hg and with an electron beam scanning them across chords in a given cross-section. An analytical relation is established between absorption reading and gas density at any point, in an either Cartesian or polar system of coordinates. The radial distribution of absorption readings is shown to fit the function $F(r) = ce^{-br^2}$ for $r \leq R$ and $F(r) = 0$ for $r > R$ (R -radius of jet). The sensitivity threshold of measuring instruments is introduced in the form $\Delta = ce^{-br^2}$, so that $r_{\max}^2 = \log(c/\Delta)/b$. Accordingly, for $r_{\max} < R$ the radial density distribution in a jet is then $\rho(r) = c(b/\pi)^{1/2} e^{-br^2}$. The two parameters c and b are evaluated by the method of least squares, whereupon an analytical smoothing function is also introduced. A comparative evaluation of experimental data on quasi-steadily flowing jets of various gases reveals that, when discharging into vacuum, a jet of a heavier gas (argon) ranges farther than a jet of a lighter gas (nitrogen). Figures 4; references 8.

Effect of Phase Transitions on Propagation of Sound Through Fog: Theory and Experiment

917F0201A Novosibirsk ZHURNAL PRIKLADNOY MEKHANIKI I TEKHNIЧЕСКОY FIZIKI
in Russian No 6, Nov-Dec 90 pp 27-34

[Article by D.A. Gubaydullin and A.I. Ivandayev, Tyumen]

UDC 532.529:534.2

[Abstract] Propagation of sound through a fog is analyzed for the effect of phase transitions on its attenuation, fog being essentially a binary medium consisting of air with two water phases: vapor and liquid droplets. Theoretical analysis is based on Nigmatulin's model of a two-velocity three-temperature continuum and the Hertz-Knudsen-Langmuir relation for the intensity of nonequilibrium condensation at the interphase boundary, assuming an acoustically homogeneous monodisperse suspension of water droplets in an air-vapor mixture. The equations of one-dimensional motion during phase transitions are linearized and, together with the equations of mass, energy, and momentum conservation, formulated in a system of coordinates relative to which the unperturbed mixture remains at a standstill. The attenuation of sound due to phase transitions with attendant mass transfer by diffusion is evaluated in accordance with Gubaydullin's dispersion relation. The decrement over one wavelength is shown to depend on the frequency as well as the phase velocity of sound and also nonmonotonically on the weight fraction of vapor in air, being maximum when the latter is approximately 10% of the saturation level (when droplets begin to form in pure vapor) under any pressure within the 0.1-1.0 MPa range and that maximum depending neither on the weight fraction of droplets in the mixture nor on the accommodation coefficient. Most strongly attenuated is sound of a frequency somewhat above the reciprocal of the characteristic time of nonequilibrium vapor-droplet interphase heat and mass transfer at a surface temperature not equal to the phase equilibrium temperature. The results of this analysis are compared with available experimental data, the latter being found to fall within the range of theoretical ones covering the 0.04- ∞ range of the accommodation coefficient. Figures 3; references 12.

Effect of Entropic Sublayer on Stability of Supersonic Shock Layer and Laminar-to-Turbulent Transition of Boundary Sublayer

917F0201E Novosibirsk ZHURNAL PRIKLADNOY MEKHANIKI I TEKHNIЧЕСКОY FIZIKI
in Russian No 6, Nov-Dec 90 pp 74-80

[Article by V.I. Lysenko, Novosibirsk]

UDC 532.526

[Abstract] An experimental study concerning the flow of a shock layer past a flat plate with a bevel front edge has yielded significant data on the effect of such a front edge on the stability of flow in the entropic sublayer and on the stability or laminar-to-turbulent transition of the boundary sublayer. Experiments were performed in the T-325 wind tunnel at the Institute of Theoretical and Applied Mechanics (Siberian Department, USSR Academy of Sciences), its test segment having a 200 mm square cross-section. A steel plate 5 mm thick, 200 mm wide, and 450 mm long was placed in the tunnel at a zero

angle of attack, its long lateral edges rigidly constrained and its nose sloping at a 20° angle. The front edge of the nose was beveled perpendicularly to the active plate surface, the length of the bevel being varied over the 0.1-10 mm wide range. The stagnation temperature of the stream was about 200 K and the temperature of the plate surface was equal to the recovery temperature of the stream. Measurements were made with a TPT-4 d.c. thermoanemometer and with wire transducers (tungsten wire 6 μm in diameter and 1.5 mm long). Other instruments included a U2-8 narrow-band amplifier, a V6-9 narrow-band microvoltmeter, and a GZ-112/1 signal generator, also a total-head Pitot tube and a GRM-2 recording manometer. Supplementary experiments were performed in the T-326 wind tunnel, with a 5 mm thick but 70 mm wide and 163 mm long steel plate. Its nose sloped at a 7° angle, with an either 0.1 mm or 1.5 mm long bevel of the front edge. Flow patterns were visually observed with a "Strioscope" shadowgraph and recorded with a "Zenit-V" photographic camera. In this T-326 wind tunnel were also measured pressure fluctuations at the plate surface, quartz pressure transducers having been mounted flush with that surface and feeding signals to a "Kistler 5006" charge amplifier. Here the quiescent velocity of the intruding gas stream was $N_{\text{Ma},\infty} = 6$ and its stagnation temperature was 423 K, its quiescent Reynolds number $N_{\text{Re},\infty}$ per unit length being varied over the $(11-57) \times 10^6 \text{ m}^{-1}$ range. The data reveals that lengthening the bevel builds up the entropic sublayer and thus destabilizes not only perturbations within it but eventually also fundamental-mode perturbations within the boundary sublayer, the entire shock layer then becoming destabilized. The author thanks A.D. Kosinov and G.P. Klemenkov for assistance. Figures 5; references 32.

Transient Processes in Free Pack Following Sudden Loss of Pressure During Gas Filtration

917F0201F Novosibirsk ZHURNAL PRIKLADNOY MEKHANIKI I TEKHNIЧЕСКОY FIZIKI
in Russian No 6, Nov-Dec 90 pp 80-89

[Article by V.A. Antipin, A.A. Borisov, and A.P. Trunev, Novosibirsk]

UDC 532.529.5

[Abstract] An experimental study was made concerning propagation of modulated rarefaction waves through packs in a 1.8 m long vertical shock tube with a 6 cm inside diameter. A diaphragm at half-height, mounted between flanges split the shock tube into an upper part serving as the high-pressure chamber and a lower part serving as the low-pressure chamber. A pack partly filling the 0.9 m long lower cylinder to a 0.75 m level acted as a piston under the 15 cm wide clearance separating it from the diaphragm, with the air here under a pressure of 1 atm. Tests were performed with a pack of cement (bulk density 0.985 g/cm^3 , grain 7 μm grain diameter) and with two packs of $\gamma\text{-Al}_2\text{O}_3$, one fine (bulk density 1.188

g/cm^3 , 50 μm grain diameter) and one coarse (bulk density 0.732 g/cm^3 , 2500 μm grain diameter, sintered). The pressure in the upper cylinder was varied over the 0.11-0.26 MPa range, three piezoelectric pressure transducers of an original design with a 1 Hz - 100 kHz frequency range and a 0.5 s time constant having been installed here 36, 54, 72 cm respectively above the diaphragm. Their output signals were fed through an amplifier and then an analog-to-digital converter to an Elektronika-60 microcomputer for processing. Sudden rupture of the diaphragm produced a pressure pulse with a steep leading edge and a mild trailing edge in the lower cylinder. Owing to the high density of the two-phase porous pack (powder and air mixture), it took a much longer time for the rarefaction wave to penetrate through the pack than for the shock wave to traverse the entire low-pressure chamber. Owing to rereflection of the shock wave at the top surface of the pack under the clearance, the pressure drop the pack was found to be almost harmonically modulated and the rarefaction front to become smoother while the amplitude of perturbations decreased. A characteristic feature of rarefaction waves in the fine-disperse packs was their low propagation velocity. For a theoretical interpretation of the results, propagation of a rarefaction wave through a pack is described by equations of dynamics of the heterogeneous Nigmatulin-Goldshtik model (R.I. Nigmatulin, "Dynamics of Polyphase Media" Part 1, Izd. Nauka, 1987; M.A. Goldshtik, "Transfer Processes in Granular Bed", Institute of Thermophysics, Siberian Department, USSR Academy of Sciences), three ordinary differential equations in the isothermal approximation. These three equations are supplemented with three relations characterizing isothermal flow, continuity of the gaseous medium, and incompressibility of the solid material. A slight velocity unbalance between the two phases of the gaseous powder concentrate is considered first, assuming that the thin pack-air interface is a light and rigid piston and that the duration of the pressure pulse is quite long. Those equations of the heterogeneous model then reduce to a single equation which, in the limiting case of the diameter of solid pack particles approaching zero, reduces to an equilibrium model. On the basis of this equation is now solved the problem of a piston in a cylinder. The problem of sound attenuation in a pack is solved on the basis of the original Nigmatulin-Goldshtik nonequilibrium model. The authors thank M.I. Gorbunov and O.V. Shapeyeva for assistance given in physical and numerical experiments. Figures 5; tables 2; references 10.

Relaxation Characteristics of Turbulent Shear Flow in Wake of Transversely Oriented Cylinder Near Plate

917F0201C Novosibirsk ZHURNAL PRIKLADNOY MEKHANIKI I TEKHNIЧЕСКОY FIZIKI
in Russian No 6, Nov-Dec 90 pp 61-67

[Article by V.I. Kornilov and D.K. Mekler, Novosibirsk]

UDC 532.526.4

[Abstract] Experimental data on turbulent nonequilibrium shear flow in the wake of a transversely oriented

circular cylinder within the boundary layer at a flat plate are interpreted in accordance with Hinze's relaxation equation (J.O. Hinze, ZEITSCHRIFT DER ANGEWANDTEN MATHEMATIK UND MECHANIK Vol 56 No 10, 1976). Experiments were performed in the T-324 low-turbulence subsonic wind tunnel at the Institute of Theoretical and Applied Mechanics (Siberian Department, USSR Academy of Sciences) with a 6 mm thick and 993x2500 mm² large rectangular plate placed horizontally in the test segment of that tunnel. A cylinder was placed across the plate at a distance of about 600 mm from its front edge and thus within the fully developed turbulent boundary layer. Cylinders of various sizes were used so that the ratio of cylinder diameter D to boundary layer thickness δ (10.6 mm under the cylinder) could be varied discretely over the 0.113-0.388 range. Their vertical distance y_0 from the plate surface was varied over the 0.094-0.94 range of boundary layer thickness. Reliable comprehensive velocity measurements made with a DISA instrument set have yielded data consistent with calculations made on the basis of Prandtl's theory, also using Prandtl-Klauser and Boussinesq's models. An analysis of the results reveals that the relations between the turbulence parameters and the vertical mean velocity profile within the region of nonequilibrium flow in the boundary layer are governed by kinematic similarity, but not quite so within the central core of that boundary layer. A single expression is accordingly found to cover the relation $v_t/v_e D = f(y/\delta_{0.999})$ (v_t - kinematic eddy viscosity, v_e - velocity at upper edge of boundary layer, y - vertical distance from plate surface, $\delta_{0.999}$ - boundary layer thickness to the distance y above the plate surface where $v/v_e = 0.999$) and Hinze's relation $L_x^* = a\Delta x$ for the longitudinal relaxation length to be valid here. Figures 5; references 12.

Axial Compression of Nonhomogeneous Cone

917F0201H Novosibirsk ZHURNAL PRIKLADNOY MEKHANIKI I TEKHNIЧЕСКОY FIZIKI
in Russian No 6, Nov-Dec 90 pp 115-118

[Article by M.A. Zadoyan and N.B. Safaryan, Yerevan]

UDC 539.376

[Abstract] Axial compression of an infinitely long cone by a concentrated force acting at its apex is analyzed, assuming that the material of the cone is an incompressible nonhomogeneous one subject to power-law strain hardening with a fractional power exponent. The analysis is based on the corresponding system of three partial differential equations of balance, in a spherical system of coordinates with the origin at the apex. Boundary conditions of zero stresses along the generatrix and zero axial velocity as well as zero shearing stress along the axis reduce the problem to compression of a fictitious conical body with a spherical base at equilibrium and the system of equations to a fourth-order nonlinear ordinary differential one. This equation is then reduced

to a system of four first-order differential equations and the corresponding boundary-value problem is solved numerically for the purpose of stress distribution analysis. A solution was obtained by the ranging method on a Standard System 1022 computer for a cone dehomogenized by a flux of elementary particles, by temperature gradients, by surface treatment, or by nonuniform strain hardening of the material. The stress distribution is compared to that of a similar homogeneous cone under axial compression. Figures 1; references 3.

Interaction of Vibration Relaxation and Dissociation Reactions During Supersonic Flow of Viscous Gas Past Blunt Body

917F0201B Novosibirsk ZHURNAL PRIKLADNOY MEKHANIKI I TEKHNIЧЕСКОY FIZIKI
in Russian No 6, Nov-Dec 90 pp 55-60

[Article by A.G. Tirskiy and V.G. Shcherbak, Moscow]

UDC 533.6.011

[Abstract] Supersonic motion of a blunt body through atmospheric air neither chemically nor thermodynamically at equilibrium is analyzed for the effect of thermodynamic nonequilibrium and attendant dissociation reactions on the vibration relaxation of body particles and on the characteristics of air flow past the body, vibration relaxation being slow because of the low density of air. The analysis is based on Navier-Stokes steady-state equations and takes into account the structure of viscous shock at the body surface, but ignores effects of longitudinal molecular mass transfer. Five components of air (N_2 , O_2 , N , O , NO) are considered to participate in dissociation-recombination and exchange reactions within the region of perturbed flow. The boundary conditions at the body surface, assumed to be noncatalytic, are those of impermeability, adhesion, heat balance, and heterogeneous recombination reactions. The effect of vibration relaxation on the dissociation reactions is manifested in the dissociation rate constant $K_D(T, T_v) = L_D(T)V(T, T_v)$ (K_D - dissociation constant at thermodynamic equilibrium at vibrational temperature $T_v = T$), according to the CVD model (P. Hammerling, J.D. Teare, and B. Kivel, PHYSICS OF FLUIDS Vol 5 No 4, 1962) where the multiplier $V(T, T_v)$ depends on the probability $F(v)$ of transition of molecules from vibrational levels to a continuous spectrum. The effect of vibration relaxation on the dissociation reactions was evaluated accordingly, using the Marrone-Treanor relation (P.V. Marrone and C.E. Treanor, PHYSICS OF FLUIDS Vol 6 No 10, 1963) for that transition probability $F(v) = \exp[-(E_D - E_v)/kU]$ (E_D - dissociation energy, E_v - energy of vibrational level, U - parameter of temperature dimension characterizing the degree of predominance of transitions from upper levels over transitions

from lower ones). The effect of dissociation reactions on the vibration relaxation was evaluated according to the CVDV model (C.E. Treanor and P.V. Marrone, PHYSICS OF FLUIDS Vol 5 No 9, 1962), using the Milliken-White relation with Park's high-temperature correction (C.A. Park, AIAA Paper No 1730, 1984) for the vibration relaxation time in a mixture of gases. Figures 5; references 17.

Effect of Reflected Particles on Flow of Gas With Suspended Particles Past Blunt Bodies

917F0201D Novosibirsk ZHURNAL PRIKLADNOY MEKHANIKI I TEKHNICHESKOY FIZIKI
in Russian No 6, Nov-Dec 90 pp 67-74

[Article by Yu.M. Davydov, I.Kh. Yenikeev, and R.I. Nigmatulin, Moscow]

UDC 532.529

[Abstract] Flow of a gas with suspended particles past blunt bodies is regarded as motion of two interpenetrable continua and analyzed on the basis of a three-velocity three-temperature model which takes into account reflection of particles by the body back into the suspension. As a specific example is considered transverse flow of a gaseous suspension past a flat plate. Particles are assumed not to collide with one another so that randomization of their motion can be ignored. Such a flow and attendant processes are described by six partial differential equations: two equations of continuity and two equations of motion, one of each for the gas and one for the particles, one equation of total energy of the mixture, and one equation of internal energy of the particles. The system is closed by two equations of state for the gas and the particles respectively. The aerodynamic drag coefficient is expressed in terms of Reynolds and Mach numbers and particle volume concentration, the force of friction between gas and particles being proportional to it. Interaction of incident and returning particles with the moving gas is expressed in terms of an effective force so as to take into account phase transition of the $3 \rightarrow 2$ kind. The system of partial differential equations was integrated numerically by the method of large particles with first-order precision. The results are found to differ by not more than 3-5% from those obtained by integration in space and time. They are found to differ by not more than 10-15% from available theoretical data on flow of a two-phase stream past a wedge and available experimental on flow of a two-phase stream past simple bodies. Figures 6; references 17.

Comparison Between Two Patterns Collision of Counterflowing Jets With Different Values of Bernoulli Constant

917F0201G Novosibirsk ZHURNAL PRIKLADNOY MEKHANIKI I TEKHNICHESKOY FIZIKI
in Russian No 6, Nov-Dec 90 pp 97-101

[Article by N.N. Lukerchenko, Moscow]

UDC 532.522

[Abstract] Collision of two jets with different values of the Bernoulli constant is considered, in which case the classical flow pattern with a critical point cannot be realized. It is demonstrated that in this case the stagnation zone shrinks infinitely down to a point rather than to finite limiting dimensions and not further as the pressure p_0 in it approaches the stagnation pressure p^* . The pattern of flow from the stagnation zone correspondingly changes into one with a cusp on the boundary line, which represents a flow reversal. For the purpose of proving this, flow from the stagnation zone is replaced with reverse flow by reversing the velocity vector at every point. The problem then becomes one of collision of two jets counterflowing along a straight solid wall. Following a conformal mapping of their complex potentials and of their Joukowski functions into parametric half-spaces, the problem is solved for three characteristic parameters: 1) ratio of their widths at infinity, 2) ratio λ of their velocity heads $(1/2)pv^2$ at infinity, 3) pressure coefficient $\kappa = (p - p_0)/(1/2)pv^2$, ranging from 0 to -1, referred to the jet a with smaller velocity head. The solution is analyzed for its behavior as $\kappa \rightarrow -1$, when $\lambda = 1.1$ and when $\lambda = 1$, and found to indeed describe a stagnation zone shrinking to a point when the $\lambda > 1$ (jets with unequal velocity heads). The author thanks L.I. Sedov and V.P. Karlikov for interest and helpful discussions. Figures 4; references 5.

Effective Third-Order Moduli of Elasticity of Composite Materials

917F0201I Novosibirsk ZHURNAL PRIKLADNOY MEKHANIKI I TEKHNICHESKOY FIZIKI
in Russian No 6, Nov-Dec 90 pp 118-123

[Article by V.A. Buryachenko and A.M. Lipanov, Moscow]

UDC 539.4

[Abstract] Macroscopic (effective) second-order and third-order moduli of elasticity of microstructurally non-homogeneous (composite) materials are calculated in the approximation of the geometrically linear theory according to Guz's second variant of small initial strains (A.N. Guz, "Basic Three-Dimensional Theory of Stability of Deformable Bodies", Izd. Vysshaya Shkola, 1986), with the relation between strain tensor and displacement vector components $\epsilon_{ij} = (u_{i,j} + u_{j,i})/2$ and the equation of state relating stress to strain $\sigma = L_{(2)}\epsilon + L_{(3)}(\epsilon \otimes \epsilon)$. The equation of balance ignoring body forces is formulated and on the basis of this theory and standard hypotheses (V.A. Buryachenko, IZVESTIYA AKADEMII NAUK SSSR: MEKHANIKA TVERDOGO TELA No 3, 1987; B.P. Maslov, PRIKLADNAYA MEKHANIKA No 7, 1979), the equation being a nonlinear one with a symmetric del operator. It is linearized, assuming a homogeneous $[\epsilon(x)]$ tensor product $\epsilon(x)$ within the X_α phase, and then reduced to an integral equation for the modified strain $e = \epsilon - q_0$ (q being a

piecewise-constant tensor of rank 2). Calculation of those effective moduli of elasticity $L_{(2)}^*$ and $L_{(3)}$ involves calculating tensors A^* of rank 4, F_1 of rank 6, F_2 of rank 8, and mean strains in tensor components. Calculation of tensor A^* involves solution of the problem for a linearly elastic medium. This tensor has been evaluated numerically by two methods, conditional moments (B.P. Maslov) and effective field (V.A. Buryachenko), for a composite material consisting of an incompressible matrix and rigid spherical equal-size inclusions. Figures 2; references 7.

Long Waves With Finite Amplitude in Polydisperse Gaseous Suspensions

917F0195M Novosibirsk ZHURNAL PRIKLADNOY MEKHANIKI I TEKHNIЧЕСKOY FIZIKI in Russian No 4, Jul-Aug 90 pp 157-161

[Article by N.A. Gumerov, Tyumen]

UDC 532.529

[Abstract] Propagation of long-wave perturbations through a rarefied polydisperse gaseous suspension is analyzed, assuming an arbitrary but low volume concentration of incompressible particles with an arbitrary size distribution in an ideal gas. Inasmuch as the suspended particles are of a material usually heavier than the gas, their weight concentration may range from low to high. The gas is furthermore assumed to be calorifically ideal, its viscosity and thermal conductivity influencing only its interaction with the suspended phase. The analysis is based on Nigmatulin's model of an effective gas (R.I. Nigmatulin, "Dynamics of Polyphase Media" Part 1, Izd. Nauka, 1987) describing propagation of one-dimensional plane waves in the small parameter $\tau/t^* \ll 1$ approximation, i.e., with a characteristic wave period τ much longer than the particle-gas velocity and temperature equalization time. In the first approximation are included both velocity and temperature differences between the gas and the particles, even though these differences are so small on account of $t^* \ll \tau$ that a quasi-steady state with linear laws of thermal and mechanical interphase interactions may be assumed. Particles in suspension are assumed to be spherical and not to interact with one another. The system of ordinary differential equations representing the laws of energy and momentum conservation for the particles and for the gas takes into account velocity and temperature relaxation of particles as well as interphase interaction. It is supplemented with two equations of state for the gas and the particles respectively. The mean density and the mean-mass velocity of the mixture and the diffusion velocities of the two phases are then introduced, which leads to a system of continuity equations. The problem is simplified by limiting the amplitudes of waves to finite ones. Replacement of the variable gas density with the ratio of particle density to gas density reduces this system of continuity equations makes this system of continuity equation reducible from the canonical form

to one equation in Lagrangian coordinates for the dimensionless density. Its linearization for small density perturbations then reduces it to one linear equation in Lagrangian coordinates. The corresponding dispersion relation is found to follow the asymptotic low-frequency convergence of the complex wave number in polydisperse suspensions. Further reduction to Burgers' relation for the wave velocity and further analysis in terms of "effective gas" parameters demonstrate that long perturbation waves propagate through a polydisperse suspensions as they do through a monodisperse one with identical thermophysical properties of both phases and identical radius of the top $a_{5,3}$ -size fraction of particles (N.A. Gumerov and A.I. Ivandayev, ZHURNAL PRIKLADNOY MEKHANIKI I TEKHNIЧЕСKOY FIZIKI No 5, 1988). References 10.

Transient Vibrations of Slim Rod in Elastic Half-Space

917F0195L Novosibirsk ZHURNAL PRIKLADNOY MEKHANIKI I TEKHNIЧЕСKOY FIZIKI in Russian No 4, Jul-Aug 90 pp 134-141

[Article by L.N. Yungerman, Novosibirsk]

UDC 539.3

[Abstract] Vibrations of a slim rod vertically embedded in an elastic medium such as soil occupying the lower half-space and the consequent emission of shear waves by that rod into such a medium are analyzed, this being a problem encountered in construction and in mining. A cylindrical elastic rod with a length-to-radius ratio $L/R \gg 1$ is considered, a rod driven vertically into the soil flush with its free top surface and then excited axially by a vertical harmonic unit-step force $Q(t) = H_0(t) \sin \omega t$ (time, frequency $[g] \gg L/c$, c -velocity of longitudinal waves in rod). Analysis of the transient process is based on the one-dimensional wave model with displacement $V(z,t)$ (z -vertical axial coordinate, r -radial horizontal coordinate) and involves solution of a boundary-value initial-value problem for the following system of three simultaneous differential equations: one equation of balance of forces on an elastic beam and two equations of dynamics of an elastic medium. The boundary conditions are: zero stresses at the free top surface of the soil ($z = 0$) and at the buried bottom base of the rod ($z = L$); rigid contact between the lateral surface the rod and the surrounding soil. Conditions of radiation are stipulated at infinity ($r = \infty$). The initial conditions are zero force and zero velocity at time $t = 0$. The problem is solved, first analytically, following a comparative dispersion analysis of four mathematically simpler models deviating from the exact theory of elasticity (model A): physically adequate model B of deformable medium with one-component displacement vector, model C of medium deformable in pure shear only with one-component displacement vector, models A', B', C' representing the respective plane (two-dimensional) versions. The problem was then solved numerically by the

method of finite differences using the explicit "criss-cross" scheme and the standard Fourier analysis. Calculations have yielded the three parameters characterizing processes in the given system: velocity of longitudinal waves propagating vertically through the rod, velocity of transverse waves propagating horizontally through the soil away from the rod, and wavelength of forced vibrations of the rod. The rod and the soil were characterized by their relevant physical properties (density, modulus of elasticity, shear modulus), the rod also by its geometrical dimensions (length). All the approximate models are found to yield consistent results, which indicate that the attenuation of forced vibrations of such a rod in soil depends on their wavelength as well as on the density and the shear modulus of the soil. The author thanks Kh.B. Tkach for defining the problem and M.V. Stepanenko for helpful discussions. Figures 5; tables 2; references 9.

Comparing Electric Field of Lightning With Electric Field of Glancing Spark

917F0195A Novosibirsk ZHURNAL PRIKLADNOY MEKHANIKI I TEKHNIЧЕСKOY FIZIKI
in Russian No 4, Jul-Aug 90 pp 10-19

[Article by Ye.A. Zobov and A.N. Sidorov, Leningrad]

UDC 537.521+621.391.821

[Abstract] Known theories and experimental data including photographs are shown to demonstrate that the principle of similitude applies to a glancing spark and a lightning, specifically to their electric fields. Tracing the discharge process from development of a leader streamer to closure of the gap reveals analogous conditions for breakdown and analogous breakdown patterns, the principal indicators of that similitude. A glancing spark may, accordingly, serve as a laboratory model for further lightning research and gathering of much needed additional experimental data. The authors thank I.V. Podmoshenskiy for helpfully discussing the implications of the results of this study. Figures 5; references 27.

Model of Interaction of High-Intensity Ion Beam and Metallic Absorber

917F0195B Novosibirsk ZHURNAL PRIKLADNOY MEKHANIKI I TEKHNIЧЕСKOY FIZIKI
in Russian No 4, Jul-Aug 90 pp 26-31

[Article by V.I. Boyko, V.P. Kishkin, N.N. Prilepskikh, and I.V. Shamanin, Tomsk]

UDC 529.124

[Abstract] A mathematical model is constructed to describe exothermic interaction of a high-intensity ion beam and an axisymmetric absorbing metal target. It includes four partial differential equations of hydrodynamics in Euler variables (density of target material ρ , total energy per unit absorber mass $E = \epsilon + W^2/2$, specific

internal energy of absorber ϵ , ion velocity vector W , temperature T , energy released by interaction Q) in a cylindrical system of coordinates plus two algebraic equations of absorber state in terms of pressure and temperature respectively, each a function of its density ρ and specific internal energy ϵ . Inasmuch as the mechanism of ion stopping changes as an ion passes through successive layers of the absorber, each layer being in a different thermodynamic state, the stopping power $(1/\rho)(dE/dx) = S_{be} + S_{fe} + S_{nu} + S_{fi}$ (x -depth coordinate in Cartesian system) of the absorber depends on characteristics of both the incident ion and of the target material (S_{be} -stopping by bound electrons, S_{fe} -stopping by free electrons, S_{nu} -stopping by nuclei of absorber, S_{fi} -stopping by ions of absorber). The stopping power can be calculated either according to Bethe's classical theory for high-energy ions (above 0.1 MeV) with appropriate correction terms for low-energy ions (below 0.1 eV) or according to the combined Bethe-Linhard theory. Calculations made both ways have revealed that stopping by nuclei and ions of the absorber material does not play a significant role in this particular interaction so that Mehlhorn's extension of Bethe's classical relation (T.A. Mehlhorn et al., COMMENTS ON PLASMA PHYSICS OF CONTROLLED FUSION, 1982) for the stopping power is appropriate here. As an example is considered an axisymmetric 50% H^+ + 50% C^+ ion beam with a power density of 1.5×10^{15} W/m² and a Gaussian current density distribution striking a 21 μ m thick aluminum foil (1.5 times thicker than the mean free path of 1 MeV protons in cold aluminum) in pulses of 50 ns duration, its current density rising from 0 to 1.5×10^5 kA/m² during the first 20 ns and remaining constant at that level over the next 20 ns before falling to 0 again within the last 10 ns. The equations of hydrodynamics were integrated numerically according to the method of large particles, in the second-order approximation in space and in the first-order approximation in time. The results indicate that the existence of two different kinds of ions in the beam strongly influences the dynamics of its interaction with an absorber. Figures 3; references 21.

Development Models for Evaluation of Heat Transfer Under Conditions of Supersonic Turbulent Separation Flow

917F0195I Novosibirsk ZHURNAL PRIKLADNOY MEKHANIKI I TEKHNIЧЕСKOY FIZIKI
in Russian No 4, Jul-Aug 90 pp 96-104

[Article by A.A. Zheltovodov, Ye.G. Zaulichnyy, and V.M. Trofimov, Novosibirsk]

UDC 536.24:532.54

[Abstract] An experimental study of heat transfer during supersonic (Mach 2, 3, 4) turbulent separation flow in a wind tunnel inside an Euler chamber was made, with the Reynolds number per unit path length at the entrance varied over the $N_{Re,1} = (30-91) \times 10^6$ m⁻¹ range. The stagnation pressure p^* and the stagnation temperature

T^* were varied over the 200-1540 kPa range and the 255-270 K range respectively. For an evaluation of the heat transfer coefficient, the data are variously interpreted: on the basis of the Zaulichnyy-Trofimov model of such a flow in de Laval nozzles (Ye.G. Zaulichnyy and V.M. Trofimov, *ZHURNAL PRIKLADNOY MEKHANIKI I TEKHNIЧЕСКОY FIZIKI* No 1, 1986), on the basis of the Zheltovodov-Yakovlev model (A.A. Zheltovodov and V.N. Yakovlev, "Development Stages, Structure, and Characteristics of Turbulence in Compressible Separation Flow Near Plane Barriers", Preprint No 27, 1986, Institute of Heat and Mass Transfer, Siberian Department, USSR Academy of Sciences), on the basis of the Kutateladze-Leontyev theory of a turbulent boundary layer and using their asymptotic method (S.S. Kutateladze and A.I. Leontyev, "Turbulent Boundary Layer of Compressible Gas", *Izd. Nauka*, 1962), and also by using Deitch's relation for incompressible flow (M.Ye. Deitch, "Engineering Gas Dynamics", *Izd. Nauka*, 1974). A comparative analysis of the results broadens the understanding of interactions taking place and of the heat transfer mechanism under conditions of supersonic turbulent separation flow. Figures 5; references 10.

Effect of Wave Processes on Viscous-Nonviscous Interaction of Subsonic or Supersonic Jet and Respectively Supersonic or Subsonic Companion Stream in Channel and in Tube

917F0195J Novosibirsk *ZHURNAL PRIKLADNOY MEKHANIKI I TEKHNIЧЕСКОY FIZIKI*
in Russian No 4, Jul-Aug 90 pp 112-117

[Article by I.S. Belotserkovets and V.I. Timoshenko, Dnepropetrovsk]

UDC 533.6.011.6

[Abstract] Interaction of a subsonic or supersonic gas jet discharged respectively into a subsonic or supersonic gas stream in a channel or tube is analyzed for the effect of wave processes, assuming that the gas in both is homogeneous and calorifically as well as thermally ideal. The analysis is based not on Prandtl's boundary layer theory but on the basis of the viscous-nonviscous interaction model. It therefore requires including, already in the first approximation, the effect of the pressure gradient due to viscosity on the nonviscous flow. This is done by adding the authors' system of three simultaneous ordinary differential equations for the pressure in the region of viscous flow and at the boundary of the effective displacement layer, in a cylindrical system of coordinates for two-dimensional flow. Solution of the problem then reduces to simultaneous integration of these and the system of Euler equations. As two examples are considered a subsonic jet in a boundless supersonic stream behind a body and a supersonic jet with a subsonic stream in a channel. The equations of gas dynamics and the equations of the boundary layer were integrated by the method of finite differences, those of gas dynamics

according to MacCormack's scheme and those of the boundary layer according to an implicit scheme in normalized Mises variables. Turbulence was treated on the basis of both the algebraic Prandtl model and the differential model involving one-parametric eddy viscosity. Correct stipulation of boundary conditions, namely zero leakage through channel or tube wall, is particularly important in the case of subsonic jet in a supersonic stream. Figures 7; references 13.

Nonisothermal Separation Flow Past Sphere

917F0195H Novosibirsk *ZHURNAL PRIKLADNOY MEKHANIKI I TEKHNIЧЕСКОY FIZIKI*
in Russian No 4, Jul-Aug 90 pp 91-96

[Article by K.B. Koshelev and M.P. Strongin, Barnaul]

UDC 532.516

[Abstract] Flow of a homogeneous gas stream past a solitary spherical particle is considered, the flow being quiescent far before the particle with a Reynolds number $N_{Re,\infty} \leq 200$ and a Mach number $N_{Ma,\infty} \leq 2$ at infinity. Vapor of the particle material generated by heat transfer from the gas is assumed to have thermophysical properties identical to those of that surrounding gas. The problem is formulated as a two-dimensional axisymmetric one, the flow of the gas being described by Navier-Stokes equations in a spherical system of coordinates with the origin at the center of the sphere. The conditions far from the sphere (radius $r = R_\infty$ and $0 \leq \theta \leq \pi/2$) are those of an unperturbed flow. The boundary conditions on the stern side of the sphere ($\pi/2 < \theta \leq \pi$) are zero gradients of both radial and tangential velocity components, also zero pressure and temperature gradients. The conditions at both axes $\theta = 0$ and $\theta = \pi$ are zero tangential velocity component and thus zero tangential gradient of the radial velocity component, inasmuch as ($v_r = \delta v_\theta / \theta$), also zero pressure and temperature gradients. Conditions of adhesion, namely zero tangential velocity component v_θ , and constant temperature at the surface are assumed for flow with small values of the Knudsen number ($N_{Kn} < 0.015$). Conditions of slippage and temperature jump at the surface are assumed for flow with large values of the Knudsen number ($N_{Kn} \geq 0.015$). For a particle at its boiling temperature the condition of impermeability, namely zero radial velocity component v_r , is replaced with the condition of a finite radial velocity component proportional to the radial temperature gradient and to the mass transfer coefficient. The system of Navier-Stokes equations is supplemented with the equation of state for an ideal gas with temperature-dependent physical properties. All equations are reduced to dimensionless form by normalization of all but two variables to their respective steady-state values, only the radial coordinate being normalized to the radius of the sphere R_s and the pressure of the gas being normalized to the quiescent velocity head at $r = R_{\infty}$. The problem is split into separate physical processes, with heat convection and dissipation accounted

for but implicitly. Each partial problem is then resolved into its directional space components, except the not thus resolvable equations of continuity. All are solved by the method of finite differences using implicit schemes, steady-state solution being obtained by the stabilization method. A numerical analysis of the results reveals a strong effect of evaporation on the separation zone and a strong dependence of the separation characteristics on the Knudsen number. It also reveals a nonmonotonic dependence of the vortex on the Mach number $N_{Ma,\infty}$, its size increasing as $N_{Ma,\infty}$ increases from 0 to 1 and then decreasing as $N_{Ma,\infty}$ increases from 1 to 2. Figures 5; references 17.

Modes of Free Oscillations in System of Four Quasi-Two-Dimensional Vortices

917F0195G Novosibirsk ZHURNAL PRIKLADNOY MEKHANIKI I TEKHNIЧЕСКОY FIZIKI
in Russian No 4, Jul-Aug 90 pp 85-91

[Article by A.M. Batchayev, Moscow]

UDC 532.51

[Abstract] An experimental study of transient processes during development of turbulence in a biperiodic flow of four quasi-two-dimensional vortices originally under steady-state conditions was made, such a flow being related to a Kolmogorov flow. It was simulated inside a rectangular 3 cm high magnetohydrodynamic cell $L_x = 24$ cm long and $L_y = 12$ cm wide resting horizontally on a plexiglas box. This box contained a symmetric pair of 3-pole electromagnets with a power rating of 11 W. The vertical component of magnetic induction in the cell could be approximately characterized by a $B_z(x,y,z) = B_0(z) \sin(2\pi x/L_x) \cos(2\pi y/L_y)$ distribution, its amplitude B_0 increasing almost exponentially in time. The electromagnet coils, connected to a TES-18 stabilized laboratory rectifier, carried a nearly constant current of 1000+/-3 mA. The cell was filled with an electrolyte, 100 g/dm³ aqueous CuSO₄ solution, into which two copper electrodes were inserted through holes in two opposite lateral walls. An electric current of density $j = (0, j_y, 0)$ sent through the cell produced an Ampere force F with an $F_x = j_y B_z / c$ component (ρ - density of fluid, c - speed of light in vacuum) acting on the fluid, a zero F_y component, and a negligible F_z component at least four orders of magnitude smaller than the force of gravity with, moreover, $N_{Re,z}$ about four orders of magnitude smaller than $N_{Re,x}$. The cell was cooled with transformer oil, the temperature being measured by a Cu/Constantan thermocouple and maintained constant within +/-0.1°C by a U10 ultrathermostat during each experiment. The velocity difference between vortices was measured with a thermoanemometer, its two identical MT-54M microthermistors being connected electrically in parallel to an instrument bridge with compensation of their nonlinearity. They were placed in the cell symmetrically with respect to the $y = L_y/2$ plane, 3 cm deep at two points ($x_1 = 7.6$ cm, $y_1 = 1.2$ cm) and ($x_2 = 7.6$ cm, $y_2 = 10.8$ cm).

At these points the Reynolds number varied over the widest range without changing sign and not exceeding $3N_{Re}^*$. The flow pattern could be completely defined in terms of three dimensionless parameters: Reynolds number "referred to the external force" $N_{Re} = (L_x/2\pi)^3(j_y B_0 / \rho c \nu^2)$, bed friction factor $\sigma_0 = (L_x/h)^2$, and geometrical eccentricity $\varepsilon = L_x/L_y = 2$. Readings were taken in nine layers of the fluid, covering the σ_0 range from 122.7 to 1963, and then appropriately processed. Together with oscillograms and photographs, they have yielded data on the primary steady-state flow in such a system and on the excitation of free oscillations. The amplitude of the thermoanemometer output signal A was found to be proportional to the square root $(N_{Re} - N_{Re}^*)^{1/2}$ as long as the difference $N_{Re} - N_{Re}^*$ remained small, the proportionality factor k decreasing as σ_0 increased, and to become an increasingly intricate sinusoidal function of time as the ratio N_{Re}/N_{Re}^* approached 1 with an attendant increase in the harmonic content. The data reveals a frequency shift of free oscillations upon change of the ripple factor, this frequency becoming lower upon excitation of higher harmonics and becoming higher upon decay of higher harmonics with an attendant decrease of nonlinear distortion (klirr factor). This evidently explains why the relative frequency shift becomes smaller as σ_0 increases while the ratio N_{Re}/N_{Re}^* remains unchanged. The author thanks A.M. Obukhov (deceased) for interest, F.V. Dolzhanskiy for discussing the results, and V.M. Ponomarev for assistance in spectrum analysis. Figures 5; references 13.

Dynamics of Condensation Front During Metal Ore Reduction by Laser Beam Under High Gas Pressure

917F0195D Novosibirsk ZHURNAL PRIKLADNOY MEKHANIKI I TEKHNIЧЕСКОY FIZIKI
in Russian No 4, Jul-Aug 90 pp 38-41

[Article by A.G. Gnedovets, Ye.B. Kulbatskiy, S.V. Sekishchev, A.L. Smirnov, and A.A. Uglov, Moscow]

UDC 536.422.4

[Abstract] Reduction of metal ore by a laser beam was studied in an experiment with a pulsed Nd-laser and a WO₃ target under a high-pressure gaseous shield, a condensation front in the form of a jump discontinuity having been found to form within the gas and metal vapor cloud. Laser radiation pulses of 20-50 J energy and 1.5 ms duration were focused by a lens (focal length of 270 mm) onto the target, forming on its surface a spot 2-6 mm in diameter. The radiation intensity was varied over the 1-10 GW/m². The target, a 1 mm thick platelet with a 10x15 mm² surface area, was placed inside a chamber filled with hydrogen after having been scrubbed. The hydrogen pressure was varied over the 0.1-5.0 MPa range. A ruby laser emitting pulses of 0.3 J energy and 20 ns duration with Q-switching was used for

tracking the condensation front by the method of double-exposure holographic interferometry. The holographic interferograms depicting the condensation front dynamics were reconstructed and then processed by numerical methods. They identify three stages of the ore reduction process, heating and vaporization of the target with attendant formation of a gas-vapor cloud and reduction of WO_3 to metallic tungsten extending beyond the duration of an incident laser pulse over a total time of about 150 μs . This first stage is followed by formation of a condensation front beginning about 1500 μs after the radiation pulse and subsequent relaxation over a remaining 2-3 μs long period. Under pressures $p \leq 1$ MPa the condensation front was found to move radially first toward the cloud during the initial fast expansion of the latter and then away from it during its subsequent slow expansion. Under pressures $p \geq 1$ MPa the condensation front was found to move first away from the target during the initial increasingly fast cloud expansion and then toward the target after the velocity of cloud has become equal to the velocity of that condensation front. Figures 4; references 4.

Absorption of Sound Near Semiinfinite Rigid Plane

917F0195F Novosibirsk ZHURNAL PRIKLADNOY MEKHANIKI I TEKHNIЧЕСКОY FIZIKI
in Russian No 4, Jul-Aug 90 pp 53-59

[Article by V.A. Murga, Leningrad]

UDC 534.2:532

[Abstract] Absorption of sound by a viscous compressible medium near a rigid plate is analyzed, considering a nondecaying incident monochromatic sound wave at a low glancing angle $\alpha \ll 1$ and sufficiently far from the edges of the plate so that the latter can be treated as a semiinfinite plane. The problem is thus reduced to a two-dimensional one, but the assumption of plane "reflected" field is necessarily waived. This "reflected" field is calculated in accordance with Kirchhoff's theory, assuming that particles of the fluid in the incident wave oscillate with velocity of a constant amplitude. The corresponding system of four vector equations describing oscillatory motion of its particles in the "reflected" wave is solved for both longitudinal and transverse components of the velocity vector, the integral describing them being transformed into Fourier integrals. Absorption of sound energy in the boundary layer is of particular interest and is evaluated in accordance with the Landau-Lifshits theorem about energy dissipation in fluids, assuming further that absorption of sound energy is due to viscosity of the fluid only. The dissipation coefficient is shown to be $d = k_0(v/2\omega)^{1/2}/\alpha^2 = M k_0 = \omega/c$, (ω - frequency of fluid oscillations, c - speed of sound, v - kinematic viscosity of fluid) for glancing angles covering the $\alpha \leq k_0(v/\omega)^{1/2}$ range, including $\alpha = 0$, and $k_0(v/\omega)^{1/2} \ll 1$. Infiniteness of d

when $\alpha = 0$ does not mean "infinite" absorption, however, but derives from the particular definition of d associated with time-averaging of energy, "dimensional" absorption of sound energy being altogether independent of the glancing angle. Figures 2; references 6.

Experimental Study of Transient Radiation Emission by Jet of Impact-Heated Gas Mixture Containing CO_2

917F0195C Novosibirsk ZHURNAL PRIKLADNOY MEKHANIKI I TEKHNIЧЕСКОY FIZIKI
in Russian No 4, Jul-Aug 90 pp 31-38

[Article by A.V. Yeregin and V.S. Ziborov, Moscow]

UDC 533.906

[Abstract] An experimental study was made concerning transient emission of infrared radiation by pulsed supersonic jets of $\text{CO}_2 + \text{N}_2 + \text{H}_2\text{O}$ -vapor mixtures during their formation stage. Such jets were discharged through a 1 mm wide orifice in a 45 mm wide flat vacuum chamber. This vacuum chamber followed the low-pressure compartment of a shock tube 50 mm in diameter. First the gas mixture was admitted into both the low-pressure compartment and the vacuum chamber, its pressure being varied over the $P_\infty = 1.3$ -26 kPa range. It was then impact-heated by a shock wave returning from the other end of the shock tube, helium gas filling the high-pressure compartment of this shock tube and its pressure being over the 2-5 MPa range. The stagnation temperature and pressure of the jet discharging upon such an impact were varied over the 1500-2500 K and 1-6 MPa ranges respectively. The velocity of an impacting shock wave was measured accurately within 1-2% on two different bases. Radiation emission by such a pulsed jet was measured by way of multichannel emission and absorption spectroscopy, Spectrum System interference filters and FSG-223A photoresistor detectors, all other optical elements being CaF_2 optics. A black body served as reference source, its temperature having been varied over the same 1500-2500 K range and measured with a TRU 1300-2350 tungsten ribbon lamp prior to the experiment for the purpose of calibration. Measurements covered two emission bands of CO_2 : 4.3 μm (4.25-4.65 μm) and 2.7 μm (2.3-3.1 μm). The data have been processed so as to indicate the population temperatures of optically active transitions and thus provide information about the energy distribution over molecules of the discharging gas mixtures, it even being possible to determined the concentration of radiation-absorbing molecules. The results are interpreted on the basis of a three-temperature energy distribution in CO_2 , assuming accordingly a Boltzmann energy distribution in the antisymmetric mode (temperature T_3) and the same Boltzmann energy distribution in both symmetric and deformation modes (T_2) as well as in the translational-rotational mode (T_1). In the first experiment with a $\text{CO}_2:\text{N}_2 = 1:10$ mixture only the vibrational temperatures of all CO_2 modes did not have sufficient time to

adapt to changing flow parameters within the compressed jet zone during the jet formation stage following discharge. In the next with H_2 vapor added and a resulting approximately 8% CO_2 + 86% N_2 + 6% H_2 mixture the vibrational-translational exchanges in all CO_2 modes proceeded much faster while both transient flow and steady flow approached each its equilibrium. A jet compression zone was evidently developing in each case, vibrational-translational and vibrational-vibrational exchanges during the transient period not being at equilibrium and differing appreciably from those in the steady state. They also depended largely on both the gas composition and the jet flow pattern. The vibrational temperatures within this compression zone were much higher during the transient period than in the steady states an relaxation processes proceeded faster in the discharging gas, as indicated by brighter infrared emission "flashes" at the start of jet discharge. The authors thank I.M. Naboko for guidance and E.I. Vitkin for helpful discussion of the results.

Aerodynamics of Apparatus With Stationary Granular Bed

917F0195K Novosibirsk ZHURNAL PRIKLADNOY MEKHANIKI I TEKHNICHESKOY FIZIKI
in Russian No 4, Jul-Aug 90 pp 128-133

[Article by Sh.A. Yershin, U.K. Zhabbasbayev, M.Sh. Kulymbayeva, and L.G. Khadiyeva, Alma-Ata]

UDC 532.546

[Abstract] Steady plane flow of a viscous incompressible fluid through an apparatus with a stationary granular bed in the displacement-type reactor is analyzed by the method of averaging the fluid phase parameters over local volumes of such a porous medium. The corresponding two-dimensional system of two Navier-Stokes equations and a continuity equation then describes flow of a viscous fluid through an isotropic porous medium, these equations becoming also becoming applicable to flow before and behind the bed if the two contiguous are characterized as porous ones but with a porosity $\varepsilon = 1$. Disregarding the inertia terms will reduce this system reduces it to the Brinkman model (H.C. Brinkman, APPLIED SCIENTIFIC RESEARCH Vol A1 No 1, 1947), while disregarding the viscosity terms will reduce it to the Waysman-Goldshtik dynamic model (A.M. Waysman and M.A. Goldshtik, IZVESTIYA AKADEMII NAUK SSSR: MEKHANIKA ZHIDKOSTI I GAZA No 6, 1978). The system can be and has been solved, for appropriate boundary conditions, by the Richards-Crane numerical pressure marching method (C.W. Richards and C.M. Crane, NUMERICAL METHODS IN ENGINEERING Vol 15 No 4, 1980). The results reveal how the flow through such an apparatus depends on its geometry and on the resistance of its bed as well as on the Reynolds number. As an example is considered flow through a metal grid or a stack of them, thin porous media, with that system of equations appropriately modified. Figures 6; references 25.

Jet Flow Pattern of Rarefied Gas Near Surface of Plane Barrier

917F0198E Leningrad VESTNIK
LENINGRADSKOGO UNIVERSITETA, SERIYA 1:
MATEMATIKA, MEKHANIKA, ASTRONOMIYA
in Russian No 4, Oct 90 pp 49-52

[Article by B.F. Pavlov]

UDC 532.525.6

[Abstract] An experimental study of jet flow patterns at flat plates parallel or perpendicular to the direction of flow was made in connection with the design of spacecraft for operation in rarefied atmospheres. Three different nozzles were used for producing free jets, a sonic one (Mach 1) and two supersonic ones (Mach 3, 4.6). The experiments were performed with rarefied air and argon, 300 K stagnation temperature, also with argon heated to 3500 K. They have yielded data on the flow pattern: distributions of both pressure p and tangential stress τ at the barrier surface, including the coordinates of their maxima and also those of the stagnation point. An analysis of these flow patterns in such jets indicates a wide gamut of patterns ranging from a continuous one to a pronounced transitional one, with the Reynolds number $N_{Re,L}$ number in the direction of flow covering the 5.6-120 range. Considering that both density and velocity distributions in such jets of rarefied gas are nearly the same as those in jets of gases relaxing under equilibrium conditions, the gas density ρ_∞ in the free jet is calculated according to an empirical formula based on this similarity. The pressure p and the tangential stress components τ_x, τ_y are calculated according to formulas based on the hypothesis of locality, the coefficients p_1 and τ_0 being functions of the rarefaction ratio and a temperature parameter. The results indicate that, as the Mach number is increased, the maxima of longitudinal distributions (along a plate parallel to the jet) shift farther away from the nozzle and the maxima of transverse distributions (across a plate parallel or perpendicular to the jet) shift toward the plane of symmetry of the flow pattern. Figures 6; references 3.

Accounting for Finiteness of Mach Numbers in Simplest Linear Model of Local Interaction Theory

917F0198A Leningrad VESTNIK
LENINGRADSKOGO UNIVERSITETA, SERIYA 1:
MATEMATIKA, MEKHANIKA, ASTRONOMIYA
in Russian No 4, Oct 90 pp 32-35

[Article by O.A. Aksenova]

UDC 533.6.011.8

[Abstract] Local interaction of a hypersonic stream of a rarefied gas and a convex body is considered in accordance with a linear model which, in a sense, is

Miroshin's model of local interaction (R.N. Miroshin, VESTNIK LENINGRADSKOGO UNIVERSITETA, Ser. 1 No 1, 1987) in the simplest form. It yields linear combinations of parameters p_k and τ_k , which are the coefficients of normal momentum and tangential momentum transfer coefficients respectively. In a somewhat different formulation the vector coefficient p of momentum transfer is resolved into its x and y components $p_x = \sum_{k=0}^l \lambda_k P_k(\cos\theta)$ and $p_y = \sum_{k=0}^{k-1} \mu_k P_k^1(\cos\theta)$ in the rectangular system of velocity coordinates (θ - angle between velocity vector of incident stream and normal to body surface). With the finiteness of a large Mach number taken into account, the two series of aerodynamic coefficients λ_k and μ_k are calculated directly by the Laplace method with asymptotic corrections. The aerodynamic coefficients can also be calculated indirectly on the basis of their relation to the momentum transfer coefficients, the expressions for the latter being the same. References 3.

Optical Methods of Studying Inhomogeneities in Gaseous Media

917F0198D Leningrad VESTNIK
LENINGRADSKOGO UNIVERSITETA, SERIYA 1:
MATEMATIKA, MEKHANIKA, ASTRONOMIYA
in Russian No 4, Oct 90 pp 46-48

[Article by S.A. Meladze]

UDC 535

[Abstract] Classical optical and laser methods of studying perturbations in gaseous media during gasdynamic experiments are reviewed, the classical ones including interferometry, shadowgraphy and schlieren, and high-speed photography. Interferometry based on the Gladstone-Dale law is one method among them suitable for quantitative as well as only qualitative analysis. The advantages of using lasers, typically a He-Ne or ruby laser, rather than a mercury lamp or sunlight are the feasibility of generating narrow light beams in short pulses. It is now technically quite possible to generate laser beams not wider than 10^{-6} m in pulses of not longer than 10^{-9} duration. Particularly interesting and widely used for diagnostic probing of turbulent media and measurement of wave velocities is the laser-Doppler velocimeter. This device operates either with a reference beam or in any of various differential schemes, the Doppler signal being extracted either by photomixing or by direct spectrum analysis and the information contained in this signal then being extracted with the aid of a Fabry-Perot interferometer. It measures velocities ranging from 0 to kilometers per second with an error not larger than 4%. Tables 1; references 8.

Accessible Region for Single-Impulse Flight From Kepler Orbit

917F0198C Leningrad VESTNIK
LENINGRADSKOGO UNIVERSITETA, SERIYA 1:
MATEMATIKA, MEKHANIKA, ASTRONOMIYA
in Russian No 4, Oct 90 pp 42-46

[Article by S.N. Kirpichnikov]

UDC 531.55:521.2

[Abstract] The problem of determining the accessible region for single-impulse flight from a given elliptical Kepler orbit is analyzed in connection with optimization of interorbital flights, assuming that the characteristic impulse velocity is given. The problem is solved by the author's method and accordingly assuming further that the characteristic impulse velocity is smaller than the orbital velocity, which leads to simple explicit equations approximately describing the boundary of the region accessible upon start from an either fixed or arbitrary point on the initial orbit. A material point is considered which moves along a given initial orbit in a Newtonian central-force gravitational field. The region accessible from a fixed starting point is calculated first for the special case where the change-of-velocity (characteristic) vector lies in the plane of the initial orbit, then for the more general case of this vector not lying in that plane, and finally for single-impulse coplanar flight. References 8.

Structural Strength of Steel-Copper Pseudoalloys

917F0194D Kiev FIZIKO-KHIMICHESKAYA
MEKHANIKA MATERIALOV in Russian Vol 26 No 6,
Dec 90 pp 95-99

[Article by V.N. Antsiferov, N.N. Maslennikov, and A.A. Shatsov, Republican Engineering-Technical Center for Powder Metallurgy, Perm]

UDC 621.762:539.4:678.076

[Abstract] The properties of copper-filled powder Cr-Mo steels are analyzed on the basis of experimental data and their theoretical interpretation, the purpose being to establish relations between their structure and strength. Such pseudoalloys were produced by mechanically mixing iron powder with Cr and Mo powders and separately but also mechanically mixing copper powder, sintering the steel compacts at 1200°C in a hydrogen atmosphere (dew point -40°C) for 4 h, then impregnating them with copper powder at 1150°C for 30 min, then quenching the composite compacts from 950°C in water, and tempering them at 500°C or 550°C for 4 h. Five specimens were thus produced, the carbon content in all being within 0.39+/-0.05%. All contained 0.5% Mo, two contained 3% Cr (one also 1% Ni), two contained 5% Cr (one also 1% Ni), one contained 4% Cr + 0.7% Ni. The principal structure of all was found to be sorbitized pearlite with a 170-230 Vickers microhardness, x-ray

spectrum microanalysis further revealing an up to 20% content of each carbide-forming element (Cr, Mo) in the hard phase. Mechanical tests have yielded reliable data on ultimate strength, 0.2% yield strength, and percentage elongation. The ductility of fracture index K_{Ic} and the increment of breaking stress $\Delta\sigma_1$ are calculated with the aid of these data and available copper solubility data, according to formulas for powder metals based on their mechanics of fracture. Lowering the tempering temperature from 550°C to 500°C has, according to these calculations and assuming no change of the 0.2% yield strength, increased the ductility of fracture index by 39 MPa.m^{1/2} and the ultimate strength by 610 MPa. Tables 2; references 12.

Mechanical Strength of VT-22 Titanium Alloy in Various Structural States

917F0194C Kiev FIZIKO-KHIMICHESKAYA
MEKHANIKA MATERIALOV in Russian Vol 26 No 6,
Dec 90 pp 84-69

[Article by V.V. Shevelkov and L.F. Kratovich, In-Plant Higher Technical Educational Institution at "Leningrad Metal Plant", Pskov Engineering Subdivision]

UDC 669.295.017:539.43

[Abstract] An experimental study of the VT-22 high-strength titanium alloy (5.45% Al, 4.85% V, 4.60% Mo, 1.06% Cr, 1.03% Fe, 0.18% Zr, 0.14% Si, 0.14% C, 0.02% O, 0.015% H) was made concerning the effects of various heat treatments on its structure, mechanical properties, and fracture. The first treatment involved standard dual annealing (heating to 820-850°C - holding for 1-3 h - cooling to 750-730°C - holding for 1-2 h, cooling in air) with subsequent aging at 600-630°C for 3-4 h and then cooling in air. This treatment increased the strength but not sufficiently the plasticity of this alloy. The second treatment involved aging at 700-800° for 10-100 h, which ensured adequate plasticity. The third treatment involved thermal cycling (heating into the β -phase range - cooling into the $(\alpha+\beta)$ -phase range - holding - reheating into β -phase range), altogether four such cycles. This treatment resulted in a widening of the separation between yield strength and ultimate strength, indicating an excellent responsiveness after this treatment to strain hardening and stress relief. Structural examination was done under an MIM-8 optical microscope and fractography was performed under an REM-200 scanning electron microscope. Specimens were tested for short-time mechanical characteristics at normal temperature, resistance to cracking under static load, fatigue strength, and V-notch impact strength. The results confirm the relative advantages of each heat treatment. Figures 4; tables 1; references 10.

Classification of Hydrogen Storage Alloys

917F0194A Kiev FIZIKO-KHIMICHESKAYA
MEKHANIKA MATERIALOV in Russian Vol 26 No 6,
Dec 90 pp 38-42

[Article by B.A. Kolachev, Moscow Institute of Aviation Technology imeni K.E. Tsiolkovskiy]

UDC 669.016.6

[Abstract] Hydrogen storage alloys are classified into homologous AB_n series, including the basic AB_n compounds and their derivatives where elements A and B have been gradually replaced by elements A, A' and B', B'', B''' respectively. Particularly noteworthy are the intermetallic compounds $MmNi_5$ (Mm- mischmetal), $Ti_x Fe$, $Ti_{1+x}Fe$, and AB_2 such as ZrB_2 with their substitutional derivatives. The relevant characteristics of each alloy in any series are the maximum hydrogen sorption H/Me and the dissociation pressure at some given temperature, usually measured at 20°C or 50°C. Typical saturation hydrides are $MmNi_5H_{6.3}$ and $LaNi_5H_{6.7}$, their dissociation pressures at 20°C being 1.3 MPa and 0.2 MPa respectively. Replacement of either one basic component A or B with two elements of the same kind in the same amounts as in complex structural alloys yields analogs of the latter, each of these substituting elements playing generally a different role: M' may increase the corrosion resistance and M'' may increase the hydrogen absorption rate. There is no limit as to the number of substituting elements, but in many cases there is no significant advantage gained with more than five of them altogether. A similar stoichiometric composition of hydrogen storage alloys does not necessarily imply similar characteristics, a case in point being the alloys $ZrV_2H_{5.2}$ and $ZrCr_2H_{3.8}$. Tables 1; references 16.

Temperature Fields in Spherisymmetric Multilayer Systems

917F0193E Minsk INZHENERNO-FIZICHESKIY
ZHURNAL in Russian Vol 59 No 6, Dec 90
pp 1024-1026

[Article by Yu.I. Dudarev, M.Z. Maksimov, and L.K. Nikonenko]

UDC 536.21

[Abstract] The nonstationary temperature field in a spherisymmetric system is described by the fundamental first-order partial differential equation of heat conduction for a sphere in an ambient medium. This nonhomogeneous equation is reduced to a homogeneous one by removal of the volume heat source $q_v(r,t)$ (r- radial coordinate, t- time) from the left-hand side. Replacement of the radial coordinate r with a new coordinate $\xi = \int_{r_0}^r dr/\kappa(r)$ (κ - thermal conductivity, an only weak function of ξ) and subsequent separation of variables lead to a second-order partial differential equation with

respect to ξ . Solution of this equation by the Wentzel-Kramers-Brillouin method, assuming $c\gamma \approx \text{const}$ (c -specific heat, γ -density), yields an expression for the temperature field $T(\kappa)$ at any time t and solution of the original equation by the Carslaw-Yaeger-Lykov method yields an expression for the temperature field as a function of time $T(\kappa, t)$. The dispersion equation is then derived for multilayer spheres, the problem being reduced to an eigenvalue problem. The first four eigenvalues have been evaluated numerically for double-layer sphere, for two values of the Biot number $N_{Bi} = \alpha R/\kappa_2 = 0$ or 0.1 (α -coefficient of heat transfer to ambient medium, R -radius of sphere) and $K_a = a_1/a_2 = 10$ or 100 ($a = \kappa/c\gamma$) with each value of the Biot number. Tables 1; references 9.

Dielectric Properties of Filled Glass-Ceramic Material

917F0193C Minsk INZHENERNO-FIZICHESKIY
ZHURNAL in Russian Vol 58 No 6, Dec 90 pp 962-968

[Article by V.V. Novikov, L.N. Tartakovskaya, Yu.P. Trizna, M.V. Dmitriyev, and T.N. Mishchenko, Odessa Polytechnic Institute]

UDC 537.226.1

[Abstract] A material consisting of $\text{BaO-SiO}_2\text{-ZnO}$ glass-ceramic and $\alpha\text{-Al}_2\text{O}_3$ powder filler for substrates of electron devices is described, of particular interest being its dielectric properties. These are calculated in accordance with the structural model of this material as one consisting of three phases: initially continuous matrix, growing filler, and interphase layer. During the sintering process a crystalline Ba-SiO_2 phase nucleates at 680°C and vanishes at 850°C , a crystalline $\alpha\text{-BaAl}_2\text{Si}_2\text{O}_8$ nucleates at 720° and remains, whereupon a crystalline interphase $\text{BaO-6Al}_2\text{O}_3$ nucleates at 1100°C and vanishes at 1300°C . First are determined the properties of filler particle clusters in accordance with the average-element model of the aggregation theory. Then are determined the effective properties of the composite material in accordance with the percolation theory. The relative electrical resistivity and dielectric permittivity of the composite material, both referred to those of pure glass, have been calculated by this method for an evaluation of their dependence on the glass weight fraction over its entire range from 0 to 1. The effective electrical resistivity was calculated for a composite material with an either 0.6 or 0.75 filler saturation volume fraction and 0.15-0.30 volume fractions of the interphase layer. Percolating transition is found to theoretically begin when the glass volume fraction reaches about 0.4, and experimental data confirm this. The effective dielectric permittivity of the composite material was calculated with the dielectric permittivity of the interphase layer varied from $\epsilon_{ip1} = \epsilon_0$ to $\epsilon = \epsilon_m$ (subscripts 0,m referring to air and glass matrix respectively). Calculations with ϵ_{ip1}

within the $(0.7-1.0)\epsilon_m$ range are found to yield the closest agreement with experimental data. Figures 3; tables 1; references 3.

Apparatus for Measuring Parameters of Air Streams at Ocean Surface

917F0193D Minsk INZHENERNO-FIZICHESKIY
ZHURNAL in Russian Vol 59 No 6, Dec 90
pp 1005-1011

[Article by S.I. Gavrilovich, S.A. Levchenko, and S.I. Shabuna, Institute of Heat and Mass Transfer imeni A.V. Lykov, BSSR Academy of Sciences, Minsk]

UDC 533.6.08

[Abstract] The principle of an acoustic anemometer for measuring the parameters of air streams at the ocean surface is explained, of most concern being determination of the vertical thermal flux and the horizontal frictional shearing stress. According to preliminary estimates, measurements covering the 0.01-20 Hz range of energy carrier frequencies at a wind velocity of 10 m/s should extend over a volume of 0.5 m cubed, readings should be taken over a period not shorter than 2000 s, and the data sampling frequency should be at least 40 Hz. The advantages of such an acoustic instrument and specifically an ultrasonic one are its fast response, insensitivity to the ambient temperature, and suitability for measuring the vertical velocity component of low wind velocities. It actually measures the time taken by a sound wave to travel from the transmitter-transducer to the receiver-transducer, considering that the wind velocity vector can be resolved into two components respectively parallel and perpendicular to the common axis of both transducers. The frequency of the sound wave must be lower than 100 kHz so as to ensure minimum absorption by the ambient medium and higher than 20 kHz so as to remain above the frequency range of turbulence and acoustic atmospheric noise. Such an instrument has been built for the 40-60 kHz optimum operating frequency range, with two UZP-2 microphones. These are capacitive transducers with a 100 ± 15 pF rating, a $4 \mu\text{m}$ thick polytetraphthalate membrane metallized on both sides each. They operate under a d.c. bias of 200 V and, with a negative electric voltage pulse of 5 μs duration, are excited into resonance. The output signal of the transmitter microphone output signal decays within 5-10 pulse periods, but not before reaching the receiver microphone. A wideband preamplifier on the receiver side compensates stray capacitances and boosts the signal. The anemometer has a time resolving power of 2×10^{-7} s. It was calibrated in a wind tunnel over the 2-50 m/s velocity range, a correction factor $K_1 = V_{\text{true}}/V_{\text{meas}} = 1.369 \pm 0.015$ having accordingly been added for measurements in longitudinal air streams and another correction factor $K_2 = 0.127 \sin^2 2\varphi + 1.061$ having been appropriately added to account for the dependence of time readings on the angle of attack φ . The final anemometer error does not exceed 3%. The instrument

can be connected to a microcomputer for data processing. This was done with the aid of an Elektronika NMS 1100.1 microcomputer for for an additional calibration aboard a ship, against a conventional MS-13 cup-type anemometer, over the 1-2 m/s velocity range. The instrument should be very useful for air stream studies in the South China Sea. Figures 4; references 4.

Thermal Expansion of Polycrystalline SiC and Nonreproducibility of Its Linear Dimensions

917F0193B Minsk INZHENERNO-FIZICHESKIY
ZHURNAL in Russian Vol 59 No 6, Dec 90 pp 958-961

[Article by A.M. Tolkachev, V.A. Tits, and G.K. Kladov, Institute of Low-Temperature Engineering Physics, UkSSR Academy of Sciences, Kharkov]

UDC 536.413:546.281'261

[Abstract] An experimental study of polycrystalline SiC was made concerning its suitability for optical devices operating over a wide low-temperature range. Its coefficient of linear thermal expansion and nonreproducibility of its linear dimensions in 280-20-280 K cooling-heating cycles were measured, several cylindrical rods 25 mm in diameters and 100 mm high having been cut from one ingot and tested without any prior special heat treatment. All specimens were first tested in a dilatometer for thermal nonreproducibility of its linear dimensions, their nominal length having been established at 280 K temperature. They were then cooled down to 20 K at a rate of 1 K/min under a vacuum of the order of 0.001 Pa in the dilatometer, for subsequent measurement of the coefficient of linear thermal expansion during reheating to 280 K. After the first cooling and reheating cycle the relative change (decrease) of their length was of the order of 10^{-5} , but after the second and third cycles their length was found to have decreased much more. Only after the fourth cycle did their relative change of length stabilize again and remain within 5×10^{-7} after further cycling, the measurement error not exceeding $\pm 2 \times 10^{-7}$. The data have been extrapolated to 300 K for a definitive determination of the temperature dependence of linear thermal expansion, the relative change of length on this basis found to increase from -2.823×10^{-4} at 20 K to -0.513×10^{-4} at 280 K and then decrease to obviously 0 at 300 K. Figures 2; tables 1; references 3.

Transverse Flow of Two-Phase Stream Past Cylindrical Heat Exchanger Surface

917F0193A Minsk INZHENERNO-FIZICHESKIY
ZHURNAL in Russian Vol 59 No 6, Dec 90 pp 917-923

[Article by N.A. Kudryavtsev, M.V. Mironova, and V.P. Yatsenko, Institute of Energy Conservation, UkSSR Academy of Sciences, Kiev]

UDC 532.529.5

[Abstract] Steady laminar flow of a gas stream with particles in suspension transversely past a horizontal cylindrical heat exchanger is analyzed following a numerical experiment on the basis of a mathematical model accounting for Magnus and Saffman forces as well as thermophoresis, gravity, and aerodynamic drag. The model, which for steady laminar flow of an incompressible fluid past a circular cylinder yields a circulation zone whose width is proportional to the Reynolds number, is based on Navier-Stokes and energy equations in natural variables in a polar system of coordinates for an infinitely long cylinder. The original system of these equations in divergence form was transformed into a system of difference equations according to Leonardo's third-order approximation scheme. Calculations were made for three values of the Reynolds number $N_{Re} = (10^2, 10^3, 10^4)$ and one fixed characteristic value of the Prandtl number $N_{Pr} = (0.73)$, on a grid of 62×100 points with a $\pi/60$ angular step tangentially around the cylinder. Adequacy of the model was confirmed by its satisfying the condition that for flow with attendant heat exchange the Nusselt number be $N_{Nu,F} \approx N_{Re}^{0.5}$ over the entire given range of N_{Re} . Friction at the cylinder wall was calculated by the method of local similitude for $N_{Re} = 10^4$, presumably the critical value of the Reynolds number. This method does not accurately account for development of turbulence behind the cylinder, not of particular concern here, but the error does not significantly influence the results pertaining to flow and heat exchange at the front side of the cylinder with attendant sedimentation of particles on its surface. The motion of particles around the cylinder is described by a system of Lagrange equation in a Cartesian system of coordinates, assuming a uniform initial distribution of particles over the stream far before the cylinder. The calculations have yielded the dependence of the sedimentation constant on the Stokes number, this dependence being characterized by an inflection ranging from a minimum value of the Stokes number below which the probability of sedimentation approaches zero to its maximum value above which the probability of sedimentation approaches unity. The results indicate that, just as in the case of isothermal flow, accounting for all the aforementioned effects increases the value of the sedimentation constant and especially so at low values of the Reynolds number. As the angular velocity of particles increases, moreover, that dependence remains self-similar with respect to that velocity only up to a critical value of the latter. When the angular velocity exceeds the critical, that dependence becomes nonmonotonic and the sedimentation constant decreases as the Stokes number increases. When the angular velocity reaches and exceeds a higher second critical, then the flow of particles around the cylinder becomes asymmetric. The magnitude of this second critical angular velocity depends on both Reynolds and Stokes numbers, also on the physical properties of the gas and the particles. It could not be calculated exactly in this numerical experiment. Figures 3; references 10.

Robot-Based Assembly Center

917F0238B Moscow MEKHANIZATSIYA I
AVTOMATIZATSIYA PROIZVODSTVA in Russian
No 2, 1991 pp 10-11

[Article by Yu.V. Kitayev, candidate of technical sciences]

UDC 621.865.8:621.757.06

[Text] The Tula Polytechnic Institute developed a modular assembly center (Figure 1) for a wide range of products. They installed it at a machine building enterprise. The assembly center, which is based on PUMA industrial robots, is divided into a number of independent functional devices: manipulator, control, information, loading, process adjustment, and end-effector modules.

The manipulator module (Figure 2) consists of a base (1) that holds two RM-012 industrial robots, two tables (3) for the loading modules (cassettes), a base (4) with a rosette (5) for connecting the process adjustment module, and two magazines (6) for the industrial robots' end-effectors.

The process adjustment modules are platforms with dimensions of 400 x 600 mm in a plane. Located on the

platform are the basic equipment and accessories adjusted for assembly operations and one connector assembly plug each. The module to press and flare six booms and mount four bearings and a product case consists of an STK-4 table-model spot riveter, two presses, attachments to trim the flash, electropneumatic

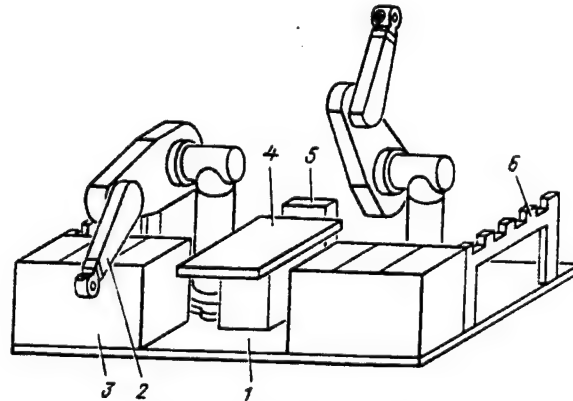


Figure 2. Manipulator Module

Key: 1. base; 2. robot; 3. table for cassettes; 4. support under the platform with the process adjustment; 5. butt-joint subassembly rosette; 6. end-effector magazine

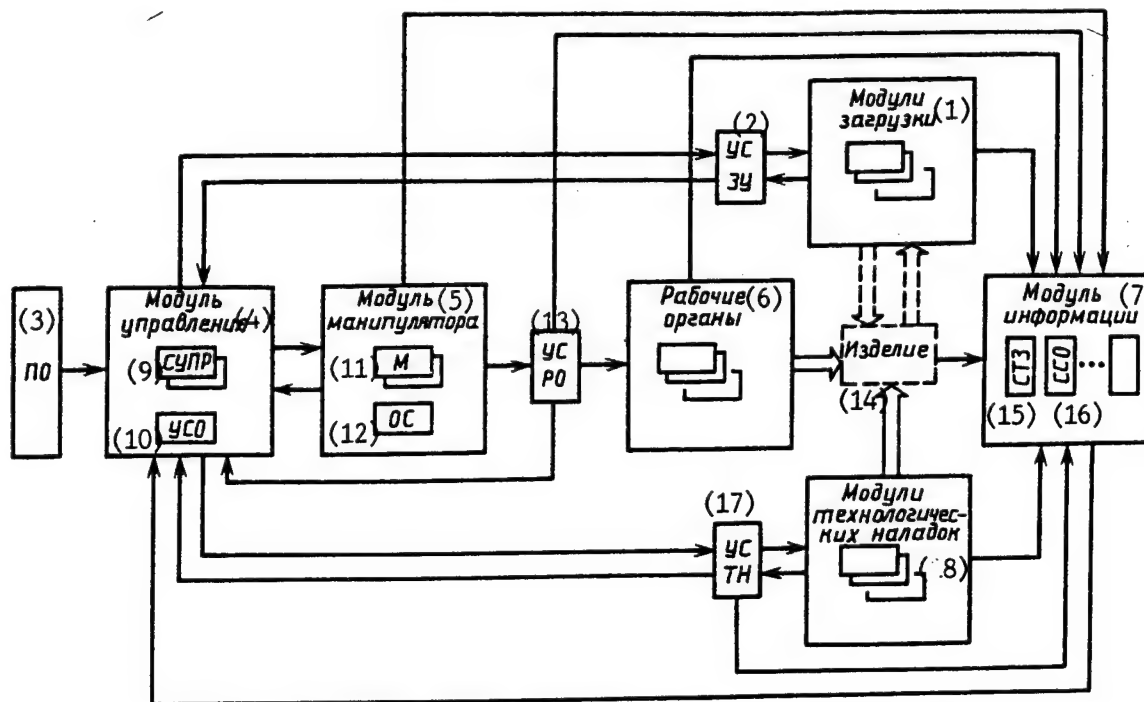


Figure 1. Composition and Structure of the Modular Assembly Center

Key: 1. loading modules; 2. device to connect loading devices; 3. software; 4. control module; 5. manipulator module; 6. end-effectors; 7. information module; 8. process adjustment modules; 9. industrial robot control system; 10. facility interface; 11. manipulator; 12. base; 13. device to connect end-effectors; 14. product; 15. robovision system; 16. force-and-moment sensor system; and 17. device to connect process adjusters

distributors, and a plug to connect to the pneumatic system, electric power supply, and control circuits. The process adjustment modules are portable and can be moved to the assembly center by a hand-operated carriage or robocar. The assembly center can also be further equipped with a unit to store platforms and a device to automatically change them.

The loading modules are cassettes consisting of a standardized case and replaceable inserts under individual assembly components. One case measuring 300 x 400 mm in a plane can hold one or more smaller inserts (measuring 300 x 200 or 200 x 150 mm). The cassettes are transported from the warehouse by hand or by robocar.

The end-effectors are standard gripping mechanisms and special tools (screwdrivers, pincer tongs, devices to apply adhesive, etc.). They are equipped with sensors, including thermometric sensors to sense forces and moments. A KOPR-1 (produced by Nokia in Finland) and supplied by the Granat Scientific Production Association in Minsk is used to connect the industrial robot and end-effectors. The device makes it possible to feed compressed air to an end-effector along three channels and to supply power through 22 contacts.

The information module combines units to process and convert data entering from the end-effector, equipment, attachments, and measuring device sensors. Provisions have been made to connect a robovision system with a stationary inspection television camera and movable camera on a manipulator to the module.

The control module (Figure 3) is created on the basis of two Sfera-36 industrial robot controllers. In addition to controlling the robots, these controllers process input information and issue instructions to peripheral equipment. They also control the incoming information by their switches. This makes it possible to expand the input bus to 64 channels. The manual control and indication unit makes it possible to control the equipment manually by channel-by-channel switches with activation display.

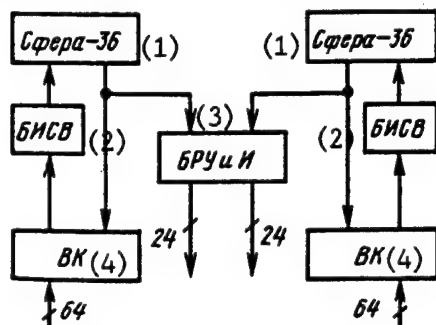


Figure 3. Diagram of the Control Module

Key: 1. Sfera 36; 2. intake status indicator unit; 3. manual control and indication unit; 4. intake switches

The control module also includes a unit to supply power to the various panel circuits.

The assembly center's equipment set is distinguished by its simplicity, and it makes it possible to greatly expand the center's technological capabilities and enables the assembly center to react quickly to any change in the products being manufactured. When necessary, it can easily be built into a higher-level flexible manufacturing system. COPYRIGHT: Izdatelstvo "Mashinostroyeniye", "Mekhanizatsiya i avtomatizatsiya proizvodstva", 1991

The Problem of Developing Domestic Conveyor Building

917F0238C Moscow MEKHAIZATSIIYA I
AVTOMATIZATSIIYA PROIZVODSTVA in Russian
No 2, 1991 pp 12-15

[Article by V.K. Dyachkov, candidate of technical sciences, under the "Mechanizing Industry" rubric: "The Problem of Developing Domestic Conveyor Building"]

UDC 621.867.2

[Text] In the USSR, conveyor building has developed primarily in commercial applications areas such as the following: for the coal recovery industry (the leading organizations being the State Research, Planning, and Design Institute of Coal Machinery Building [Giprouglemash], the Donetsk State Research, Planning, and Design Institute of Coal Machinery Building [Don-giprouglemash], and the Mining Institute imeni Skochinskii); for the baked goods storage and processing industry (the VNIKEIPRIDMASH [not further identified], the TsNIIPROMZERNOPROYEKT [not further identified]); for agriculture (All-Union Scientific Research Institute of the Mixed Feed Industry [VNI kombikormovoy promyshlennosti], VNIIZHIVMASH [All-Union Scientific Research and Technological and Design Institute of Machinery for Integrated Mechanization and Automation of Animal Husbandry Farms], etc.); for enterprises in the metallurgy, power, and chemical industries; for the machine building industry in all its extensiveness; and for the pulp and paper, construction materials, and construction industries (Union Industrial Mechanization State Planning and Design Institute [GPKI Soyuzprommekhanizatsiya], All-Union Scientific Research Institute of Hoisting and Transport Machinery Building [VNIPTMASH], and Conveyor Building Planning and Design Institute [PKI konveyer-stroyeniya]).

The Soyuzprommekhanizatsiya GPKI is involved in developing a wide range of general-purpose conveyers (belt, apron, car, screw, and bucket elevator) that are being series-produced at plants of the Ministry of Heavy Machine Building. The VNIPTMASH is involved in scientific research on continuous-transport machines, and its design section is developing trunk and special-purpose conveyers with boosted parameters on a special-order basis, as well as new machines (vibrating and flight) not included in the product list of the Soyuzprommekhanizatsiya GPKI.

Such has been the historic division of labor in the field of the development of conveyor building in our country.

The VNIPTMASH has in its primary organizational structure a scientific laboratory (department) of conveyers (continuous-transport machines) and design departments in its central design office. Recent years have seen the creation of integrated departments with scientific laboratories and design sectors devoted to machines of a given profile (including conveyers).

The main direction of scientific research at the VNIPTMASH has been exploratory developments; experimental research on machine prototypes; creation of the scientific bases of a theory of designing, making the calculations for, and developing standard materials (type size parameter series, type size lists, engineering design and design methods) for new series of continuous-transport machines and to improve existing machines.

The characteristic distinction and fundamental direction of these scientific works is the conduct of experimental research on prototypes of industrial type sizes of equipment, thus avoiding modeling. This has significantly complicated research processes but has made it possible to obtain immediate reliable results that are suitable practical use.

Experimental prototypes of machines and units (often rather complex) have been manufactured by the experimental plant Krasnyy Blok [Red Block] of the VNIPTMASH.

This brief article cannot possibly examine even a portion of the works that the VNIPTMASH has completed. We will just confine ourselves to listing several characteristic developments with respect to individual types of conveyers.

Vibrating Conveyers

The efficiency and possibility of using vibrating conveyers are determined by the properties of the load being transported; for example, finely dispersed dustlike cargo moves very slowly on a vibrating conveyor and with a low capacity. For this reason, the main theme of the research conducted from 1957 to 1960 was the transportability of granular cargoes as a function of their properties (granulometric makeup, moisture, etc.) and vibration condition (frequency and amplitude of vibrations). Studies were conducted of the transportability of more than 30 different characteristic granular cargoes on troughed one- and two-tube vibrating conveyers with centrifugal and eccentric drives (Figure 1). Experimental cargo transportability coefficients were determined for the chemical, metallurgy, construction, and other branches of industry. Recommendations were developed regarding the vibration parameters (frequency, amplitude, angle of direction, and vibration mode) for different types of conveyor drives and transported cargoes. The coefficient of the adjusted mass of a transportable cargo as a function of vibration mode, which is very important for practical calculations, was established.

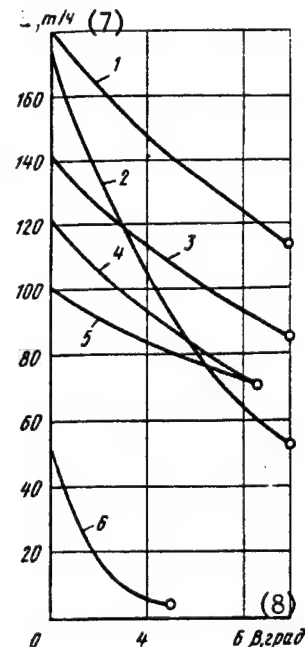


Figure 1. Graphs of the Dependence of the Capacity Q of a Vibrating Conveyor on Its Slope When Transporting Granular Loads

Key: 1. blast furnace slag; 2. sand; 3. coke; 4. clinker, 5. gravel; 6. dry cement

In 1960, original research on the motion of whorled steel chips on a vibrating conveyor with different vibration modes was conducted jointly with specialists from the Automotive Plant imeni Likhachev. The research was conducted by using high-speed filming (a "gun camera" with a speed of 24 to 48 frames per second). The chips moved in a trough with transparent walls. The trajectory of the chips' motion was determined on the basis of a special dimensional grid with rectangular coordinates.

The research conducted in 1961-1963 was used to develop a method of making the calculations for and designing troughed and tube vibrating conveyers and their parameter type size classification. To date, this type size classification has been used to develop and introduce commercial conveyor prototypes.

The Soviet Union's first standard "General-Purpose Vibrating Conveyers" (All-Union State Standard [GOST] 11732-66) was developed jointly with the VNIISTROYDORMASH.

In accordance with the established type classification, the design department of the VNIPTMASH developed a whole array of horizontal vibrating conveyers—single-trough (trough widths of 200, 320, 500, and 750 mm and lengths up to 30 m), two-trough, and single-tube.

A characteristic feature of these structures is their small overall dimensions with respect to height and the lengthwise balance of their vibrating parts.

One prototype vertical conveyor developed was 3.5 m high and had a trough 200 mm wide and an eccentric drive. The conveyers were manufactured in individual batches at the plant Krasnyy Blok and at the Gorokhovets Hoisting and Transport Equipment Plant.

Overhead Conveyers

This work was conducted in close cooperation with the Soyuzprommekhanizatsiya GPKI, the Conveyor Building Planning and Design Institute in Lvov, the Central Design Office for Automation, and the Automotive Plant imeni Likhachev.

Two directions characterize this research. The first direction included the development of the foundations of the theory and methods of calculating the strength and wear of pull chains, rollers, carriage brackets, and other conveyor components. Calculated coefficients for use in making the traction calculations for a conveyor were experimentally determined as a function of operating conditions.

A set of research studies was conducted on cars under conditions of high (up to 300°) temperatures in an original running heating chamber. Theoretical and experimental work was done to further develop the caterpillar drive and several types of traps for the chain designed by the Soyuzprommekhanizatsiya GPKI that were adopted after modification for series production at the Lvov Conveyor Building Plant.

Selected problems of the dynamics of overhead conveyers were researched.

The parametric type classifications of overhead cargo-carrying and push conveyers developed in 1960-1965 have since been fully assimilated in commercial prototypes at the Lvov Conveyor Building Plant. This confirms the correction of the direction taken in developing the type classifications.

The second direction included experimental development of new conveyor models. The first such machines were overhead cargo-carrying and push conveyers with a two-hinged chain ($D = 160$ to 200). Prototypes of it were developed at the Central Design Office for Automation.

Joint tests based on an extensive program on special-purpose conveyers were with the Central Design Office for Automation in 1965-1966.

A characteristic distinction of these machines was the extensive standardization of their equipment and their use of plastics. Research was conducted with regard to selecting the type of plastic for the chain rollers and their useful life. As a result of the test, commercial conveyor prototypes were developed (and manufactured at the pilot-production plant of the Central Design Office for Automation) that later served as the basis for setting up their series production at the Lvov Conveyor Building Plant.

An original design for a carrying and pushing vibrating with a car that had a load-carrying capacity of 500 kg was tested and developed in 1962. This design was created in the Soviet Union first; only much later did it achieve popularity abroad. Its main advantages were a significant savings in the amount of metal used and a reduction in cost coupled with maximal equipment standardization. Its optimal parameters were determined on the basis of tests, and recommendations regarding its applications areas were developed. These conveyers were introduced into industry.

At the request of the Automotive Plant imeni Likhachev, a single-path push conveyor was subjected to joint tests by the design department of the Central Design Office for Automation and the VNIPTMASH in 1959-1960 (no similar designs existed abroad at the time). The originality of the design lay in the fact that a single-path conveyor combines the cargo and traction paths into one path consisting of two channel irons, which reduced the height of the path and the amount of metal used.

Wide-scale introduction of the single-path push conveyor was later halted because the design adopted did not permit extensive standardization along with cargo-carrying overhead conveyers. Series production of two-path push conveyers developed jointly by designers from the VNIPTMASH and the Conveyor Building Planning and Design Institute was set up at the Lvov Conveyor Building Plant.

Flight Conveyers

The theory of moving granular cargoes and a method of making the calculations for and designing a conveyor with submerged and contour scrapers were developed on the basis of extensive tests in 1948-1952 on an original integrated unit consisting of three prototype conveyers with contour scrapers of a commercial type size (a trough width of up to 320 mm). The unit consisted of mutually connected (steeply inclined, Z-shaped, and vertical [i.e., loop]) conveyers operating in a closed-loop cycle with different chain and scraper speeds. No such device had previously existed either in the USSR or abroad.

A theory of moving granular cargoes in a tube flight conveyor with a three-dimensional route was developed (the round scraper moves in a closed standard tube with a round cross section). This theory was tested on an experimental tube flight conveyor unit (tub diameter, 108 mm) with a complex vertical-horizontal route, and coefficients were calculated for a wide list of granular cargoes used in different sectors of industry.

Several commercial prototypes of tube conveyers were developed to transport hot cinder (with water cooling), chemicals used in the paint-and-varnish industry, cast iron chips, and other cargoes. Tube flight conveyers were later introduced into the mixed feed industry. The introduction of tube conveyers with scrapers made of polymer composites and tubes made of ultrastrong glass is especially promising. Our first experiments confirmed the reality of this prospect.

The design department of the VNIPTMASH developed a large set of flight conveyers with low submerged scrapers to transport cold and hot (with water cooling) cargoes for the chemical, metallurgy, food, and other sectors of industry. Trough widths of 125, 200, 320, 500, and 650 mm were used, and capacities ranged from 21 to 280 m³/h. The route was straight, horizontal, and gently or horizontally sloping with a lift angle of 15 to 75°.

Car Conveyers

In 1974, in cooperation with the special laboratory of Kiev Polytechnic Institute, the VNIPTMASH developed and manufactured the Soviet Union's first prototype trunk-type horizontal-closed car conveyer powered by translatory linear induction motors. The moving part of the conveyer received its translatory motion directly from one or two linear motors without reducing gears or clutches. The conveyer's characteristics were as follows: car platform dimensions, 500 x 800 mm; car spacing, 1 m; load-carrying capacity, 200 kg; speed, 1.0 to 2.0 m/s; and maximum capacity, 720 to 1,440 t/h.

The conveyer demonstrated good serviceability when operating with one or two motors simultaneously. The drawback of a linear motor is its low efficiency ($\eta = 0.4$). In the design office's current developments related to linear motors (Kiev), however, new models of linear motors have an efficiency of $\eta = 0.79$, which is complete efficiency inasmuch as the motor transmits its motion without any additional mechanisms.

Also noteworthy among the general theoretical work conducted by the VNIPTMASH is the development in 1970-1972 of the guide material "Klassy ispolzovaniya i rezhimy raboty konveyerov" (Conveyer Use Classes and Operating Modes) as a base for making strength and durability calculations for conveyer elements and for estimating their operating efficiency. These developments were not only of practical value but were also included in textbooks and curricula for higher educational institutions.

Belt Conveyers

Work in the field of belt conveyers should be examined in three directions: improvement of existing designs, development of the theory and normative materials, and creation of new designs.

In the first direction, joint work was conducted with the Soyuzprommekhanizatsiya GPKI. This work dealt with lining drive pulleys and extensive laboratory and commercial tests of various idler designs and with calculating the coefficients of the motion resistance of a belt along idlers. Recommendations were issued on the basis of all results.

The guide technical materials RTM 24.093.04-80, "Osnovnyye trebovaniya k proyektirovaniyu lentochnykh konveyerov s lentoy shirinoy 400-2,000 mm" (Main Requirements Regarding Designing Belt Conveyers With a Belt Length of 400 to 2,000 mm) were

developed and achieved wide-scale popularity. In 1981-1982 this material was used as a basis for compiling general-purpose computer programs to design different types of unified-series belt conveyers on a computer.

In 1983-1984 the VNIPTMASH developed "Osnovy rascheta vysokoproizvoditelnykh magistralnykh lentochnykh konveyerov s lentoy shirinoy do 3,000 mm" (Principles of Designing High-Capacity Trunk Belt Conveyers With a Belt Width up to 3,000 mm).

Between 1946 and 1950 the wide-scale popularization of belt conveyers was held back by a shortfall in the production of rubberized belts owing to a shortage of rubber and cotton pulp fabrics. In view of this, the VNIPTMASH was handed the problem of developing conveyers with a metal belt (continuous steel belts rolled in one piece and wire-and-mesh belts).

Joint research with the Central Scientific Research Institute of Ferrous Metallurgy imeni I.P. Bardin was conducted on commercial prototypes of belt conveyers (belt width, 600 mm; conveyer length, 50 and 16 m) on special running machines. The research resulted in the development of a design, design method, conveyer operating rules, and specifications for manufacturing a one-piece steel belt.

An important design problem was that of selecting the pulley diameters because a steel belt undergoes the greatest stress in the event of sagging on a pulley. According to foreign recommendations, a pulley's diameter should be at least 1,000 to 1,200 belt thicknesses. Given a minimal belt thickness of 1 mm, a pulley diameter would have to be 1,000 to 1,200 mm, which sharply increases a conveyer's overall dimensions. Research on the fatigue strength of a steel belt on running machines made it possible to recommend differential selection of pulley's diameters as a function of the belt loading cycles, i.e., as a function of the conveyer's length and belt's speed. In a number of individual cases, this made it possible to reduce the pulley diameter to 800 mm without reducing the belt's durability.

Development of conveyers with a troughed steel belt on spring-loaded idlers ensuring even buckling of the belt under a load aroused particular interest. A commercial prototype of such a conveyer was developed in 1963 and operated successfully in transporting sand and stone at the Lyubertsy Reinforced Concrete Products Plant.

Research on conveyers with a wire belt made it possible to select the optimal design for a hinge-and-link belt of plane spirals, a method of manufacturing it, and a method of making the calculations for and designing conveyers.

As the shortage of rubberized belts was eliminated, the use of steel one-piece belts became limited to conveyers for the food industry, whereas wire belts became popular

as a conveyor hearth for hardening and tempering furnaces. Series production of conveyers with a metal belt was halted; individual orders were filled on a one-time order basis.

Integrated research was conducted in 1975-1976, and a belt conveyor design with a pliable supporting structure was developed to transport heavy large-piece cargo up to 600 mm in size and weighing up to 500 kg.

Research was conducted on an original experimental conveyor unit with a belt 1,600 mm wide and piece cast iron cargo weighing 500 kg.

From 1959 until the present, the VNIPTMASH has been involved in developing and testing conveyers with an increased slope and equipped with a belt with a fluted surface and corrugated sides and enclosures. The introduction of these machines into industry has proceeded very slowly, however, owing to problems with the shipment of belts by mechanical rubber goods plants. Only one type size of fluted belt designed by the VNIPTMASH with a width of 400 mm is manufactured at the Kursk Mechanical Rubber Goods Plant. A fluted belt designed by the VNIPTMASH and 1,000 mm wide was manufactured in the amount of 6 km at the Kursk Mechanical Rubber Goods Plant. It was installed and is operating successfully on a type 2LN100 inclined-lift conveyor at the Severokuzbassugol [North Kuzbass Basin Coal] First of May Production Association. Now other type sizes of fluted belts are manufactured.

A new original design for a fluted belt has been developed that is better than foreign prototypes. It has not been introduced into industry, however.

Overall, the mechanical rubber goods industry owes a great deal to conveyor building. It has failed to develop and introduce belts with a dirt-repellent working surface (which would sharply improving belt-cleaning conditions, particularly in the case of sticky cargo); belts with an increased friction capacity that would make it possible to reduce the belt's initial and design tension given a constant traction force (Figure 2); belts with interlayerings of high-strength polymers (instead of heavy rubber cable belts); or a number of other types of belts whose introduction would result in a great savings.

A steeply inclined conveyor with a belt 650 mm wide and with corrugated sides and enclosures was developed at the VNIPTMASH in 1988 to mechanize mineral fertilizer warehouses. A commercial prototype was manufactured in 1990.

In 1975-1976 a prototype commercial two-belt conveyor for steeply inclined and vertical transport of granulated fertilizers was developed, manufactured, and tested at the request of the chemical industry. The foundations of its theory and design were developed along with design recommendations. Introduction of the conveyor into industry is being held up, however, owing to the lack of a manufacturing plant.

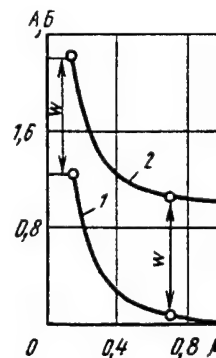


Figure 2. Graphs of the Dependence of the Indicators A (1) and B (2) on the Friction Coefficient μ of the Belt Against the Surface of the Belt Conveyor's Drive Pulley Given a Constant Traction Force W : $A = S_{off}/W = 1(e^{\mu} - 1)$ and $B = S_{on}/W = e^{\mu}/(e^{\mu} - 1)$, where S_{off} and S_{on} are respectively the tensions of the branches of the belt running off of and onto the drive pulley.

The VNIPTMASH has been devoting a great deal of attention to solving the pressing and complex problem of creating long belt conveyers to transport cargoes along a three-dimensional route with a vertical rise and a horizontal turn without reloading.

In 1969 the Soviet Union's first commercial prototype of a multidrive belt conveyor with a main and three intermediate belt drives intended for normal operation in an open pit mine's transport system instead of dump trucks was introduced in an open area at the Tuchkovo Sand and Gravel Open-Pit Mine (Moscow Oblast). It was designed on the basis of a theory developed at the VNIPTMASH and manufactured at the Krasnyy Blok Plant.

Testing and operation of the conveyor (belt width, 800 mm; speed, 1.67 m/s; capacity, 300 to 400 t/h) demonstrated its total serviceability at all times of the year (including winter) given different drive load combinations. The prototype conveyor was accepted by an interdepartmental commission and recommended for commercial production.

In 1972, after development of the Tuchkovo Open-Pit Mine the conveyor was transferred to the Khomyakov Open-Pit Mine (Tula Oblast), where it was installed and is successfully operating and transporting gravel.

In 1980-1985 the VNIPTMASH developed several (Table 1) multidrive belt conveyers to transport coarse gravel at the Rogan Hydroelectric Generating Station [GES]. Most of these conveyers have already been installed and put into operation. All of the conveyers have been installed in an open area without cover.

Table 1. Technical Characteristics of Multidrive Belt Conveyers

Characteristic	KLMK	KLMN	KLM-1	KLM-4
Belt width, mm	1,200	1,200	2,000	2,000
Capacity, t/h	1,100	1,100	4,400	4,400
Belt speed, m/s	2.86	2.86	2.0	2.0
Length of horizontal projection, m	1,280	744	993	1,949
Lift height, m	91	86	73	11.2
No. drives	3	2	3	3
Power of one drive, kW	500	320	800	800
Type of rubberized belt	TK-300	TK-300	TK-400	TK-400
No. belt interlayerings	6	6	6	6

The KLMK conveyor has a three-dimensional route with a turn in a horizontal plane along a 700 m radius and a rise of 91 m. This multidrive curvilinear conveyor, which we were the first to create, has demonstrated good operating results.

In 1987-1988 the VNIPTMASH developed a type size series of intermediate belt drives (belt width, 1,000 to 2,000 mm; drive power, 200 to 1,600 kW; belt speed, 2 to 6.3 m/s) and an engineering method for traction calculations for multidrive belt conveyers with intermediate, main, and idle drives.

Development of the basic set of materials to make the calculations for and design multidrive belt conveyers has been completed.

In 1968-1970 the VNIPTMASH completed a theoretical and experimental study of belt conveyers with a curvilinear route in a horizontal plane and developed a design method and design recommendations.

A design for a curvilinear conveyor has been developed on the basis of a USSR inventor's certificate and patented in the United States, England, France, and West Germany.

Also noteworthy among the design developments of the VNIPTMASH are a system of conveyers with a belt 2,000 mm wide to transport ore in the inclined column of the Artem shaft and a set of technical documentation for an original belt conveyor design for transporting short lengths of wood under the severe northern conditions of pulp and paper combines. Series production of these conveyers has been set up at the Uzlovoye Machining Building Plant.

In 1973 the VNIPTMASH developed the Soviet Union's first unique inclined belt conveyor to feed charge into the throat of the blast furnace at the Krivoy Rog Metallurgy Plant imeni Lenin (belt width, 200 mm; speed, 2 m/s; capacity, 2,000 m³/h; lift height, 86.8 m). The conveyor operates around the clock. On the basis of the first

prototype, the VNIPTMASH developed similar conveyers to feed charge into the blast furnaces of the Lipetsk and Cherepovets metallurgy plants.

All of the conveyers are presently operating successfully to ensure a continuous metallurgical process in the blast furnaces.

In 1981 the VNIPTMASH developed a conveyor to feed charge into a blast furnace at a metallurgy plant in India.

A system of trunk belt conveyers with a total length of about 15 km to transport coal at the Berezovka Section (capacity, 4,500 t/h; belt width, 2,000 mm; speed, 4 m/s; section length, 3.3 km; drive for each section, a main two-pulley drive with two 1,600-kW motors; idle drive, a single-pulley drive with one 1,600 kW motor) was developed and put into operation. The system operates in an unheated gallery with an annual environmental temperature range from +40°C to -40°C.

The most important task for the future is to develop high-speed belt conveyers with a magnetic belt suspension and no idlers. As belt widths increase, idlers' mass and cost increase sharply (Figure 3), and idlers become more complicated to repair and operate. Preliminary research on magnetic belt suspensions conducted at the Kuzbass Polytechnic Institute yielded positive results. This research should be expanded and continued.

This brief list of the main projects conducted shows that the VNIPTMASH has made a noticeable contribution to the development of domestic conveyor building and has the advanced scientific-technical development needed to introduce new machines into industry.

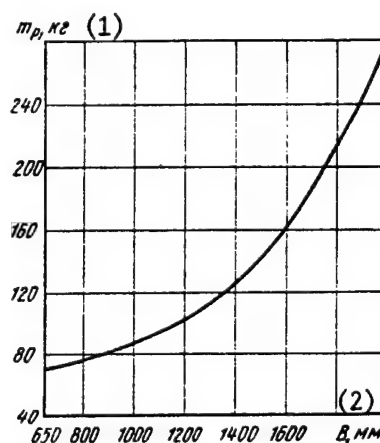


Figure 3. Graph of the Change in the Mass_n of a Three-Roller Idler on Belt Width B

Key: 1. kg 2. mm

The VNIPTMASH is presently devoting a great deal of attention to creating a CAD system to design powerful belt conveyers and applications packages to calculate and optimize equipment parameters.

COPYRIGHT: Izdatelstvo "Mashinostroyeniye", "Mekhanizatsiya i avtomatizatsiya proizvodstva", 1991

Control System for a Multicoordinate Manipulator

917F0238D Moscow MEKHANIZATSIYA I
AVTOMATIZATSIYA PROIZVODSTVA in Russian
No 2, 1991 pp 23-24

[Article by V.A. Muravitskiy and A.V. Melnichuk, engineers]

UDC 681.51/.54;621.7.077

[Text] The Rovno Scientific Research Institute of Machine Building Technology has developed and manufactured a system to control a multicoordinate manipulator by using an inexpensive program controller—a low- or medium-speed controller.

The control system provides numeric position control with the formation of a unit-counting code for the manipulator's drives and control instructions for the basic equipment.

Process control instructions are used to switch the manipulator's actuators (gripping mechanisms, clamps, etc.) on and off and also to control the basic equipment (press, shears, etc.).

The control system developed does not require a branched or high-speed interface with the controller and makes it possible to use simple-to-control drives with type ETA unit-pulse control for a direct-current motor or a BUSH1 for stepping motors.

In the control system, a high-speed counter based on series TTL digital microcircuits performs the function of forming the unit-pulse code of the electric drive.

The unit issues a pulse burst, and the controller K shapes the number of bursts in the required pulse series.

Figure 1 is a schematic of a control system for the drive of one of a manipulator's programmable coordinates.

Control of the motion along this coordinate is accomplished as follows.

The number of pulses in a burst is established in a parallel code by a set-point adjuster and determines the minimal discrete value of movement along the given coordinate (the distance between all of the positioning points should be multiples of the discrete value of the movement).

When the control system is switched on, the controller conditions a "clear" signal, and the code is rewritten

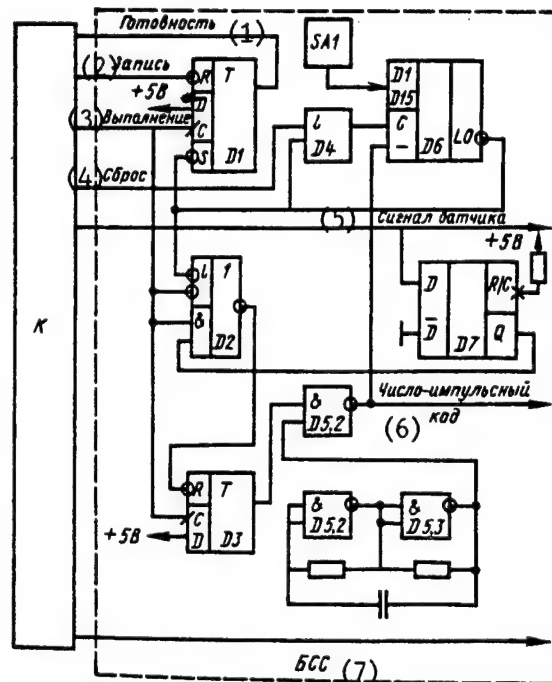


Figure 1. Schematic of the Control System for the Drive of One of a Manipulator's Programmable Coordinates

Key: 1. ready; 2. write; 3. execute; 4. reset; 5. sensor signal; 6. unit-pulse code; 7. high-speed counter

from the set-point adjuster into a four-decade counter D6 (K 155 IY6 microcircuits).

The signal passes through the element D4 to the parallel-load sync inputs D6. On the basis of a "+/-" bus, the controller issues information regarding the direction of the motion and conditions an "execute" signal that enters the control input of the multiplexer D2 (the multiplexer is based on K 155 LA3 and K 155 LR 1 microcircuits) and the sync inputs D, i.e., the flip-flops D1 and D3 (K 155 TM2). Both flip-flops are set in a single state. The signal from the output of the flip-flop D3 opens the AND NOT element D5.1, and the frequency from the generators D5.2 and D5.3 passes to the subtracting input of the counter D6. This same signal is a unit-pulse code for the electric drive. The signal from the output of the flip-flop D1 arrives at the "ready" bus and informs the controller of the beginning of the first pulse burst. The controller shapes a pulse along the "write" bus and resets the flip-flop D1. After the number at the output of the counter D6 has been counted, a signal is conditioned that proceeds to the second input of the AND element of the microcircuit D4, and the code is rewritten into the counter. It also arrives at S, i.e., the input of the flip-flop D1 and again sets it in the 1 state. After having read the "ready" signal, the controller conditions a "write" signal and resets the flip-flop D1.

This cycle is repeated until the total number of pulses in the "ready" bus equals the required number of bursts in the pulse series. After this, the controller picks up the "execute" signal. In this manner, D2 switches to R (i.e.,

the input of the flip-flop $D3$) the signal that has come from the output of the counter $D6$, which continues counting pulses in the last burst.

After the unit has been counted, the signal from the output of $D6$ activates the flip-flop $D3$. The signal from the output $D3$ closes the element $D5.1$. The shaping of a series of pulses in it ceases.

The control system uses an absolute readout system. At the output at beginning of a readout, a signal from the sensor indicating the beginning of a readout arrives at the conditioner $D7$ (K 155 AG3). When an "execute" signal is present, the multiplexer $D2$ switches a short pulse from the output $D7$ to R , i.e., the input of the flip-flop $D3$, thereby halting movement along the coordinate.

A signal from the sensor's output is also fed to the controller's input to inform it of the positioning at the point of the beginning of the readout. The control system is capable of increasing the program-controlled coordinates by proportionally increasing the number of high-speed counter units (one high-speed counter—one coordinate drive). The system is geared toward using a GSP MikroDAT MB57.0 commercial controller (which executes I/O operations in 10 ms) as a program controller. This speed is sufficient to simultaneously control the motion of a manipulator's actuating mechanisms with respect to three coordinates. The number of controllable coordinates can only be further increased by using sequential motion along the coordinates or by using a faster controller.

The control algorithm developed is simple to use and reduces to a minimum the number of operations required to change the sequence of functions executed by the control system.

Figure 2 is a flowchart of the general algorithm, and Figure 3 is a flowchart of the motion control algorithm, which is included in the general algorithm as a subroutine. To control a manipulator it is sufficient to have a set-point adjuster establish the increment of the discrete values of the minimal motion.

The discrete values of the minimal motion divide the manipulator's entire working space into a coordinate grid. The manipulator can only be positioned on points of intersection on the coordinate grid. Data about the coordinates of positioning points, process instructions, and the time requirement to execute them are successively placed in the controller's working memory and may be changed by an operator. After the manipulator has reached its positioning point, the process instruction should be executed. When it is required that several instructions be executed successively without movements, it is necessary to enter the coordinate of one and the same positioning point into memory.

In addition to the aforementioned information, the control system also uses signals from emergency state

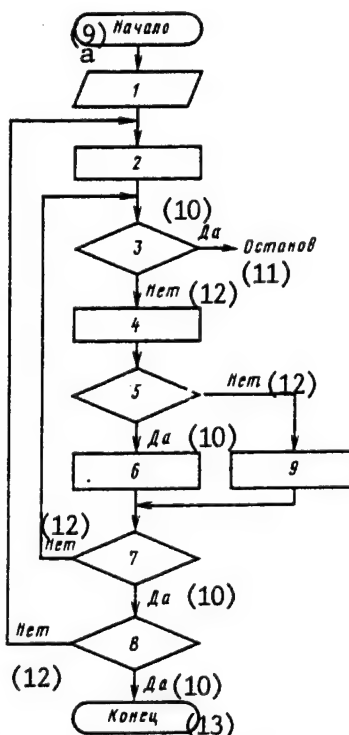


Figure 2. Flowchart of the General Algorithm

Key: 1. input of initial data; 2. initial configuration of condition bits; 3. are there emergency situation signals from the sensors?; 4. transmission of data about one step of motion and initial configuration of program counters to count pulse bursts; 5. is motion occurring?; 6. call to the drive control subroutines; 7. end of a cycle?; 8. end of the control?; 9. formulation of a process instruction; 9a. start; 10. yes; 11. stop; 12. no; 13. end

sensors during its operation. When such signals arrive, the entire system is shut down.

The control algorithm may be executed in two modes: cyclic and one-time. This is determined by the input data or an external signal, which makes it possible to connect the control system for operation with other robotic systems without changing the software.

Technical Characteristics of the System

No. simultaneously controllable programmable coordinates	3
No. positioning points on the programmable coordinate axes	Determined by software
Amount of instruction memory, words	1,903
No. programmable instructions and readouts from basic equipment, at least	104
Programmable time delay, s	0.1-409.5 (every 0.1 s) or 1-4,095 (every 1 s)

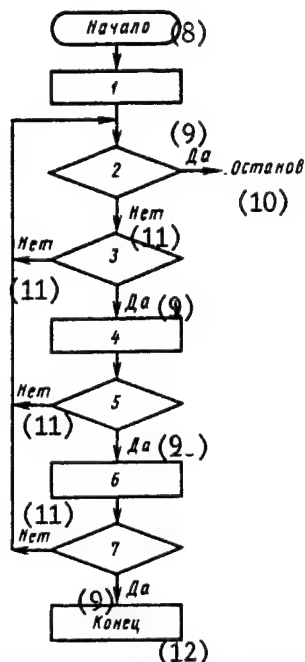


Figure 3. Flowchart of the Motion Control Algorithm

Key: 1. onswitching of the active drives; 2. are there emergency situation signals from the sensors?; 3. are "response" signals present?; 4. a change in the contents of the program counters to count pulse bursts; 5. is the content of the active program counter equal to 0?; 6. offswitching of the inactive drive; 7. have all the drives been switched off?; 8. start; 9. yes; 10. stop; 11. no; 12. end

The system costs 12,500 rubles and results in an annual savings of 15,000 rubles.

COPYRIGHT: Izdatelstvo "Mashinostroyeniye", "Mekhanizatsiya i avtomatizatsiya proizvodstva", 1991

Rotary Automated Assembly Line

917F0238A Moscow MEKHANIZATSIYA I AVTOMATIZATSIYA PROIZVODSTVA in Russian No 2, 1991 pp 5-7

[Article by L.T. Pasholok, I.V. Shchiviyev, and L.I. Bogachev, engineers]

UDC 621.757.62-13

[Text] A rotary automated assembly line has been developed for product assembly under mass production conditions. The line has been designed on the basis of the principle of a process transport flow during which workpiece subassemblies are assembled and inspected as they are transported.

The assembly process consists of the following operations: issuing a cap that has been oriented bottom-down from a vibrating bin and feeding it into the loading rotor,

pressing the cap into a base, checking for the presence of the starting workpieces and for the depth to which the cap has been pressed, unloading the finished product, and sorting products as either acceptable or defective.

The process of inspecting the linear dimensions of the subassembly being assembled and checking for the presence of starting workpieces is automatic and based on the pneumatic principle.

All of the line's subassemblies and mechanisms (Figure 1) are mounted on a common base (1) located on vibratory supports (2). The line has two loading rotors (3) and (4), two inspection rotor (5) and (6), and a sorting rotor (7). Their rotation is initiated by an electric drive through a screw reducing gear (8) located on the working shaft of the inspection rotor (6). It is then transmitted through cylindrical gears (9) and (10) to the remaining rotors. The workpieces are transferred from rotor to rotor by a transport chain (11).

Each rotor consists of a shaft with a disk secured to it. Mounted on the disk are sets of quick-change working units for assembly and control of the workpieces and mechanisms, i.e., rams, effecting the required tool movements.

In the loading rotors, workpieces are fed by slide gate feeders (12) and (13) that the workpieces enter along chutes (14) and (15); "case"-type workpieces enter from a cassette (7), and "cap"-type workpieces enter from a vibrating bin (16). A mechanical memory (17) in the form of a chain with sleeves secured on every fourth of its links is used for a memory and to unload blocked products. Pins that can occupy two fixed positions are located in the sleeves: The bottom position is for a finished product, and the top position is for a defective product.

The base members that have been loaded (already oriented) into the cassette (a cassette holds 600 pieces) are fed along a feed chute (14) into the feeder. To break up groups of workpieces that have become hung up, the cassette is equipped with a cam agitator. The agitator is set into motion by the rotor via pinions and a V-belt transmission.

As the rotor turns continuously, the tongs (1) (Figure 2) located on the disk approach the feeder (2) one after the other. When the tongs' jaw coincides with the feeder, a slide pusher (3) that is set into motion by a disk cam (4) pushes the workpiece into the tongs. When the rotor turns an angle of 20° relative to the feeder, the top pusher/ram (5) unloads the base member from the tongs into the sleeve (6) of the transport chain, which carries the workpiece to the loading rotor (4) (see Figure 1).

When the transport chain holding a base member (1) arrives at the tool block (2) of the loading rotor (in which the assembly is to occur), the bottom pusher/ram (3) mounts it in the base socket of the tool block.

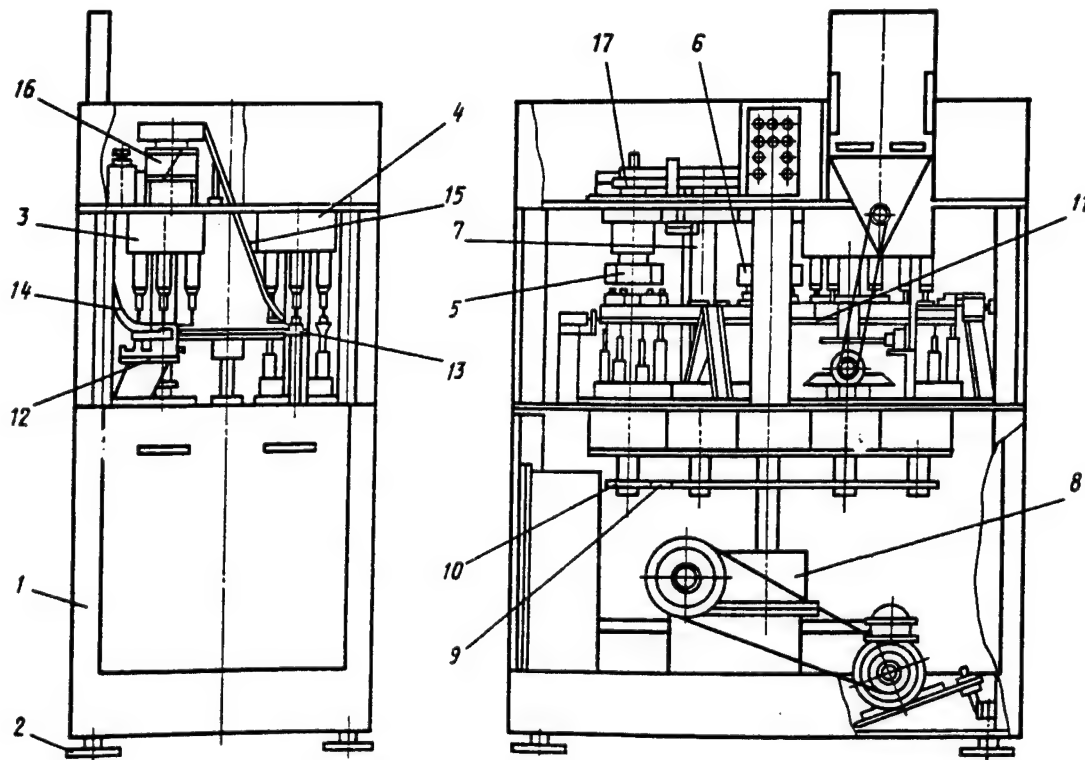


Figure 1. Design of the Rotary Automated Assembly Line

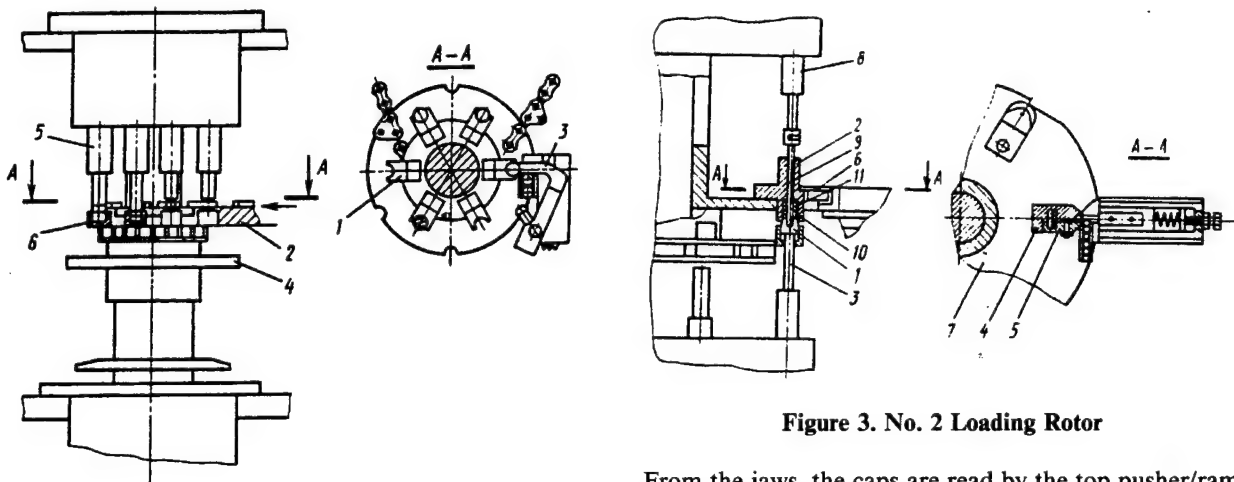


Figure 2. No. 1 Loading Rotor

The little caps that have been dumped into the vibrating bin (16) (see Figure 1) are oriented bottom down as they move along the vibrating bin's chute (15) and are fed into the feeder (13). The moment the jaw of the tongs (4) and (5) (Figure 3) coincides with the feeder, the slide pusher (6) (which is set into motion by cams located on the disk (7)) feeds them one cap each.

Figure 3. No. 2 Loading Rotor

From the jaws, the caps are read by the top pusher/ram (8) and punch (9) along the guide opening of the tool block and into the base member. The cap is pressed into the base member with a force of up to 39.2 N that is provided by a spring mounted on the top pusher/ram. As the rotor continues to turn, the bottom and top pusher-rams return to their initial position, and the assembled subassembly is pushed out from the tool block by the sleeve under the action of the spring (11) and into a transport chain sleeve.

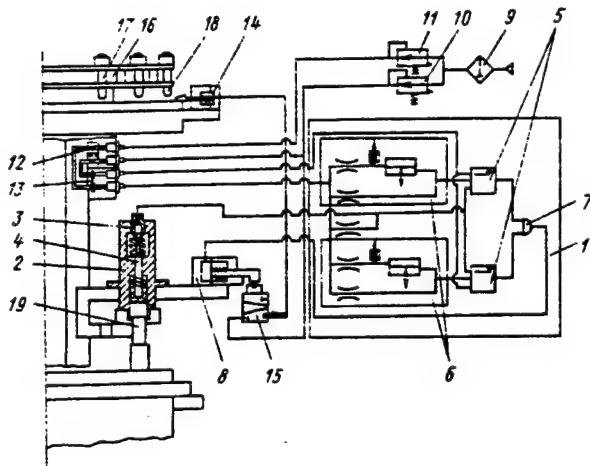


Figure 4. Inspection Rotor

The assembled subassembly arrives for inspection. The inspection-and-sorting device consists of two inspection rotors, a sorting rotor, a memory device, and an air preparation unit. The first inspection rotor checks for the presence of a workpiece; the second checks the depth to which the cap has been pressed into the base.

Six measuring stations consisting of a threshold device (1) and measuring unit (2) that in turn contains a pneumatic sensor (3) and contacting feeler gauge (4) are located in the inspection rotor (Figure 4).

The threshold device consists of two pneumatic comparison element (5), two sensors (6), a logical element (7), and an actuating pneumatic cylinder (8). The threshold device's activation error does not exceed ± 14.7 Pa; when the meter is operating in reverse, it does not exceed ± 24.5 Pa (which corresponds to 1μ in a linear characteristic). The device has an activation time of 0.15 to 0.3 seconds (at respective delivery nozzle diameters of 0.8 to 0.5 mm).

The compressed air preparation unit consists of a moisture separator (9) with a filter, a pressure regulator providing a compressed air pressure of 1.37 Pa, a pressure stabilizer (11), and a measuring device. Compressed air is fed to the inspection rotor through collector-type air collectors (12). Air passes from the air collectors to a distributor (13); from there it is sent along channels to the measuring stations.

The memory device consists of a pneumatic cylinder (14), pneumatic valve (15), and memory circuit that encompasses the two inspection rotors and the sorting rotor.

The memory circuit moves in sync with the transport chain: after having been assembled, each product that is in a transport chain sleeve and sent on for inspection along the guideway has its own corresponding sleeve (17) with a pin (18) in the memory circuit.

The memory process is implemented as follows. If it is determined at an inspection transport measuring station that the size of an assembled product is outside the tolerance range or if the absence of workpieces is established, the pneumatic valve issues an instruction to the rod of the pneumatic cylinder carrying the plate at a skew. The rod moves out and feeds the plate under the chain passing over it. The pin, moving at a skew, occupies the top position, which corresponds to remembering that a product is defective. If the size of the product being inspected is within the tolerance range, no instruction is sent to the pneumatic cylinder, and the chain pin remains in the bottom position, which corresponds to remembering that a product is acceptable.

Product size is checked in the following manner. As the transport chain arrives at the rotor's inspection position, the assembled product is fed by a pusher/ram (19) into the base socket of the measuring unit. In this unit the product interacts with a pneumatic sensor through a contacting feeler gauge. The pneumatic sensor is a shutter/nozzle that has been made in the form of a sleeve with a conical valve seat and little ball covering the intake opening. The feeler gauge occupies different positions depending on the actual size of the dimension being checked. The small ball, upon coming into contact with the top end of the feeler gauge, rises from the valve seat and opens the sensor's outlet opening. Depending on the flow rate of the compressed air leaving to the atmosphere through the sensor's outlet opening, a specified pressure is established at the inlet of the comparison elements.

Single signals to the logic element in the following combinations are issued from the comparison elements, which have been adjusted by set-point adjusters for two activation pressure thresholds (depending on the limiting dimensions of the product being inspected):

$p_1 = 0, p_2 = 0$ —the product size is less than allowed;

$p_1 = 1, p_2 = 0$ —the product size is within the tolerance range;

$p_1 = 1, p_2 = 1$ —the product size is greater than allowed;

where p_1 is an instruction from the comparison element adjusted for the nominal size and p_2 is an instruction from the comparison element adjusted for the maximal size.

The logic element, which has been designed on the basis of the inhibit function $p_1 p_2$, issues the following respective instructions to the actuating pneumatic cylinder: $p_{out} = 0; p_{out} = 1; p_{out} = 0$. The first and third output instruction states correspond to products that are defective with respect to the upper and lower bounds; the second corresponds to an acceptable product.

Consequently, when $p_{out} = 0$, the pneumatic cylinder's rod does not turn, and the plate that has been secured to the end of the rod at a skew acts on the pneumatic valve as the rotor turns. The pneumatic valve is then turned on

for 0.3 seconds. During this time, the memory process occurs—the activation of the pneumatic cylinder (14), the entry of the skew plate under the memory chain, the movement of the pin from the lower to the upper position, and the return of the pneumatic cylinder to its initial position.

When $p_{out} = 1$, the pneumatic cylinder's rod moves out, and the plate moves to the side of the pneumatic valve; accordingly, the pneumatic cylinder (14) is not activated, and the pin remains in the bottom position.

After having been inspected, the product moves to the sorting rotor. This rotor is a device with a disk mounted on its shaft. The arrangement of the openings on the disk corresponds to the position of the pusher/rams. An offtake chute with two branches approaches the disk (see Figure 1): the left branch is for acceptable products, and the right branch is for defective products.

The top end of the flag indicator mounted on the upper cup of the sorting rotor interacts with the memory chain pin (see Figure 4) through a lever system. A sorting shutter is secured to the bottom end of the flag indicator at a distance of 1 to 1.5 mm from the disk. If a product that has been established as defective arrives at the rotor, the flag indicator will, by interacting with the pin, turn and open the shutter. A pusher-ram raises the product from the transport chain sleeve through the disk opening to its top surface. The product passes freely through a moving shutter and is directed through a fixed shutter along the right branch of the chute in the receptacle for defective products. If the product is acceptable, the sorting shutter does not turn, and the product is directed along the left branch of the chute.

To ensure accident-free operation of the line, each rotor is equipped with a disabling device (see Figure 1). This device is a solid-state limit switch that is mounted on a bracket and secured to the axis of the flag indicator. The flag indicator enters the gap between the transport chain and disk. When a product is hung up in a rotor's tool or measuring unit, the flag indicator turns on its axis after interacting with the product. A small shutter (made of nonmagnetic material) secured to the flag indicator enters the slot of the limit switch, which issues an instruction to turn off the line's electric motor and turn on the electric brake.

The lengthy operation of the rotary lines has demonstrated the high reliability of all their mechanisms. The sizes of the workpieces that can be assembled are as follows: base members can be 14 to 25 mm high and 14 to 20 mm in diameter; caps can be 1.5 to 8 mm high and 2.5 to 7 mm in diameter. Between 2 and 3% of the assembled components are erroneously labeled defective. The line can perform 6,000 to 7,000 assemblies per hour.

COPYRIGHT: Izdatelstvo "Mashinostroyeniye", "Mekhanizatsiya i avtomatizatsiya proizvodstva", 1991

Ministry Becomes Joint-Stock Association

917F0262A Moscow IZVESTIYA in Russian 2 Jul 91
Union Edition p 2

[Interview with N. Panichev, president of the state joint-stock association Stankoinstrument, by V. Romanyuk, place and date not given: "Minister Becomes President"]

[Text] Beginning 1 July 1991, the USSR Minstankoprom [Ministry of the Machine Tool and Tool Building Industry] was converted into the state joint-stock association Stankoinstrument. The first question is banal: What is it—another sign change in order to keep the staff and high salaries?

"Not at all," objects GAO [joint-stock association] President N. Panichev. "When I took over the ministry several years ago, it had 1,450 employees. The association's current staff is 348 people."

[Romanyuk] Former Prime Minister N. Ryzhkov had also been tightening administrative apparatus and merging ministries. Some branches-conglomerates had become totally unmanageable.

[Panichev] We have 511 enterprises and organizations for our 348 administrative staff members. We see our task not in commanding and administering them, but in creating favorable conditions for enterprises—the main producers of goods—to work.

[Romanyuk] Most enterprises reject ministerial structures. What sense do they see in creating all sorts of associations after they have barely acquired the desired economic freedom?

[Panichev] The ministry worked by government directives and by plans put together in the USSR Gosplan [State Planning Agency]. Then, when the economy started to disintegrate to such a degree, it became necessary to search for new forms of economic administration. Since the idea is to move toward a market, we, together with the enterprises, had to create structures that would allow enterprises to operate successfully in a market environment. We became interested in the structure of the Austrian firm Voerst Alpine, four-fifths of whose property is in the state sector; we learned many useful things at Italian FIAT and in the American company General Electric. In the end, we voluntarily gave up management by order and began building our relations with enterprises on the basis of partnership.

[Romanyuk] Are you trying to say that you have already been operating as an association for quite a while?

[Panichev] Absolutely correct. We have already formed all the necessary market structures. For instance, the department of material and technical supply had 120 functionaries with a guaranteed salary whose business was to copy papers received from the USSR Gosplan [State Committee on Technical and Material Supply]. We have converted it into a self-supporting Stankosnab

[Machine Tool Material Supply Company] which deals with enterprises on a contract basis. To help Stankosnab, we created a GAO stabilization fund, for which we allocated 10,000 machine tools and 3,000 presses. In exchange, we will be receiving metal, ball bearings, and other things.

There was another unmanageable task—obtaining credits. Instead of relying on other banks, we formed our own Stankinbank with a charter capital of 100,000 rubles [R]. Now its turnover is about R1 billion. In addition, we introduced financial pools into practice. If, for instance, we need to buy a license, we collect money from interested enterprises and buy it. As of today, 42 financial pools are in operation in our industry branch. We try to join various republic programs. For instance, the Government of Russia is allocating R70 million for a program to build 200 brick factories in the republic.

[Romanyuk] Much is now being written about the fiasco of the Ivanovo machine tool association where they used to make manufacturing centers with foreign-made components; now there is no hard currency to buy components and they have to switch to making woodworking universal boring. Is this your baby?

[Panichev] All this sham at Ivanovo was created under the sponsorship of the CPSU Central Committee Politburo in opposition to the ministry. There was an attempt to resolve the problem of disposable syringes through the same apparatus methods. The CPSU Central Committee Politburo ordered us to produce rotor lines for this purpose, although it was clear from the very beginning that this technology was not workable from an engineering point of view. We have wasted much time and resources but not a single line is working to this day. Thank goodness, we put in a parallel operation a discretionary version and produced thermoplastic automatic machines with multiple press forms.

[Romanyuk] Nikolay Aleksandrovich, what have you lost as a minister and what have you gained as a GAO president?

[Panichev] I have lost an ambiguous position of a man without rights and economic levers whose only duty was to sit at government meetings and to be held responsible. I have gained much. If you mean the financial side, my personal salary is now R2,000, twice higher than the one I had as a minister. By established norms, expenses on the maintenance of GAO apparatus comprise 0.08 percent of the volume of realized production, but not more than 0.65 percent of profits remain at enterprises' disposal.

[Romanyuk] So what is it—GAO Stankoinstrument? Each fragment of this abbreviation brings out questions...

[Panichev] This is a voluntary association. Not a single enterprise had been accepted without a protocol of its collective's general meeting making a decision to join the GAO. Why joint-stock? Because we are convinced that

this is a realistic way to make each employee an owner of the productive capacity, to stimulate him to invest not only his labor, but also his money into the development of production. So far, six plants have switched to a joint-stock form. Now the largest in the industry collective—Krasnyy Proletariy—is going joint-stock. A new form of administration is being introduced at the plant imeni Lenina in Sterlitamak. Here they created 14 self-supporting entities on the basis of factory shops and issued shares. By the way, there is now a department that will be involved in the implementation of new ownership forms.

[Romanyuk] The republics declared their sovereignty. Can it happen that the GAO will fall apart after the Union Treaty is signed?

[Panichev] I have in my hands an inter-republic agreement signed by the prime ministers of four republics—the Ukraine, Russia, Belorussia, and Armenia. Our branch is, so to speak, the chief technologist of the machine-building complex. Internal cooperation encompasses up to 45 percent of production volume. To destroy the unity of the branch is to allow the production to fall to one-half of its present level. Enterprises can work on a joint-stock basis, on leaseholds, and even convert into cooperatives, but at the same time they need to be a part of the system of internal technological cooperation inside the branch.

In this respect we have things to learn from Europe. For instance, from the European Committee on Machine Tool Building. Its task is formulated this way: If a manufacturing center arrives in Germany from Italy, five hours later it has to be assembled into a system of machines and start producing output. Something else: If today you are making grinding machines, you cannot switch to making harrows tomorrow. You can fail in the market today, but you have no right to lose your skills. This is the basis of many European firms' good reputation.

[Romanyuk] Have all enterprises in the branch joined the association?

[Panichev] Not all! Two plants located in Lithuania have not joined, as well as two in Lvov. Two concerns were formed before the GAO was organized: Seven out of 24 woodworking plants and 14 tool building plants went there. Just recently five plants returned to us, and two more from the defense industry joined in—our doors are open for everybody. They come to us because we do not try to run them; instead, we provide a unified technical policy, science support, take upon ourselves foreign economic activities, and support the functioning of market structures we ourselves have created.

Development of Control Programs for NC Machines in a Manufacturing Process CAD System

917F0218F Moscow STANKI I INSTRUMENT
in Russian No 12, Dec 90 pp 14-16

[Article by A.M. Gilman and Yu.B. Yegorov]

UDC 681.3.06:621.9.06-529:658.512.011.56

[Abstract] The process of designing technological processes entails two tasks. The first is that of compiling the sequence of operations and transitions required to manufacture a component meeting its stipulated specifications. The second consists of making technological calculations; selecting cutting, measuring, and auxiliary tools; designing optimal machining modes and time norms; and compiling control programs for the NC machines to be used. Control programs contain instructions specifying the trajectory of tools' motions and their technological instructions. Because a significant portion of the data needed to compile control program codes forms the technological operations chart, compiling a control program is a part of the technological design process. Historically, at least in the accepted practices of automating manufacturing in the CEMA member-countries, control program compilation has not been considered or implemented as part of the technological design process. In view of the advantages (to developers and users alike) of including control program compilation as part of the technological design process, the authors of this article discuss Soviet efforts to combine control program compilation with the other aforesaid tasks addressed in designing technological processes. One method proposed is that of combining a technological process CAD system with the TEKHTRAN system (one of the most popular systems for automated compilation of control programs in the USSR). Another approach considered is that of introducing a preprocessor to design the operations entailed in technological processes. The TAU-TM [not further identified] system is cited as one such attempt. The distinctive features of designing a technological process CAD system for use in designing all output technological documents including an NC machine control program are examined in detail by way of the example of the Korund technological process CAD system. Particular attention is paid to the considerations that go into selecting a method of synthesizing a technological process and to compilation of a control program for an NC machine. References 10 (Russian).

A System for the Computerized Exploratory Design and Manufacture of Tools for Resource-Saving Machining Processes

917F0218 Moscow STANKI I INSTRUMENT
in Russian No 12, Dec 90 pp 11-13

[Article by G.N. Kirsanov]

UDC 658.512.011.56:621.9.02.002

[Abstract] Automation of the production of engineering objects has created the need for computer-aided design

[CAD] systems that can be used to design tools in an automated exploratory design and manufacture mode. Such systems could be used in creating both familiar and fundamentally new designs of tools that could in turn be used to implement resource-saving machining processes. One of the key processes in developing the methodological and data base support for such a tool CAD system is that of designing and constructing universal tool systematics. These systematics should be based on unified and generalized principles and methods of designing tools of different configurations based on the internal links of the machine tool pair "tool-workpiece." The tools being designed should be looked upon as instruments performing functions, i.e., eliminating allowances and shaping workpieces, and the CAD system should be capable of producing classical tools and tools for new machining methods. The systems of the proposed CAD system should be based on the open-network system so as to allow for further development and modification and should serve as a methodological foundation for computer-aided exploratory design and manufacturing. The proposed tool CAD system discussed in this article includes the following: a software tool system, source data regarding workpiece parameters and tool types, a tool retrieval system, a source data bank, and a system to implement the actual CAD process. The tool CAD system described contains the following components: subsystems to design, manufacture, operate, and overhaul tools; an information identification subsystem; a system to designate cutting modes; an information and measuring system; an adaptive control system; a system executing the processes entailed in manufacturing the tools designed; a quality control system; and a tool-coding system. The proposed system is intended to be implemented in accordance with a modularized technology including assembly/disassembly equipment and manufacturing accessories. Figures 2; references 4 (Russian).

A Unified Intelligence Structure for Engineering and Biological Systems

917F0218B Moscow STANKI I INSTRUMENT
in Russian No 12, Dec 90 pp 4-7

[Article by G.N. Rapoport and A.G. Gerts]

UDC 007:62+57

[Abstract] Just like biological systems, modern engineering systems consist of a set of multidimensional interconnected objects that are controlled by means of a hierarchical multilevel control strategy. Each level has its own unique purpose, survivability, importance, and free action that reflects its own particular purpose and intelligence capabilities. Each subsequent level is responsible for the correctness of the action of the elements of the preceding level and for coordinating their actions. This is

accomplished primarily by collecting and processing information as to the interactions of the individual components of the lower level and issuing control responses. Decentralization is one of the most important requisites of the efficient control and survivability of engineering systems. Redundancy (both physical and structural) is another important factor in survivability. This article examines the essential characteristics of control systems as hierarchical systems. The following aspects of hierarchical control systems are discussed: sequential vertical arrangement of the subsystems constituting the system, priority of actions effected by the subsystems, and the dependence of upper-level subsystems' actions on the actual execution of their functions by lower-level subsystems. Also discussed is the concept of a function-oriented system based on a hierarchically designed knowledge bank and software mechanisms of adapting to and interacting with the external and inner world. The process of designing and storing instruction chains and sets thereof is discussed. The functions of the operating systems (specifically, supervisors and interpreters) used in the aforesaid function-oriented system are covered in detail. The system described may be classified as a real-time artificial intelligence system (actually an expert system implementing condition control of some engineering objects in real time). The capabilities afforded by such systems, their hardware implementation, and their similarities to biological systems are considered. References 2 (Russian).

The Survivability of Flexible Manufacturing Systems

917F0218D Moscow STANKI I INSTRUMENT
in Russian No 12, Dec 90 pp 9-10

[Article by V.G. Mitrofanov and A.S. Starostin]

UDC 658.52.011.56.012.3

[Abstract] When used in relation to any complex manufacturing system, the term "survivability" refers to the system's capability of responding to various external disturbances related to failures in the operation of equipment and engineering subsystems. This response can be either in the form of a change in workpiece-machining routes or in operating modes such that the specified disturbances do not result in any impairment of the course of the manufacturing process. Responses of this type minimize the negative consequences of external disturbances associated with equipment failures without resulting in any additional costs. This article examines strategies for ensuring the survivability of flexible manufacturing modules and systems thereof in the design stage. One strategy discussed is to give each flexible manufacturing module a reserve of time that can be used instantaneously in the event of an equipment failure so as to keep the flexible manufacturing module from interacting with the failed equipment and experiencing any negative consequences that would be involved in

such interaction. Another strategy discussed is to give the flexible manufacturing system the capability of changing its configuration in the event of an accident. Another option considered is to make flexible manufacturing modules mutually replaceable so that manufacturing assignments can be redistributed among equipment that is in good working order when other similar equipment has failed. These options are analyzed from a mathematical standpoint.

Modeling Computer-Integrated Manufacturing

917F0218C Moscow STANKI I INSTRUMENT
in Russian No 12, Dec 90 pp 7-9

[Article by V.V. Pavlov]

UDC 658.011.56.001.57

[Abstract] When attempting to unify research, design, technological, manufacturing, and administrative subsystems into a unified computer-integrated manufacturing system, designers are faced with the problem of representing (for use on a computer) a set of interconnected mathematical models of diverse objects and processes. One way of accomplishing this is to develop a set of algorithms, software, and data base support materials for a computer-aided design [CAD] system based on a unified modeling system. This article describes one such system. The system is based on disjunctive and conjunctive forms of linking the various loops of the model. Procedures for modeling positive, negative, and neutral actions on a product by the production system producing it are outlined. The proposed modeling method may be used in executing CAD procedures and in analyzing the technological capabilities of a manufacturing system, determining product design requirements, and developing recommendations regarding the structure and modification of a manufacturing system. The modeling method has been used at the Mosstankin. Figures 2; references 4 (Russian).

Information Science Problems in Computerized Manufacturing

917F0218 Moscow STANKI I INSTRUMENT
in Russian No 12, Dec 90 pp 2-4

[Article by Yu.M. Solomentsev]

UDC 681.3:658.011.56

[Abstract] The development of automation equipment and the use of the latest progress in information science and computer technology, automation equipment, and engineering cybernetics have resulted in great strides in creating promising technologies and significantly increasing the level of commercial relationships in the national economy. This thematic review examines information science problems in computerized manufacturing. The reasons why the anticipated cost savings

resulting from introducing flexible manufacturing systems in the USSR never materialized are examined. Several possible ways of reducing the time periods required to create computerized manufacturing and automation equipment are examined, including the parallel implementation of design, technology planning, and manufacturing processes at the Ivanovo Machine Tool Production Association imeni 50th Anniversary of the USSR and the efforts to streamline the process of manufacturing components by developing a computerized manufacturing system at the Krasnyy proletariy [Red Proletarian] Machine Tool Plant imeni A.I. Yefremov. The elements of computer-integrated manufacturing systems and plant-level operations management systems are examined. The following recommendations are made regarding the parameters of the hardware used to develop computerized manufacturing systems: 1) a 16- or 32-bit microcomputer having interface controllers with sensors and actuators, digital-to-analog and analog-to-digital converters, and communications channel adapters or local area network [LAN] controllers to link with a central computer; 2) computer-aided design [CAD] systems, graphic workstations with resolutions ranging from 600 x 400 to 1,200 x 1,000 points on a screen, black-and-white or 16- to 256-color monitors with a screen size of 14 to 23 inches, a central computer performing 0.5 to 20 million operations per second, a design and technological information data bank, and an interface to LANs or distributed networks; and 3) an administrative management, planning, and accounting system including a network of personal computers with a pictographic interactive interface, printers, information-archiving devices, I/O and processing devices, speech I/O devices, and interface to LANs and distributed networks. Figure 1; references 3 (Russian).

Prospective Automated Transport and Warehousing Systems

917F0216A Moscow MEKHANIZATSIYA I
AVTOMTIZATSIYA PROIZVODSTVA in Russian
No 1, Jan 91 pp 6-8

[Article by S.I. Bochek and A.G. Solomina, engineers]

UDC 658.011.56:658.78

[Abstract] This article describes an automated transport and warehousing system that is intended for use in servicing production lines based on the conceptually new technology of flexible individual assembly. Final product assembly is performed on mobile transport platforms. Feed of the platforms to the assembly sites is loosely controlled depending on the specific conditions of the given manufacturing process. Using the new technology of flexible individual assembly makes it possible to establish a free rhythm when implementing assembly operations. Several versions of a specific product can be assembled simultaneously, thus allowing assemblers' skills to be used to maximum advantage. The new automated transport and warehousing system consists

consists of a warehouse module for the workpiece sets being completed along the transport and storage system and a warehousing module for finished products. The first of these two modules is based on automated warehousing units with load capacities of 500, 250, 100, and 50 kg. The module features double-row racks that are serviced by rail-type stacking conveyers. The control system features a microprocessor component base and is capable of integration with a higher-level computer in an Elektronika MS 0585-type configuration. The system also features driven transport platforms with load capacities of 100, 50, and 25 kg. The finished-product warehousing module is based on a series of automated warehousing units with a load capacity of 100 kg. Products being assembled are moved automatically from workstation to workstation and, when finished, directed to the finished-product warehousing unit. The new automated transport and warehousing system is recommended for use in assembling processes geared toward the manufacture of radio receivers, televisions, tape players, electric ranges, refrigerators, and washing machines. Figure 1.

A Robot Vision System for Determining the Color, Shape, and Position of Objects in a Robot's Live Zone

917F0216B Moscow MEKHANIZATSIYA I
AVTOMTIZATSIYA PROIZVODSTVA in Russian
No 1, Jan 91 pp 8-11

[Article by V.I. Syryamkin, candidate of technical sciences, V.S. Titov, doctor of technical sciences, and O.S. Borovik, A.A. Fomin, and Yu.A. Nikitina, engineers]

UDC 681.5

[Abstract] Robot vision systems intended for analyzing color objects in a robot's live zone have been receiving increasing attention. One way of implementing a robot vision system is to create vision systems based on general-purpose microcomputers and effective devices to input color images into a computer. Existing robot vision systems working with color images are either cumbersome and expensive or else cannot be quickly readjusted to perform new manufacturing process tasks. The robot vision system described herein is intended for use in assessing the color, shape, and position of objects in a robot's live zone. Color images processed in the new robot vision system may be described by determining the color coordinates corresponding to red, green, and blue for each pixel in the image. The color of any pixel can be reflected by a combination of the levels of the main colors, and the pixel's brightness can be described by an expression based on weight coefficients. The new robot vision system contains a color television camera (Hitachi), buffer storage, color television, video monitor, telecommunication device (type BDS-85), and microcomputer (Elektronika MS 0585). The new robot vision system boasts the following technical characteristics: color image resolution, 256 x 256 pixels; monochrome

image resolution, 512 x 512 pixels; number of gradations of an image's brightness, 16; image-reading time, 80 ms; number of analyzable color shades, 4,096; probability of correct recognition of color and shape, 0.99 to 0.995; precision of estimating linear coordinates, mean square deviation, and systematic error, 0.1 to 0.4% of the image frame size; and time required to process one image frame, 0.2 to 50 seconds. The new robot vision is ready for operation. Figures 4.

Overhead Transport Robot To Automate Loading, Unloading, Transport, and Warehousing Operations

917F0216C Moscow MEKHANIZATSIYA I
AVTOMTIZATSIYA PROIZVODSTVA in Russian
No 1, Jan 91 pp 11-12

[Article by V.I. Burenkov, engineer, and V.N. Kazakov, candidate of technical sciences]

UDC 69.057.7:621.86.06

[Abstract] Electric hoists are widely used to mechanize transport operations in the manufacturing process. They are simple and reliable, but operating them requires a great deal of manual labor and control and observation time. In an attempt to eliminate these shortcomings, the authors of this article have proposed an overhead transport robot to automate loading, unloading, transport, and warehousing operations. In essence a conventional electric hoist is mounted on a monorail, and the hoist is equipped with a system of gripping mechanisms and an automatic control system. The cargo is suspended on a telescopic column, and a system of transducers with very simple logic devices is used to control the electric hoist's drives. The proposed system can be implemented by using inexpensive components so that the control system does not cost more than 700 rubles. The system examined herein has been developed and used to automate the loading, unloading, transport, and warehousing operations entailed in manufacturing sharply angled pipe. Using the system resulted in an annual savings of 5,150 rubles. Figures 3.

Scientific-Technical Progress in Machine Building

917F0216I Moscow MEKHANIZATSIYA I
AVTOMTIZATSIYA PROIZVODSTVA in Russian
No 1, Jan 91 pp 35-38

[Article by A.A. Panov, candidate of technical sciences, and Yu.N. Losev, engineer]

UDC UDC 621:002.5

[Abstract] The Main Directions for Economic and Social Development of the USSR From 1986 to 1990 and for the Period to the Year 2000 calls for marked intensification of production. Recognizing the impact that scientific-technical progress has on industrial development and product quality, the USSR State Committee for

Science and Technology switched to the special-program method of planning and created its Integrated Program of Scientific-Technical Progress of the USSR in 1991-2010. A large number of branch special-purpose and integrated programs were created. In the USSR Ministry of the Machine Tool Industry alone, 38 special, integrated, and regional programs were developed. Most of the emphasis was placed on quotas, and program measures and indicators were developed without balanced ties to the entire set of industrial processes conducted at given enterprises. A lack of systematization in the formulation of indicators resulted in programs that were not well thought out, that duplicated other programs, or that did not attempt to address big or complex problems. In view of these problems, this article focuses on the creation of a consolidated scheme of planning scientific progress in which the development of scientific-technical research and development would be planned in much the same way as production programs are planned. Under the proposed planning model, branch integrated programs would encompass all phases of the activity entailed in developing and manufacturing a product including the scientific research and design work that is conducted before a product reaches the production stage and all of the stages entailed in the product's eventual production. This article details all of the individual stages entailed in developing long-range (20-year) plans beginning with research and development, moving on to the actual manufacture of products, and retooling and updating the technologies used at enterprises at specified intervals. Flowcharts outlining a consolidated scheme for planning scientific-technical progress and a system for formulating a branch program for scientific-technical progress in a specified technological direction are included. Figures 2.

Methods of Increasing and Stabilizing Precision When Manufacturing Products

917F0216G Moscow MEKHANIZATSIYA I
AVTOMTIZATSIYA PROIZVODSTVA in Russian
No 1, Jan 91 pp 25-27

[Article by I.M. Baranchukova, candidate of technical sciences]

UDC 62-187

[Abstract] Practice has shown that the precision capabilities of any manufacturing system are determined above all by its dynamic characteristics. These in turn depend on a number of factors. Analysis of test data indicates that besides being affected by changes in the magnitude and sign of the three-dimensional motions occurring between a blank and a tool, the precision indicators of blanks are also affected by changes in the speed of the aforesaid motions. Theoretical research conducted by the author and reported herein indicates that the parameters of these motions (amplitude and frequency) are governed by the behavior of the rotating masses of the manufacturing system's spindle groups. This behavior is

in turn governed by the nature of the motion of the tip of the kinetic moment vector upon the interaction of external and internal moments due to disturbances and resistance forces under conditions of constraints. This results in related three-dimensional motions in the zone of contact between tool and blank. Establishing such connections between the parameters of these motions and machining conditions enabled the author to develop an integrated method of controlling the motions occurring in the zone of contact between a tool and a blank. The method entails control in three stages: idle rotation, incision, and complete cutting. The procedures entailed in implementing the control method are described in detail, as are algorithms to control the functioning of a spindle group in a manufacturing system with an alignment controller and an algorithm to determine the initial application of a tool's smooth cutting edge. Figures 4.

The Entropy Approach in Determining the Ultimate Bounds of the Development of an Automated Control System

917F0216H Moscow MEKHAIZATSIYA I
AVTOMTIZATSIYA PROIZVODSTVA in Russian
No 1, Jan 91 pp 33-34

[Article by A.A. Smekhov, doctor of technical sciences]

UDC 65.011.56

[Abstract] Automated control systems are generally designed and constructed as developing systems. Developing an automated control system entails increasing the number of tasks it can perform and the amount of information used to perform these tasks. This article examines the issue of the limits to which developing an automated control system remains economically feasible. The conventional approach entails direct calculations to determine the costs and economic impact of developing the given automated control system and results in identification of the ultimate bound of the system's engineering development. The academician V.A. Trapeznikov has proposed another approach termed the entropy approach. The idea underlying this approach is that the running costs associated with the operation of a manufacturing system depend on its degree of disorganization (disorder), which is of course known as entropy. When the disorganization of a controlled system increases, its efficiency decreases. Conversely, applying control actions reduces entropy and increases efficiency. Because control actions are a function of the amount of control information available, efficiency (i.e., reduction in entropy) is also related to control information. V.A. Trapeznikov also postulates that the amount of information needed to control a system under new conditions is proportional to the costs of developing it. The interrelationship between these factors and their relationship to determining the ultimate bounds to which development of a given automated control system remains feasible are analyzed mathematically by way of the example of two interacting

transport systems. Mention is also made of the fact that when entropy is determined as a measure of the indeterminacy of the information regarding a system (i.e., the system's disorganization), consideration must also be given to noise resulting from various environmental effects. These various instances of noise generated represent external events that must be added to the "base" entropy of a system to obtain a system's total entropy. Figures 2.

Equipment for Remote Control of Underground Hoisting Units

917F0216F Moscow MEKHAIZATSIYA I
AVTOMTIZATSIYA PROIZVODSTVA in Russian
No 1, Jan 91 pp 18-91

[Article by N.P. Prokhorenko, engineer, and N.P. Matviyenko and Yu.P. Deynekin, candidates of technical sciences]

UDC 622.67;62-519

[Abstract] The Avtomatuglerudprom Institute [Institute for the Automation of the Coal Mining Industry] of the Krasnyy Metallist [Red Metalworker] Plant has developed the ADU-1.1M unit for remote control of underground hoisting units equipped with underground machines used in underground workings of coal and shale mines that pose a high risk of explosion in connection with their gas and dust. The new remote control unit comes in eight versions (ADU-1.1M through ADU-1.8.1M). Its technical characteristics are as follows: delay in offswitching the brake when lowering a load, about 0.8 seconds; number of track switches, no more than 20; controllable hoisting vessel velocity, 1 to 8 m/s; velocity control error, $\pm(0.1$ to $0.31)$ m/s; speed limiter activation time, no more than 0.1 seconds; and power consumption of the ADU-1.1M set, no more than 1.3 kW. Prototypes of the ADU-1.1M have passed acceptance tests, and an interdepartmental commission has recommended the ADU-1.1M for series production at the Krasnyy Metallist Plant. The savings from using and producing the ADU-1.1M are estimated at about 4,000 rubles. Figures 2, table 1.

Designing Mechanisms To Move Blanks

917F0216D Moscow MEKHAIZATSIYA I
AVTOMTIZATSIYA PROIZVODSTVA in Russian
No 1, Jan 91 pp 12-13

[Article by V.A. Zaderenko, engineer]

UDC 621.7.077:62-521.001.24

[Abstract] The engineering level and capacity of modern hoisting mechanisms are largely determined by the quality of their drives. Using thyristors in induction motors' control circuits makes it possible to improve the control of electric drives and thus expand their applications area. Changing the voltage fed to the motor is

among the simplest ways of continuous control of a mechanism's speed by means of thyristors and requires the least number of additional elements. Voltage changes are accomplished by phase control of thyristors connected to the motor's stator circuit in a specified manner. Changing the voltage in a closed-loop control system provides stable reduced speeds in drive and braking modes. In view of these facts, the Starooskolskiy Mechanical Plant undertook a research project to develop an optimal version of a mechanism based on using semiconductor transducers. The results of this study and recommendations regarding selecting an optimal (from the standpoint of minimal losses) induction motor controlled by thyristor voltage regulators are reported herein. Specifically, recommendations are given regarding changes that need to be made when using a general-purpose motor with a rated slip of up to 5%. The data presented may be used to design a hoisting mechanism as a function of service load. Figure 1.

Determining an Industrial Robot's Work Space

917F0216E Moscow *MEKHANIZATSIYA I AVTOMTIZATSIYA PROIZVODSTVA in Russian* No 1, Jan 91 pp 14-17

[Article by V.F. Krasnikov, candidate of technical sciences]

UDC 007.52

[Abstract] Automating manufacturing based on extensive use of industrial robots and manipulators is an effective and promising direction in heavy and light industry alike. The success of introducing industrial robots and manipulators depends largely on the optimal "compatibility" of their characteristics with the other automation equipment. One important aspect of making industrial robots compatible with other automation equipment is determining the industrial robot's work space. This article proposes a method for determining and optimizing the size of an industrial robot's work space (V_p) and the size of its service area (F). The proposed method is based on the use of analytical models representing the set of positions of the robot's gripping mechanism given different link turning angles. The author establishes an analytical dependence between the structure, kinematic parameters, and coordinates of the industrial robot and the shape of the work space described by the robot's gripping mechanism. Also presented is a technique for determining the optimal lengths for a given industrial robot's links by using a random method with elements of a heuristic approach involving a four-step optimization algorithm. The proposed methods are illustrated by way of calculations for robots intended for applying paint and varnish coatings and packing and removing empty and full bottles. Figures 3, table 1.

Development of a Technology for the High-Speed Milling of Cast Iron Components for the Krasnyy Proletariy Automated Plant

917F0233J Moscow *PROBLEMY MASHINOSTROYENIYA I NADEZHNOСТИ MASHIN in Russian* No 3, 1991 pp 19-23

[Article by G.V. Borovskiy, I.G. Kondratyev, Yu.V. Solin, A.I. Pozdeyev, S.K. Belyayev, M.M. Filin, and M.N. Pokhmelnikh]

UDC 658.2.011.056

[Abstract] Productivity at the Krasnyy proletariy [Red Proletarian] Production Association should be eight- to tenfold higher than that of existing industry thanks to the introduction of high-speed machining by tools with mechanically secured multifaceted replaceable cutting plates made of promising tool materials such as polycrystalline cubic boron nitride. Because 64% of all time in a manufacturing process is typically spent on machining, the All-Union Scientific Research Institute of Tooling developed and tested face mills equipped with plates of the aforesaid material for use in high-speed milling of cast iron base members on universal machine tools. Tests of these cutting plates conducted on a model IR500PM1F4 mill at the Krasnyy proletariy Production Association in Moscow indicated that using such plates can increase machining productivity and tool strength by a factor of 3 to 6. This article details the tests conducted on the new cutting plates and on ways of improving machining productivity under the conditions of an automated plant and presents specific recommendations regarding such machining process parameters as face mill diameters, machining speeds and time, and power and motor capacity requirements. Figures 5, tables 3; reference 1 (Russian).

Ways of Developing Conventional Machining Methods Under the Conditions of an Automated Plant

917F0233I Moscow *PROBLEMY MASHINOSTROYENIYA I NADEZHNOСТИ MASHIN in Russian* No 3, 1991 pp 18-19

[Article by M.A. Esterzon]

UDC 658.2.011.056

[Abstract] The technical and economic indicators of computerized manufacturing are determined by the level of the technology and equipment used to perform conventional cutting operations (turning, drilling, milling, grinding, etc.). Under the conditions of an automated plant, these operations account for nearly 98% of machine tool capacity and 98.5% of labor input. These figures explain the extreme importance of adopting conventional machining methods to conditions of flexible manufacturing systems so as to make more efficient use of these systems' capabilities. The Experimental

Scientific Research Institute of Metal Cutting Tools [ENIMS] conducted a scientific research project directed toward creating the scientific-technical know-how needed to develop high-quality, reliable, high-productivity, and flexible machining processes that can be executed at automated plants. This project included the following: general theoretical research on machine building technology; planning work related to technology, cutting and auxiliary tooling, accessories, and measurement equipment; experiments entailing various machining modes conducted on existing equipment; and the manufacture and testing of mockups and prototypes of new machining equipment for use in automated plants. Research was also conducted in the area of improving the properties of cast irons and steels for use in machine tools and their components and on new methods of thermal hardening and on developing composites. The research conducted indicated several promising ways of improving conventional machining processes under conditions of automated plants. Included among these promising paths were the following: organizing the machining process in accordance with a "machine tool-warehouse-machine tool" scheme to as to maximize the time for which equipment is actually used, make the shapes of blanks closer to the shapes of their respective finished product counterparts, use new materials and cutting tool designs as well as combined tooling and multihead machining, and integrate the machining process by connecting machine tools to a central computer and to the transport and warehousing system. The research conducted also provided information regarding the possibilities of reducing labor input in automated plants and the benefits of new cutting materials and improved tool designs.

Selected Features of the Technological Design of Flexible Manufacturing Systems

917F0233H Moscow PROBLEMY
MASHINOSTROYENIYA I NADEZHNOСТИ MASHIN
in Russian No 3, 1991 pp 17-18

[Article by V.I. Buveykovskiy]

UDC 658.2.011.056

[Abstract] The main distinguishing features of computer-integrated [CIM] and flexible manufacturing systems [FMS] are their multilevel, extensively branched information and management system based on computer technology and their deeply integrated mechanical system (consisting of machine tools and auxiliary equipment) that can be automatically reconfigured to optimize the technical and economic characteristics of a manufacturing system when its input parameters are revised. Because of the significant differences between conventional manufacturing systems and computer-integrated manufacturing systems, conventional technological design methods are not suitable for designing the latter. Attempts to develop computer-integrated manufacturing systems based on expensive metal-cutting

equipment have greatly complicated the task of formulating a manufacturing system with positive technical and economic indicators. To further complicate matters, the currently existing technical languages for coding design information (i.e., for sketching the plan for configuring equipment, developing a test description of the manufacturing system's operation, etc.) do not permit complete, precise, and unequivocal description of computer-integrated manufacturing systems as they are being created. Because the language of design has not yet been adequately developed, it is still impossible to work out technological decisions in the system design stage. For this reason, efforts to create domestic computer-integrated manufacturing and (as the first stage in this process) work out the technological design of such systems must first concentrate on the following: researching the distinctive features of designing manufacturing systems; developing new technological design methods, including methods supported by computer technology; developing technological processes for manufacturing components under conditions of computer-integrated manufacturing; intensifying work within the framework of technological design to formalize descriptions of the operation of manufacturing systems and to create automated management systems; solving the economic problems entailed in developing computer-integrated manufacturing; tying the new manufacturing systems created with the existing manufacturing environment; and creating new methods of organizing planning efforts, including methods using computers throughout all stages of the technological design and actual operation stages. Figure 1.

Monitoring, Testing, and Diagnosis in Computerized Manufacturing

917F0233G Moscow PROBLEMY
MASHINOSTROYENIYA I NADEZHNOСТИ MASHIN
in Russian No 3, 1991 pp 15-17

[Article by A.I. Kamyshev]

UDC 658.2.011.056

[Abstract] The role of monitoring, testing, and diagnosis has increased dramatically under the conditions of computerized manufacturing for a number of reasons. Monitoring, testing, and diagnosis in any form of computerized manufacturing including automated plants are the main means of acquiring the information needed to integrate and manage manufacturing. In an automated plant producing machine tools and machine tool subassemblies, monitoring, testing, and diagnosis encompasses the following areas: intake inspection of materials and components used to complete other products, monitoring of the machining and other processes entailed in manufacturing components, testing and diagnosis of assembled subassemblies and machine tools, preventive monitoring, forecasting and diagnosis of the equipment in use, and testing and studying the machine tools and subassemblies being produced so as to improve them.

The processes of intake inspection and monitoring, testing, and diagnosis can be combined in a computerized assembly process control system. Such systems consist of automated inspection and diagnosis stations and sections that are equipped with stands, instruments, and computer technology unified by a central computer. Rational configuration of such stations can help reduce the transport routes entailed in a manufacturing process and reduce the costs of eliminating defective production. Automating the process of information gathering and processing in such a system make the inspection and testing process faster, easier to visualize, and more objective. Unifying several such monitoring, testing, and diagnosis system in local area networks within an automated plant further increases the efficiency of such systems. This article diagrams and discusses the key elements of such systems. Figures 2; references 2 (Russian).

NC Systems as a Part of the Hierarchical Structure for Managing an Automated Plant

917F0233F Moscow PROBLEMY
MASHINOSTROYENIYA I NADEZHNOСТИ MASHIN
in Russian No 3, 1991 pp 14-15

[Article by V.A. Ratmirov]

UDC 658.2.011.056

[Abstract] Two contrary trends are observed in the multilevel management structure of automated plants. On the one hand, the top levels of the hierarchy possess more powerful computer technology, and the remaining levels in the system are all subordinate to these upper levels (i.e., the principle of vertical subordination is used). On the other hand, the development of computer technology and creation of personal computers have resulted in a decentralization of management and other intelligent functions and in the creation of local data bases. This has expanded the functions performed by the lower levels of the hierarchy and given them some degree of autonomy. That fact that each NC machine tool in a system can now have its own ongoing diagnostic information and data about the machining process that it is executing has reduced the load on information transmission channels and increased the reliability of automated plant management systems overall. The conventional method of designing NC machine tool systems called for the aforementioned vertical subordination. It is now possible, however, to use a modular principle and a distributed structure when designing NC machine tool systems. NC tool systems designed in accordance with this principle rely on personal computer hardware and software. Such systems can be expanded and adapted to various types of production equipment without changing the basic software. Configuring a flexible manufacturing system to operate in a self-contained mode makes it possible to set up a two-shift operating scheme. The Relief-M NC machine tool system is one such system. It is intended for use with a wide range of manufacturing

equipment and is based on the personal computer. From both conceptual and design standpoints, the new NC machine tool system operates at three levels: dispositional, coordinative, and executive. The Relief-M system can control 12 coordinates (5 of which can be controlled simultaneously), provides a discreteness of movement of 0.001 or 0.0001 mm, has a working feed speed of 25 m/min (a fast speed of 30 m/min), requires 1 to 2 milliseconds between signals issued to the drive, has 356 kbyte of memory for the control program adjuster, has a sensor signal frequency of 150 kHz, has a power of 200 VA, and weighs 50 kg. The new system is equipped with a color graphic display and can operate interactively. Figure 1.

Principles of Creating an Automated System for the Technological Preparation of Production for an Automated Plant

917F0233E Moscow PROBLEMY
MASHINOSTROYENIYA I NADEZHNOСТИ MASHIN
in Russian No 3, 1991 pp 12-14

[Article by A.M. Berman]

UDC 658.2.011.056

[Abstract] Using an automated system for the technological preparation of production dramatically reduces the time and cost of preparing production and increases the quality and optimality of design decisions. The implementation of an automated system for the technological preparation of production should be based on the same type of local area network [LAN] on which computer-integrated manufacturing is based. When a computer is used to perform the tasks entailed in the technological preparation of production, all of the documentation needed for the automated plant to function should be formulated and stored on machine carriers (what has been termed paperless technology), and the information should be sent along the communications channels of the LAN. Automated systems for the technological preparation of production can function both at the level of the automated plant and at the level of individual automated shops. When automated systems for the technological preparation of production are designed, a distinction is drawn between external and internal system integration. External integration includes development of the automated system for the technological preparation of production based on the methodological support, language, software, and hardware that are common to automated operations support systems; the use of unified data and knowledge bases and graphic data banks; and a LAN plus feedforward and feedback to and from a computer-aided design and automated management system. Internal automation includes the creation of a technological process CAD system, preparation of a control program and special accessories based on unified source information and the data and knowledge bases, and simultaneous preparation of a control program for the machining and monitoring processes. Automated

systems for the technological preparation of production typically contain two groups of subsystems—design subsystems and technological/organizational subsystems. Efforts to develop automated systems for the technological preparation of production should focus on the following tasks: analysis and investigation of the main tasks in the technological preparation of production at automated plants and the interconnections existing between these individual tasks; development of methods of designing technological processes by using such tools and knowledge bases and expert systems; creation and/or updating of existing application software for use with promising computer technology and, above all, personal computers; efforts to improve the efficiency of the components of automated systems for the technological preparation of production by improving their key characteristics; and development of work in the field of integrating tasks within an automated system for the technological preparation of production and within the framework of computer-integrated manufacturing. Figures 2.

The Automated Plant CAD System of the Krasnyy proletariy Machine Tool Production Association in Moscow

917F0233D Moscow PROBLEMY
MASHINOSTROYENIYA I NADEZHNOСТИ MASHIN
in Russian No 3, 1991 pp 9-12

[Article by A.I. Levin]

UDC 658.2011.056

[Abstract] Because the adequate and efficient operation of automated plants depends on the adequacy of available means for the engineering (design and technological) preparation of production, an advanced system for the computer-aided design of products (referred to as the SAPR-AZ [CAD-API]) has been created within the framework of the automated plant at the Krasnyy proletariy [Red Proletarian] Machine Tool Production Association in Moscow. The new CAD system is intended to provide a comprehensive and gradual transition to a "paperless" technology of formulating and developing design and technological information. Thanks to the fact that the automated plant makes extensive use of modern methods of mathematical modeling and optimization of the designs of machine tools and machine tool subassemblies manufactured at the plant, the new CAD system is expanded to increase the engineering level of the products produced at the automated plant and sharply reduce the time required to complete the cycle of design and interaction preparation of production. The new CAD system is expected to have an especially beneficial effect inasmuch as a significant number of the 6,000 machine tools produced yearly at the automated plant are custom-designed to meet client specifications. The new CAD system use a single methodological approach throughout all stages of the design process. This approach entails the formulation of structured morphological models of

design objects from a pre-existing set of components of lower hierarchical rank (for example, machine tools are designed from a set of existing subassemblies, subassemblies are designed from a set of existing components, and components are designed from existing structural/technological elements). The principle of similarity is used as a basis for creating type-size series of standard element. Sets of such standard elements are formulated into special data bases that can be continually supplemented and updated. The new CAD system includes six functional subsystems (data base, expert system, computer graphics, text documents, design management, and plan quality control) and a long list of object-oriented subsystems (composite design of machine tools from standard subassemblies; a main drive with a working spindle [headstock]; a set of basic manufacturing equipment; accessories for this basic equipment; electrical, hydraulic, and pneumatic equipment; and fixed members, assorted plane components and components made of sheet material, and packaging). The CAD system is organized into three levels. The problems to be solved in designing and making the calculations required for machine tools, components, and subassemblies in accordance with the composite principle are dealt with at the first level. It is also at this level that text and graphic documents are prepared. Information sharing between automated workstations and concentrated and intermediate storage of information within the bounds of the design office occur at the second level. Included among the tasks addressed at the third level are the following: design of complex components; execution of refined calculations of configurations and bearing structures to determine their precision, rigidity, and dynamics; and simulation of dynamic processes. Table 1; references 3 (Russian).

Simulation in Problems of the Design and Functioning of Automated Plants

917F0233C Moscow PROBLEMY
MASHINOSTROYENIYA I NADEZHNOСТИ MASHIN
in Russian No 3, 1991 pp 6-9

[Article by V.T. Portman and Ye.I. Sklyarevskaya]

UDC 658.2.011.056

[Abstract] A system of simulations encompassing all of the stages in the life cycle of an automated plant has been developed for use in modeling the diverse organizational and technological structures of automated plants. The simulations provided for use in the predesign analysis and actual design stages serve as tools for selecting structure parameters. The simulations provided for use in the operation stage may be used as actual components of automated management systems to analyze versions of long-range and operations plans. Both analytical and stochastic models are used in the predesign analysis. The former are used to select equipment and make a consolidated estimate of the capacity of the facility being modeled. The latter are used to formulate a preliminary

estimate of the load on basic and transport equipment, volumes of incomplete products, and the required capacity of warehouses when the available initial planning and interaction data are in the form of estimates and thus uncertain. Sets of simulations are provided for use in designing an automated plant overall (higher-level models) or a specific flexible manufacturing system (lower-level models). The simulation system can include 1) an automated data bank of such data as equipment parameters, routing information, information regarding the interaction processes entailed in machining workpieces, and versions of organizing manufacturing processes and 2) an expert system intended to automate the decision-making process based on the consideration of a number of factors and evaluation criteria. The simulation system is currently being developed through the efforts of a number of scientific research and academic institutions. Development of the models of an automated plant overall is still in the initial stage. Work on the simulations of individual flexible manufacturing systems has proceeded farther and includes simulations for use in three machining schemes (sequential, sequential-parallel, and parallel). The use of the system of simulations is illustrated by way of two detailed examples. Figures 7.

Forecasting the Economic Indicators of an Automated Plant's Production Activity

917F0233B Moscow PROBLEMY
MASHINOSTROYENIYA I NADEZHNOСТИ MASHIN
in Russian No 3, 1991 pp 4-6

[Article by L.Yu. Lishchinskiy]

UDC 658.2.011.056

[Abstract] The general formulation of the problem of forecasting the economic indicators of the production activity of an automated plant is based on the modern idea of the economic effect of production: It is the difference between the cost estimates of the aggregate results of production activity and the aggregate costs of resources for the period of the enterprise's life cycle or for some other sufficiently representative time period. Forecasting the structure and activity of an automated plant entails the following: 1) determining directions for improving an automated plant's economic activity (including formulating an economically well founded manufacturing program and making decisions regarding reconfiguring the automated plant), 2) formulating an automated plant's optimal manufacturing program and optimal manufacturing dynamics given a specified plant structure, 3) optimizing the automated plant's structure given a specified manufacturing program, 4) reconfiguring the automated plant given a specified change in its manufacturing program and determining acceptable reconfiguration costs, 5) formulating a model to calculate manufacturing quotas for the plant's shops and

sections in accordance with their technological specialization, and 6) simulating the automated plant's operation on the macrolevel. These tasks can be accomplished by doing the following: 1) generation of versions of the manufacturing program based on source information about the status of output in the given time period based on an assessment of product demand, market conditions, price forecasts, etc.; 2) preliminary design of the automated plant's structure followed by optimization of this preliminary design for the respective version of the manufacturing program adopted; 3) economic assessment and selection of versions of the automated plant's manufacturing program and structure; and 4) formulation of an economically optimal manufacturing program for the automated plant structure selected. Figure 1.

Prospects and Concepts of Creating Automated Plants

917F0233A Moscow PROBLEMY
MASHINOSTROYENIYA I NADEZHNOСТИ MASHIN
in Russian No 3, 1991 pp 2-4

[Article by O.I. Averyanov, B.I. Cherpakov, and V.N. Yefrimov]

UDC 658.2.011.056

[Abstract] There has been a worldwide movement away from creating individual flexible manufacturing systems toward computer-integrated systems, i.e., automated plants, operating in a closed-loop manufacturing cycle. About 20 such plants are in operation throughout the world today. Creating automated plants will enable the USSR to operate manufacturing facilities at the level of the best world prototypes, automate the machine building industry, organize the spread of entire automated plants or fragments thereof, develop fundamentally new technological processes for many of the operations involved in machine building, develop manufacturing processes requiring few or no workers, and standardize products and automation equipment based on a unified classification system for machine building products. The main impetus for creating automated plants is the increasing individualization of user demands for various products and increasingly stringent product quality requirements. The main prerequisites stimulating the creation of automated plants include the appearance of relatively inexpensive intelligent programmable controllers, the wide-scale popularization of local area networks with standard architectures and protocols, the increasing reliability of computer equipment, and the appearance and increasing popularity of relatively inexpensive supermicrocomputers and personal computers. The main objectives of creating automated plants are as follows: 1) formation of new industrial facilities; 2) expansion of domestic industrial experience in the area of large-scale machine building

projects and in the creation and use of highly organized series-production processes; and 3) creation of a scientific-technical stockpile in the field of organizing manufacturing, technology, and equipment. Creating automated plants will require combining two approaches to design and management: the empirical approach (based

on the experience and intuition of specialists) and the theoretical approach (based on formalized scientific knowledge about the subject area). These approaches can be combined by using expert systems that include knowledge bases and systematized decision-making rules. Figures 2.

NTIS
ATTN: PROCESS 103
5285 PORT ROYAL RD
SPRINGFIELD, VA

2

22161

This is a U.S. Government publication. Its contents in no way represent the policies, views, or attitudes of the U.S. Government. Users of this publication may cite FBIS or JPRS provided they do so in a manner clearly identifying them as the secondary source.

Foreign Broadcast Information Service (FBIS) and Joint Publications Research Service (JPRS) publications contain political, military, economic, environmental, and sociological news, commentary, and other information, as well as scientific and technical data and reports. All information has been obtained from foreign radio and television broadcasts, news agency transmissions, newspapers, books, and periodicals. Items generally are processed from the first or best available sources. It should not be inferred that they have been disseminated only in the medium, in the language, or to the area indicated. Items from foreign language sources are translated; those from English-language sources are transcribed. Except for excluding certain diacritics, FBIS renders personal and place-names in accordance with the romanization systems approved for U.S. Government publications by the U.S. Board of Geographic Names.

Headlines, editorial reports, and material enclosed in brackets [] are supplied by FBIS/JPRS. Processing indicators such as [Text] or [Excerpts] in the first line of each item indicate how the information was processed from the original. Unfamiliar names rendered phonetically are enclosed in parentheses. Words or names preceded by a question mark and enclosed in parentheses were not clear from the original source but have been supplied as appropriate to the context. Other unattributed parenthetical notes within the body of an item originate with the source. Times within items are as given by the source. Passages in boldface or italics are as published.

SUBSCRIPTION/PROCUREMENT INFORMATION

The FBIS DAILY REPORT contains current news and information and is published Monday through Friday in eight volumes: China, East Europe, Soviet Union, East Asia, Near East & South Asia, Sub-Saharan Africa, Latin America, and West Europe. Supplements to the DAILY REPORTs may also be available periodically and will be distributed to regular DAILY REPORT subscribers. JPRS publications, which include approximately 50 regional, worldwide, and topical reports, generally contain less time-sensitive information and are published periodically.

Current DAILY REPORTs and JPRS publications are listed in *Government Reports Announcements* issued semimonthly by the National Technical Information Service (NTIS), 5285 Port Royal Road, Springfield, Virginia 22161 and the *Monthly Catalog of U.S. Government Publications* issued by the Superintendent of Documents, U.S. Government Printing Office, Washington, D.C. 20402.

The public may subscribe to either hardcover or microfiche versions of the DAILY REPORTs and JPRS publications through NTIS at the above address or by calling (703) 487-4630. Subscription rates will be

provided by NTIS upon request. Subscriptions are available outside the United States from NTIS or appointed foreign dealers. New subscribers should expect a 30-day delay in receipt of the first issue.

U.S. Government offices may obtain subscriptions to the DAILY REPORTs or JPRS publications (hardcover or microfiche) at no charge through their sponsoring organizations. For additional information or assistance, call FBIS, (202) 338-6735, or write to P.O. Box 2604, Washington, D.C. 20013. Department of Defense consumers are required to submit requests through appropriate command validation channels to DIA, RTS-2C, Washington, D.C. 20301. (Telephone: (202) 373-3771, Autovon: 243-3771.)

Back issues or single copies of the DAILY REPORTs and JPRS publications are not available. Both the DAILY REPORTs and the JPRS publications are on file for public reference at the Library of Congress and at many Federal Depository Libraries. Reference copies may also be seen at many public and university libraries throughout the United States.